Insights into Current Tropomyosin Receptor Kinase (TRK) Inhibitors: Development and Clinical Application

Wei Yan,[a] Naga Rajiv Lakkaniga,[a] Naresh Gunaganti,[a] Fengping Lv,[a] Francesca Carlomagno,[b,c] Massimo Santoro,[b] Neil McDonald,[d,e] Brendan Frett,[a,*] and Hong-yu Li[a,*]

[a]Department of Pharmaceutical Sciences, College of Pharmacy, University of Arkansas for Medical Sciences, Little Rock, AR 72205, USA

[b]Dipartimento di Medicina Molecolare e Biotecnologie Mediche, Università Federico II, Via S Pansini 5, 80131 Naples, Italy

[c]Istituto di Endocrinologia e Oncologia Sperimentale del CNR, Via S Pansini 5, 80131 Naples, Italy

[d]Signaling and Structural Biology Laboratory, The Francis Crick Institute, London, NW1 1AT, UK

[e]Institute of Structural and Molecular Biology, Department of Biological Sciences, Birkbeck College, Malet Street, London, WC1E 7HX, UK

Abstract: The use of kinase-directed precision medicine has been heavily pursued since the discovery and development of imatinib. Annually, it is estimated that around ~20,000 new cases of TRK-driven cancers are diagnosed, with the majority of cases exhibiting a TRK genomic rearrangement. In this perspective article, we discuss current development and clinical applications for TRK precision medicine by providing the following: (1) The biological background and significance of the TRK kinase family, (2) A compilation of known TRK inhibitors and analysis of their co-crystal structures, (3) An overview of TRK clinical trials, and (4) Future perspectives for drug discovery and development of TRK inhibitors.

Introduction

The tropomyosin receptor kinase (TRK) family of enzymes are transmembrane, receptor tyrosine kinases (RTK) that regulate synaptic strength and plasticity in the mammalian nervous system.[1-8] In this role, the TRK family regulates cell differentiation, proliferation, survival, and pain.[9-23] There are three members of the TRK family: TRKA (encoded by *NTRK1* gene), TRKB (*NTRK2*), and TRKC (*NTRK3*), which have all been implicated to drive initiation and progression of malignancies.[24-41] Similar to the BCR-ABL gene fusion product that drives chronic myelogenous leukemia (CML),[42] *NTRK* rearrangements and fusion gene products have been observed in numerous tumor types, which has been comprehensively reviewed by Vaishnavi, *et al* and Amatu, *et al*.[43-44] Unlike CML, however, the incidence of *NTRK* fusion genes in each specific tumor type overall is rare. This generates profound difficulties for patient identification and adequate recruitment for clinical trials. For instance, *NTRK2* gene fusions have been identified in 0.2% of lung adenocarcinoma,[45] which represents approximately 184 patients of 92,138 diagnosed in 2010 in the USA.[46] On the other end of the spectrum, *NTRK3* fusion genes have been identified in virtually all secretory breast carcinomas and of mammary analogue secretory carcinomas (MASC), an extremely rare tumor of the salivary (in general, of the parotid) gland.[47] In fact, the defining characteristic of MASC, when compared to other salivary carcinomas, is an *NTRK* gene fusion.[47] In addition, *NTRK* fusions are found in about 50% of pediatric diffuse intrinsic pontine glioma and non-brainstem glioblastoma.[48] In major cancer subgroups, *NTRK* fusions occur in 3.3% of lung cancers,[45, 49] 2.2% of colorectal cancers,[45, 49-52] 16.7% of thyroid cancers,[45, 53-54] 2.5% of glioblastomas, and 7.1% of pediatric gliomas.[43, 55] Finally, similar to the receptor tyrosine kinase RET (rearranged during transfection), *NTRK* fusions (particularly ETV6-NTRK3) are common in post-Chernobyl radiation-induced papillary thyroid carcinomas.[56-57] Thus, targeting TRK oncogenes is an attractive therapeutic approach for a diverse, frequently rare set of cancers.

The primary method to target TRK oncogenes is the use of small molecule kinase inhibitors. Because gene fusion products are the major oncogenes observed, other targeting strategies, such as antibody therapy, will not be effective since transmembrane tyrosine kinase fusions frequently lack an extracellular domain.[58] In this case, the fusion proteins are only susceptible to small molecule inhibition.[59-61] In general, small molecules are designed to target the adenosine triphosphate (ATP) binding site of TRK to block catalytic activity. This is based on the principle that protein kinases catalyze a phosphoryl transfer to a downstream substrate and only have micromolar affinity for ATP.[62] Since turnover is rapid and

kinase affinity for ATP is weak, small molecules can effectively bind and inhibit TRK despite a high cellular concentration of ATP. Because of the druggability of the TRK enzyme class, a number of attempts to target TRKs have been completed. In this perspective article, we discuss current development and clinical application of TRK-targeted cancer therapy including (1) The biological background and significance of the TRK family, (2) A compilation of known TRK inhibitors and analysis of TRK/inhibitor co-crystal structures, (3) An overview of TRK clinical trials, and (4) Future perspectives for drug discovery and development of TRK inhibitors.

TRK Biology and Signaling

The TRK oncogene was initially discovered in colon cancer in which the cytoskeletal protein tropomyosin was fused to an unknown, catalytically active kinase domain.[50, 63] Further studies identified the kinase as a single-pass receptor tyrosine kinase expressed in the developing central nervous system and was given the name tropomyosin receptor kinase. In the extracellular region of TRK, there is a leucine rich motif, two cysteine-rich domains, and two immunoglobulin-like domains and all are essential for ligand recognition and binding.[64-66] Unlike typical RTKs, the TRK intracellular region is small and comprised of roughly 70 amino acids before and 15 amino acids after the kinase domain.[64-65] In comparison to other RTKs, TRK is most similar to the insulin receptor and has been implicated in insulin signaling.[67]

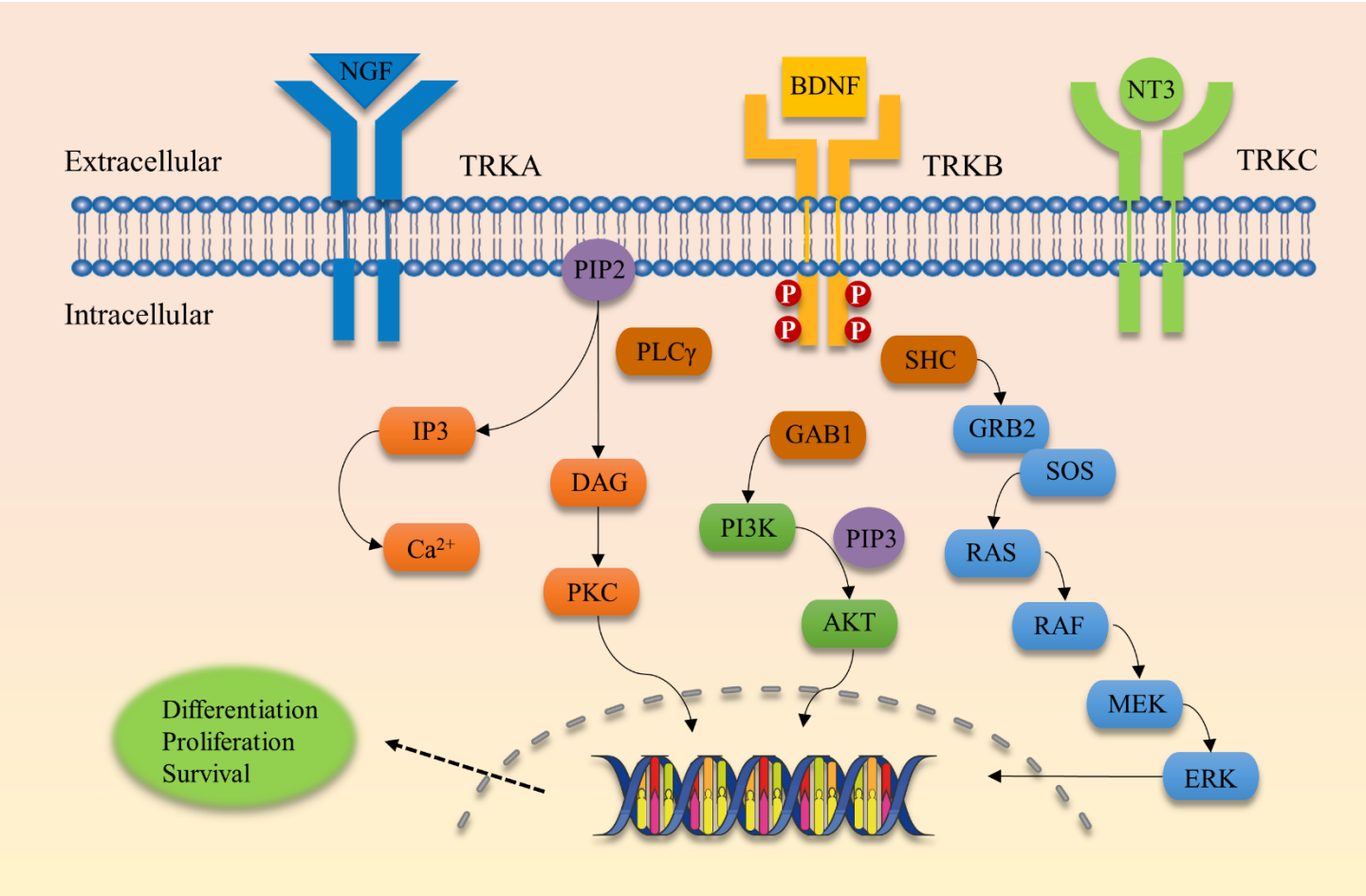

Figure 1. Schematic view of TRK receptor tyrosine kinases and major signal transduction pathways involved in cell differentiation, proliferation, and survival. TRKA is activated by nerve growth factor (NGF), TRKB is activated by brain-derived neurotrophic factor (BDNF), and TRKC is activated by neurotrophin-3 (NT3). RAS, rat sarcoma oncogene; RAF, rapidly accelerated fibrosarcoma oncogene; MEK, mitogen-activated protein kinase; ERK, extracellular signal-regulated kinase; GRB2, growth factor receptor-bound protein 2; SHC, SRC homology 2 domain containing; PI3K, phosphatidylinositol-4,5-bisphosphate 3-kinase; AKT, v-AKT murine thymoma viral oncogene homologue; PLCγ, phospholipase C-γ; DAG, diacyl-glycerol; PKC, protein kinase C; IP3, inositol trisphosphate.

The TRK family is comprised of three distinct isoforms: TRKA, TRKB, and TRKC. A major difference between all three isoforms is the ligand that activates the receptor. TRKA is activated by nerve growth factor (NGF),[68-70] TRKB is activated by brain-derived neurotrophic factor (BDNF),[69-70] while TRKC is primary activated by neurotrophin 3 (NT3) (Figure 1).[71-72] The kinase domains of TRKA, TRKB, and TRKC share between 72% and 78% sequence identity.[73] When looking at the residues that interact directly with ATP in the active site,[74] TRKA and TRKB share 95% sequence identity

while TRKB and TRKC are completely identical.[73] In the TRK domain, the TRKA hinge is more structurally constrained compared to TRKB and TRKC, suggesting the hinge environment differs between TRK isoforms.[74] Further, the kinase insert domain of the TRK family is not structurally conserved, which is another key difference within the family.[74]

Similar to the RTK superfamily, TRKs dimerize in response to ligand binding (Figure 1 and 2).[75] After ligand binding, TRKs autophosphorylate each monomer followed by rapid phosphorylation of the kinase activation loop.[76-78] These phosphorylation events enhance catalytic activity of the kinase. To generate attachment sites for adapter proteins, the NPXY motif (Y490 in TRKA) in the juxtamembrane domain and the YLDIG motif (Y785 in TRKA) in the carboxy terminus are phosphorylated.[79-82] These phosphorylation events create docking sites for SRC Homology Domain 2 (SH2) and Phosphotyrosine binding domain (PTB) containing proteins, such as SHC and phospholipase C-gamma (PLC-gamma). After binding, SHC and PLC are activated through TRK-catalyzed phosphorylation.[44, 83]

SHC was the first adaptor protein identified to bind to the phosphorylated NPXY motif of TRK, which results in the activation of the AKT and RAS canonical pathways.[80-82, 84] After SHC is activated, a secondary adaptor protein, growth factor receptor-bound protein 2 (GRB2),[85] is recruited and facilitates GTP-loading of RAS via the guanine nucleotide exchange factor, SOS.[86] The activated, GTP-bound form of RAS activates the MAP kinase cascade, which includes activation of RAF, MEK, and ERK.[87] The ERK kinase translocates into the nuclear membrane activating transcription of target genes involved in cell growth, survival, and proliferation.[88]

Activation of the AKT pathway occurs via recruitment of SHC and GRB2 to the NPXY motif of TRK, which signals through the intermediary molecule, GRB2-associated-binding protein 1 (GAB1). This simulates activity of phosphoinositide 3-kinase (PI3K) leading to phosphorylation of PI4,5 lipids at the 3'-position.[89] On AKT, there is a conserved pleckstrin homology (PH) domain, which interacts with the 3'-phosphorylated lipids leading to AKT activation.[90-93] AKT activation leads to increased expression of cell survival and proliferation genes that enhance pro-survival phenotypes mediated through TRK receptors.[94-98]

TRK Implication in Cancer

Genetic mutations in the TRK family have been reported in many cancers, namely carcinomas of the colon, thyroid, lung, ovary, breast (secretory breast carcinoma), salivary gland (mammary analogue secretory carcinoma),

pancreas, melanoma, spitzoid neoplasms, cholangiocarcinoma, stromal tumors (congenital fibrosarcoma, congenital mesoblastic nephroma, soft tissue sarcoma, gastrointestinal stromal tumor, inflammatory myofibroblastic tumor), brain tumors (pediatric glioma, astrocytoma and glioblastoma) and leukemia (Table 1 and Figure 3).[43,99-100 49,51,53,57,101] Within the TRK family, TRKA is the most commonly identified oncoprotein, which is found at a rate of approximately 7.4% across multiple tumor types.[43] Following is TRKC and then TRKB, which are found at rates of 3.4% and 0.4%, respectively. The majority of TRKB mutations have a frequency of less than 0.5% and many TRKC mutations have a frequency of less than 1.0%.[49]

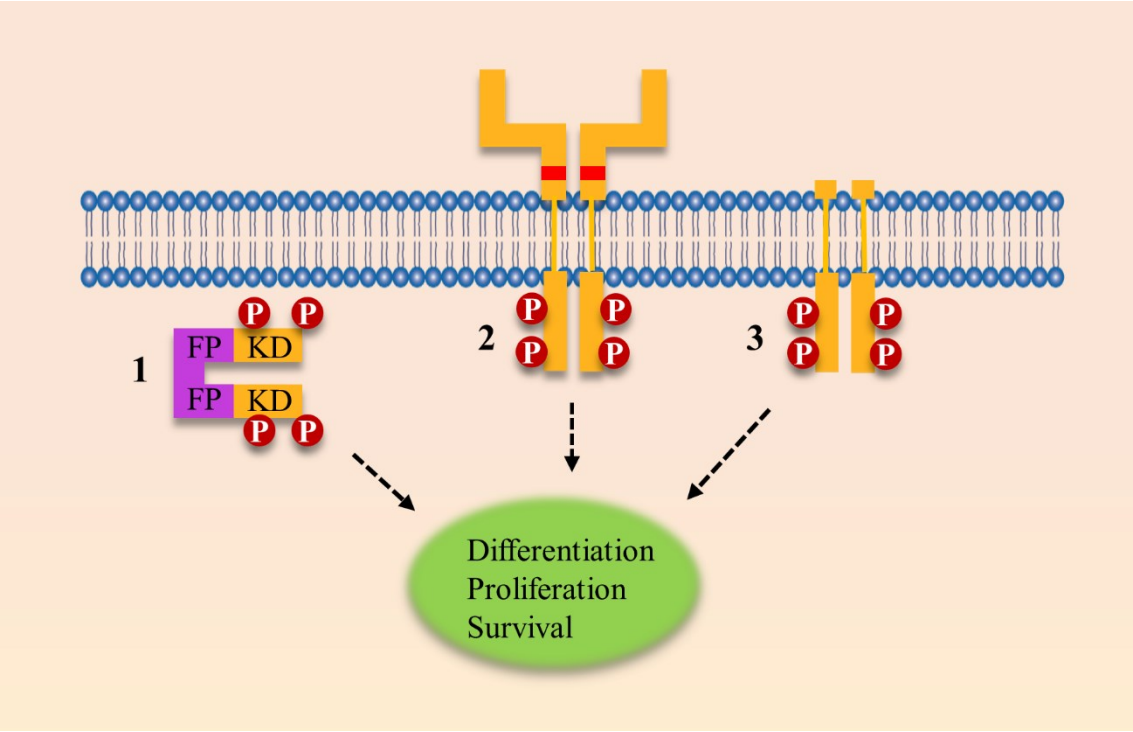

Figure 2. Ligand-independent signaling leading to constitutive TRK activation can occur through three, distinct mechanisms: A genomic rearrangement event; Extracellular point mutations; or Truncations of the extracellular domain. (1) In a genomic rearrangement event the kinase domain of TRK is fused to an unrelated protein, typically called the fusion partner. In this example, a cytoplasmic chimeric TRK fusion is shown without the transmembrane (TM) domain. Of note, TRK fusions can occur with or without the TM domain.[102] (2) Point mutations can occur in the extracellular domain of TRK, generating a TRK oncogene with transforming abilities. Point mutations that are transformative under laboratory conditions have been identified at P203A and C345S.[103-104] (3) Through in-frame deletions and alternative

splicing events, the TRK kinase can present with a truncated extracellular domain. These aberrant gene products have been identified in AML and neuroblastoma.[105-107] FP: fusion partner. KD: kinase domain.

When an *NTRK* gene fusion occurs, the translocation event generates a hybrid oncogene composed of the active TRK kinase domain linked to an unrelated gene or fusion partner, triggering constitutive activation or overexpression of the TRK protein (Figure 2).[44, 53] The resulting aberrantly expressed, novel oncogene can occur with or without the transmembrane domain.[43, 102] Certain mutations in the extracellular domain of TRKA, namely P203A and C345S, have been identified as transforming under laboratory conditions but have yet to be identified in human tumor samples.[103-104] On the other hand, in-frame deletions (ΔTRKA) and splice variants (TRKAIII) of *NTRK1* have been functionally identified and characterized in human tumor samples.[52, 105-107] The ΔTRKA in-frame deletion, identified in acute myeloid leukemia (AML), contains a truncated extracellular domain that can transform both epithelial and fibroblast cells.[107] The TRKAIII splice variant, identified in neuroblastoma, has deletions in exons 6, 7, and 9, which results in the loss of Ig-like C2-type I (IG-C2) and glycosylation sites in the extracellular domain (Figure 2).[52, 106] TRKA activating mutations from either genomic rearrangements, point mutations, deletions, or splice variants compromise the ability to regulate the kinase domain. This suggests that a key attribute to the oncogenic potential of TRK is the loss of the extracellular domain and/or its function.

Table 1. Oncogenic TRK fusions are found across multiple tumor types[a]

Cancer Site	Estimated US Cases / yr	TRKA%	TRKB%	TRKC%
Lung Adenocarcinoma (NSCLC)	92,138[46]	3.3[49]	0.2[45]	/
Colorectal	135,430[108]	1.5[49-50, 52-51]	/	0.7[45]
Intrahepatic cholangiocarcinoma	2,970[109-110]	3.6[111]	/	/
Papillary thyroid cancer	45,496[108, 112]	12.3[53]	/	14.5[54, 113]
Glioblastoma	11,376[108, 114]	1.25[55, 115]	/	/
Head and neck squamous cell carcinoma	63,030[116]	/	0.2[45]	0.2[117]
Mammary analogue secretory carcinoma	151[108, 118]	/	/	100[119]
Ph-like acute lymphoblastic leukemia	1,192[120-121]	/	/	0.7[122]
Acute myeloid leukemia	15,976[121, 123]	/	/	0.0125[57, 124]

Skin cutaneous melanoma	87,110[121]	/	/	0.3[45]
Secretory breast carcinoma	252[121, 125]	/	/	92[126]
	Estimated Total Cases / yr	10,917	310	8,325
	Estimated Percent of Cases / yr	55.8%	1.6%	42.6%

[a] Only positive studies are listed, and thus the actual prevalence may be lower than reported.

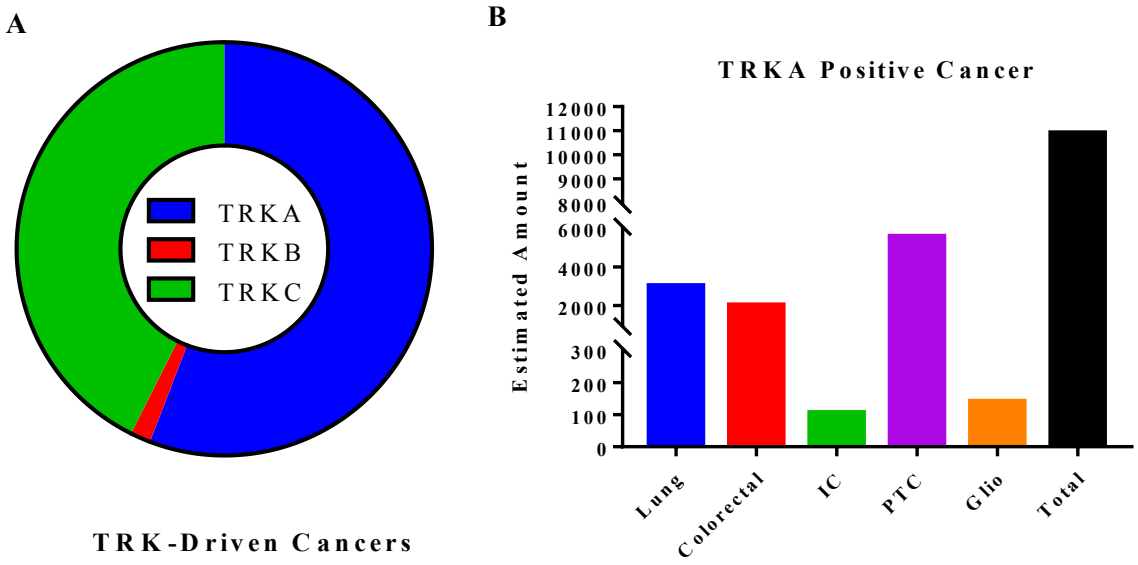

Figure 3: (A) Estimated contribution of TRKA/B/C mutations to all TRK-driven malignancies. Data is based on estimated incidence of cancers at major sites and contribution of TRK mutations at each site. It is estimated that a total of 19,552 cancers are diagnosed each year that have a TRK oncogene. Of the new cases, 55.8% (10,917) are TRKA, 42.6% are TRKC (8,325) and 1.6% (310) are TRKB. Because of the limited sequencing data, the actual amount of TRK-driven tumors could be significantly greater or lower depending on robustness of sample size, sample selection, and data analysis. Also, tumors with a TRK mutation could be dependent on a separate pathway. (B) Estimated number of cancers positive for TRKA. Lung (lung adenocarcinoma), IC (intrahepatic cholangiocarcinoma), PTC (papillary thyroid cancer), and Glio (glioblastoma).

In the tumor environment, TRK oncogenes stimulate uninhibited signaling through the RAS/RAF and PI3K/AKT pathways[49, 127-129] The preferred signaling cascade is cell-specific, with dominance from the RAS/RAF pathway observed in both colorectal (KM-12) and lung (CUTO-3) cancers. In certain cell types, TRK oncogenic signaling also occurs through the PI3K/AKT and STAT3 signal transduction pathways[49], and in other cases the RAS/RAF and PI3K/AKT

cascades are activated in concert.[130] Because of multifaceted pathway activation, TRK oncogenes are potent and highly oncogenic by stimulating both antiapoptotic and proproliferative pathways.[131] Further, TRK fusion oncogenes have been identified as important mediators to stimulate early tumor progression.[132] Taken together, inhibition of TRK oncogenes can have chemotherapeutic and chemopreventive effects and, subsequently, has become a hotbed for therapeutic discovery efforts. In this perspective, we summarize TRK inhibitors from peer-reviewed literature; compounds from patents have been previously reviewed by McCarthy and Bailey *et al.*[133-135]

TRK Inhibitors

The following section represents a comprehensive overview of known TRK inhibitors and their corresponding discovery and development efforts. Because most TRK-activating mutations alter or eliminate the extracellular domain,[59-61] antibodies directed at TRK or TRK growth factors will not be effective as anticancer agents. Thus, all inhibitors reviewed are small-molecule kinase inhibitors that primarily target the TRK kinase domain. The inhibitors are at various stages of development from exploratory research, pre-clinical research, to clinical trials. Inhibitors have been classified based on their interactions with TRK[136] and are presented according to their binding modes. TRK inhibitors can be broken down into four, distinct subtypes based on ligand/binding interactions. The classifications are (A) Type I, (B) Type II, (C) Type III, and (D) Type IV.[137] (A) Type I TRK inhibitors are ATP competitive and bind to the ATP-binding site. The majority of TRK inhibitors under clinical investigation are Type I. (B) Type II TRK inhibitors are ATP non-competitive and exhibit non-competitive or *pseudo*-competitive binding kinetics. Type-II inhibitors bind at the ATP-binding site and also to an adjacent allosteric pocket. Only a subset of kinases permit such binding, including TRK, a binding mode which can be incorporated into compound design to increase selectivity. (C) Type III TRK inhibitors bind to the kinase domain outside of the ATP-binding site. Unlike Type II inhibitors, Type III inhibitors are true allosteric inhibitors and can exploit unique, kinase-specific functionality to help achieve selectivity among TRK isoforms. (D) Type IV TRK inhibitors bind to a region other than the kinase domain. The majority of kinases are expressed as multi-domain proteins with a catalytic domain and a regulatory domain. Type IV inhibitors can interrupt key protein-protein interactions or ligand interactions that limit activity of the kinase domain.[138] Because TRK genomic rearrangements often pair the TRK kinase domain to an

unrelated gene, it is unclear how effective the anticancer properties will be for Type IV TRK inhibitors. Type IV TRK inhibitors are not reviewed in this perspective.

Type I TRK Inhibitors

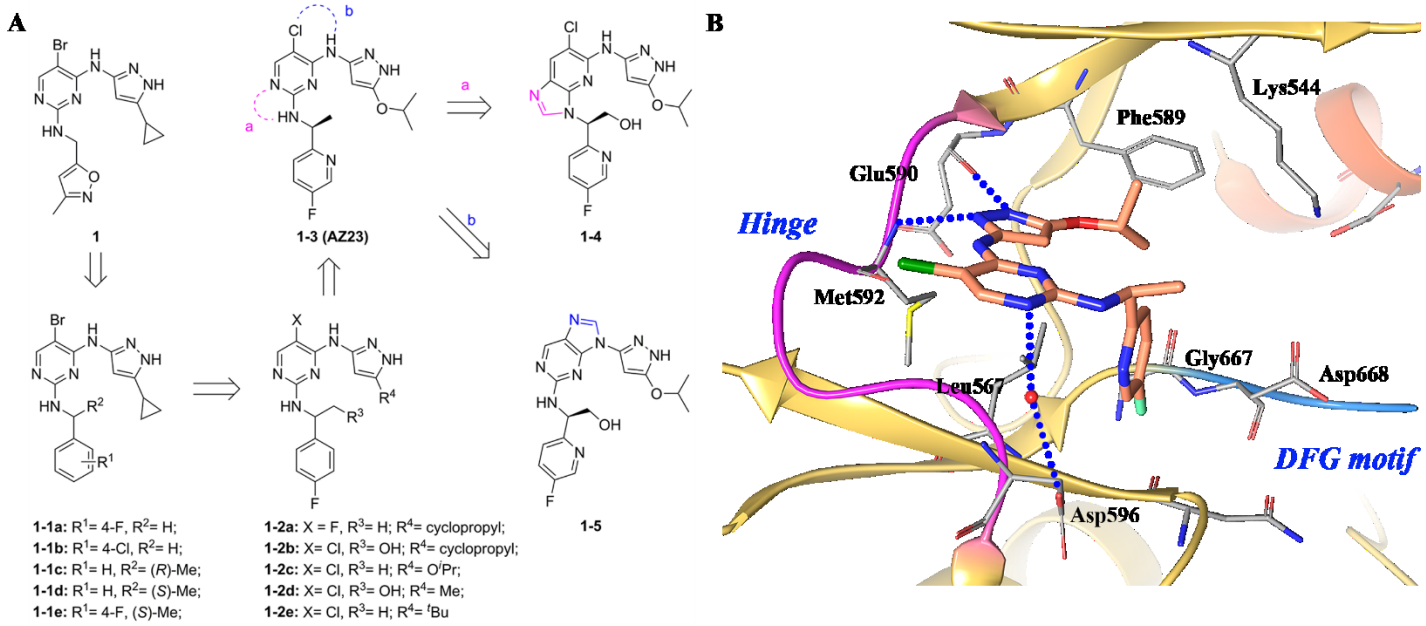

Figure 4. (A) Identification of compounds **1-3**, **1-4**, and **1-5**; (B) Co-crystal structure of compound **1-3** in TRKA (PDB ID: 4AOJ, 2.75 Å). The kinase is depicted in yellow ribbons and the hydrogen bonds are illustrated in blue dashed lines.

Type-I TRK inhibitors exhibit vast diversity in compound architecture, which will alter activity and selectivity profiles of the compounds. This helps to better define chemical space that is relevant to TRK inhibition and suggests points of refinement for future drug discovery efforts. Wang *et al* reported 4-aminopyrimidines with TRK inhibitory activity from a high throughput screening effort against TRKB (Figure 4A).[139] The group discovered compound **1** with activity on TRKA and B (IC_{50} = 0.27 μM and 1.1 μM, respectively). To complete SAR studies on **1**, the isoxazole was replaced with a phenyl group, and halogen substitution at the 4-position of phenyl was found to improved potency (**1-1a** and **1-1b**, TRKA IC_{50}s were 0.10 μM and 0.36 μM, respectively).[139] SAR studies at R^2 indicated that the (*S*)-enantiomer is preferred over the (*R*)-enantiomer (**1-1c** *vs* **1-1d** and **1-1e,** TRKA IC_{50}s were 0.65 μM *vs* 0.10 μM and 0.006 μM, respectively). On the pyrimidine ring system, substituting bromine to fluorine or chlorine had little effect on TRKA activity (**1-2a** and **1-2b,** TRKA IC_{50}s were 0.017 μM *vs* 0.004 μM, respectively).[139] Replacement of cyclopropyl at R^4

with isopropoxy is tolerated (**1-2c,** TRKA IC_{50} = 0.006 μM), but altering aliphatic length or bulk decreases potency likely from geometric constraints at the TRKA hinge region (**1-2d** and **1-2e,** TRKA IC_{50}s were 0.081 μM and 3 μM, respectively). Further optimization and refinement strategies furnished orally bioavailable compound **1-3** (**AZ23**).[139] Compound **1-3** was active against TRKA and B (IC_{50} = 0.002 μM and 0.008 μM, respectively) and exhibited anticancer activity by oral dosing in a TRKA-driven allograft model and TRK-expressing xenograft model of neuroblastoma.[140] In 2012, a ring fusion study of this scaffold was reported by the same research group.[141] Two different ring fusion strategies were employed to generate imidazo[4,5-*b*]pyridine and purine derivatives. Representative compounds of the two scaffolds, **1-4** and **1-5**, exhibited potent TRK inhibition. Both compounds displayed IC_{50} values of 0.0005 μM against TRKA-dependent MCF10A cells (MCF10A-TRKA-Δ), and were also active in mice bearing 3T3-TRKA-Δ tumors.[141]

In the co-crystal structure of compound **1-3** with TRKA (Figure 4B), TRKA is found in an inactive conformation with the C-helix pushed into a non-catalytically active orientation.[141] Compound **1-3** forms two hydrogen bonds at the hinge region with the pyrazole-moiety, and interacts with the amide backbone of Glu590 and Met592. The isopropoxy group is oriented toward Phe589, which is the gatekeeper amino acid. The fluoropyridine ring engages in an interaction with Leu657, and the fluorine atom is in close proximity to Gly667.[142] Numerous TRK kinase inhibitors exploit this region to increase selectivity and potency.[141] Based on the crystal structure, compound **1-3** is a Type-I kinase inhibitor.

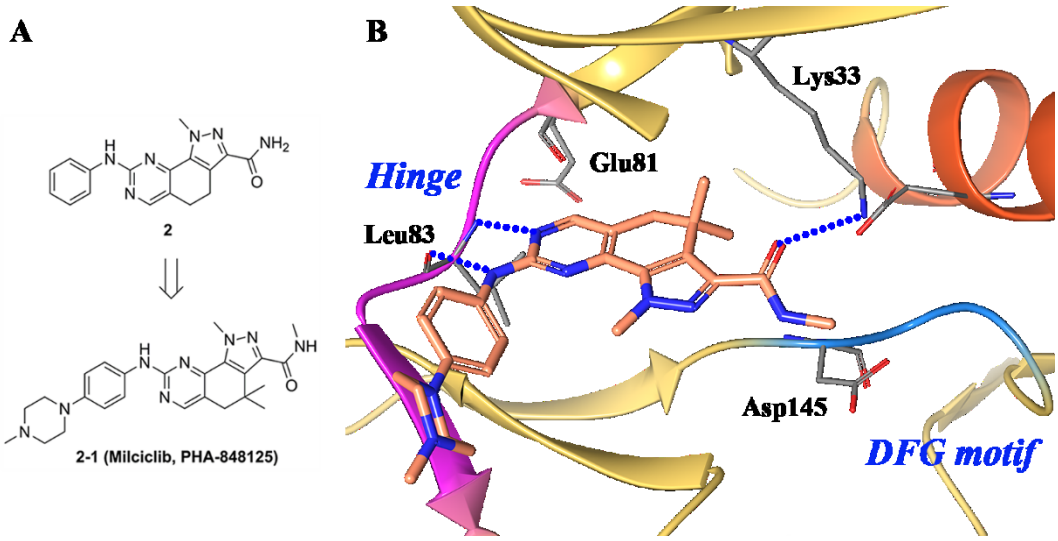

Figure 5. (A) Identification of **2-1**; (B) Co-crystal structure of compound **2-1** in CDK-2/cyclin A. (PDB ID: 2WIH, 2.5 Å). The kinase is depicted in yellow ribbons, and the hydrogen bonds are illustrated in blue dashed lines.

Further exploration of Type-I TRK inhibitors was reported by Brasca *et al.*[143] The group initially identified compound **2** as a potent CDK-2 (cyclin dependent kinase) inhibitor (Figure 5A).[143] Enhancement in selectivity, antiproliferative activity, and optimization of the physiochemical and pharmacokinetic properties led to the identification of compound **2-1** (**Milciclib, PHA-848125**) (Figure 5A) with high potency (CDK-2 IC_{50} = 0.045 μM) and high bioavailability (F = 85%). Serendipitously, this compound exhibited near equal potency against TRKA (IC_{50} = 0.053 μM) with selectivity in the greater kinome (IC_{50}s > 0.15 μM).[143]

Figure 5B illustrates the crystal structure of compound **2-1** in complex with CDK2/cyclin A.[143] The compound binds in the ATP pocket of the kinase with the pyrazoloquinazoline ring system occupying the adenine region, while the phenyl moiety points toward the solvent accessible region. Compound **2-1** creates two hydrogen bonds with the protein backbone of the hinge with residue Leu83. The amide carbonyl group of **2-1** is within hydrogen bonding distance of the conserved lysine (Lys33).[143]

Albanese *et al.* further evaluated the dual inhibitory activity of compound **2-1** against CDK-2 and TRKA.[144-145] *In vitro*, **2-1** was able to inhibit NGF-induced phosphorylation of TRKA as well as downstream signaling in the DU-145 human prostate carcinoma line. *In vivo*, **2-1** inhibited tumor growth in a human prostate DU-145 xenograft model in a dose dependent manner. Because of the dual inhibitory properties of **2-1**, the compound shifts the paradigm for precision medicine. Instead of generating a 'magic-bullet' with high TRK kinase selectivity, Albanese *et al.* focused on validating and developing a 'smart-bomb' with activity on the oncogene lesion (TRK) paired with cell cycle inhibition (CDK).[146]

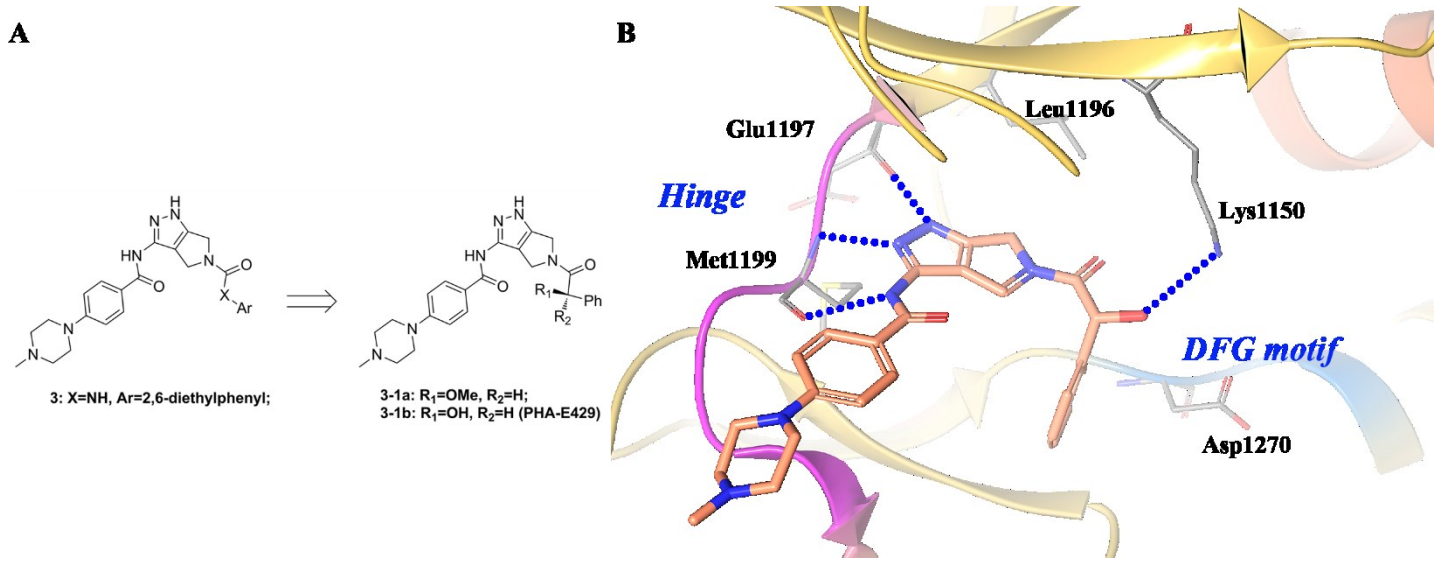

Figure 6. (A) Identification of compound **3-1b**; (B) Co-crystal structure of compound **3-1b** with ALK (PDB ID: 2XBA, 1.95 Å). The kinase is depicted in yellow ribbons, and the hydrogen bonds are illustrated in blue dashed lines.

In line with developing TRK inhibitors with dual activity, Fancelli *et al.* identified a series of 5-phenylacetyl 1,4,5,6-tetrahydropyrrolo[3,4-*c*]pyrazole as Aurora kinase inhibitors (compound **3**, Aurora-A IC_{50} = 0.027 μM) (Figure 6A).[121] Further medicinal chemistry efforts lead to the discovery of compound **3-1b**. Compound **3-1b** was found to have dual activity on TRKA (IC_{50} = 0.03 μM) and Aurora A (IC_{50} = 0.013 μM)[121] with weak ALK (anaplastic lymphoma kinase) inhibitory activity (IC_{50} = 0.091 μM).[147] Akin to **2-1**, compound **3-1b** obtained dual activity on the oncogene lesion (TRKA) as well as cell cycle inhibition (Aurora A).[147]

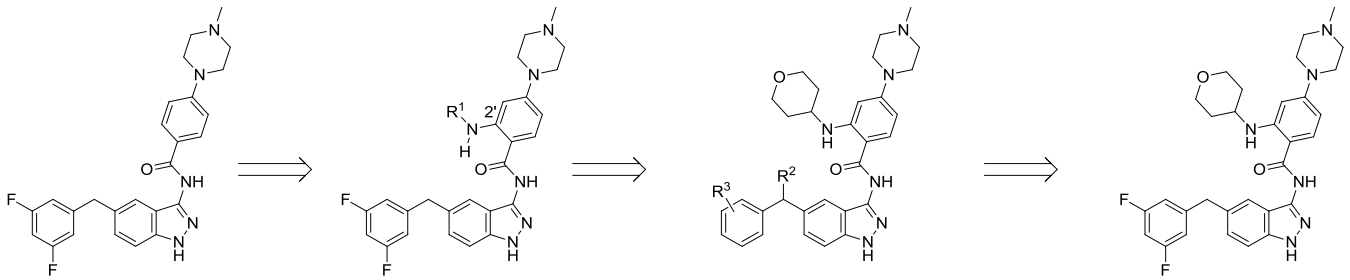

Figure 7. Structural optimization from compound **4** to **4-3**.

Recently, Menichincheri *et al.* disclosed research efforts to generate compound **4-3** (**Entrectinib**, **RXDX-101**) for ALK (IC_{50} = 0.012 μM) (Figure 7).[148] To develop ALK inhibitors from compound **4** (ALK IC_{50} = 0.073 μM), the co-crystal complex of ALK with compound **3-1b** was studied (see Figure 6B).[148] Analysis of the complex suggested that a mono-substitution at 2'-position would generate derivatives that occupy the ATP sugar pocket region while simultaneously displacing a water molecule. In addition, NH-R substituents at this position were able to stabilize the bioactive conformation through intramolecular hydrogen bonding. Based on this concept, different amines were attached to the 2'-position of the central phenyl ring.[148]

The introduction of a primary amine at 2' led to compound **4-1a** with similar ALK potency (IC_{50} = 0.067 μM).[148] This was consistent with modeling analysis as compound **4-1a** lacked the substituent necessary to fill the sugar pocket. At R^1, a methoxyethyl or methoxy propyl group generally led to a moderate loss in activity (**4-1b**, and **4-1c**, ALK IC_{50} = 0.21 μM and 0.135 μM, respectively) while a fluorine or a hydroxyl group increased activity (**4-1d**, and **4-1e**, ALK IC_{50} = 0.014 μM and 0.026 μM, respectively).[148] On the contrary, phenyl or cyclohexyl significantly decreased affinity because of size constraints of the sugar pocket (**4-1f**, and **4-1g**, ALK IC_{50} = 0.684 μM and 0.56 μM, respectively).[148] Interestingly, introduction of a hydroxyl group furnished **4-1h** of which the *trans*-isomer displayed 10-fold higher activity (ALK IC_{50}= 0.01 μM) than the *cis*. When R^1 is 4-amino-N-methylpiperidinyl (**4-1i**) or 4-aminotetrahydropyranyl (**4-3**), the resulting compounds exhibit excellent potency on ALK (IC_{50} = 0.015 and 0.012 μM, respectively). The latter of the two had better cellular activity (Cell IC_{50} = 0.438 μM *vs* 0.031 μM), which might be due to a difference in cell permeability.[148] Introduction of a methyl group to R^2 generated two enantiomers (**4-2a**), with one enantiomer being 3-fold more active than the other (ALK IC_{50}= 0.059 μM and 0.019 μM, respectively, absolute configuration not determined).[148] Due to labor-intensive chiral separation and stability of the benzhydryl stereogenic center further development of these compounds was terminated. Strong electron withdrawing groups on the phenyl ring are crucial for ALK activity. Removing the 3,5-difluoro substitution, changing the position of the fluorine, or replacing with methyl all decreased activity (Compounds **4-2b** to **4-2e,** ALK IC_{50} = 0.106 μM, 0.03 μM, 0.038 μM, 0.181 μM, respectively).[148]

After initial development for ALK, compound **4-3** was subsequently found active on ROS1 (IC_{50} = 0.007 μM) and TRK (IC_{50}s for TRKA/B/C were 0.001 μM, 0.003 μM and 0.005 μM, respectively).[148-149] In antiproliferative studies, compound **4-3** was active against the colorectal cancer cell line KM-12 (IC_{50}= 0.0017 μM) and also induced tumor stabilization (>90% TGI) when administered P.O. to mice bearing KM-12 xenografts.[150] Compound **4-3** is currently in clinical trials for the treatment of patients with ALK-, ROS1- and TRK-dependent tumors and is exhibiting remarkable signs of efficacy.[148-149] In a Phase 2 clinical trial, **4-3** is being investigated for advanced or metastatic solid tumors that harbor TRKA/B/C, ROS1, or ALK gene rearrangements (NCT02568267).

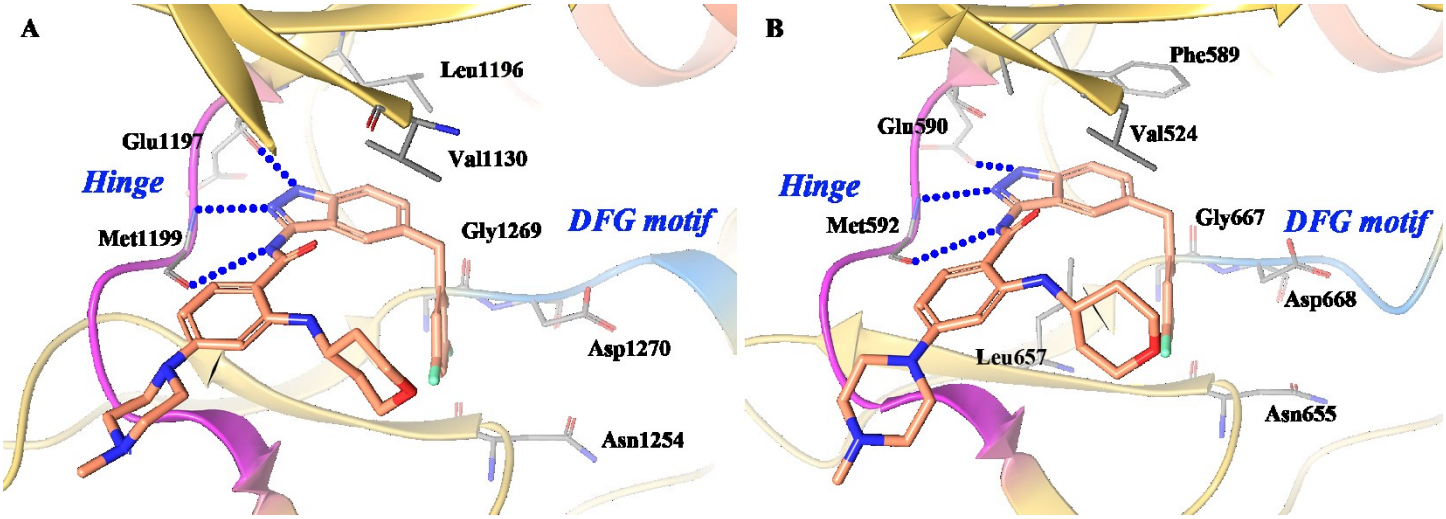

Figure 8. (A) Co-crystal structure of compound **4-3** with ALK (PDB ID: 5FTO, 2.22 Å): (B) Co-crystal structure of compound **4-3** with TRKA (PDB ID: 5KVT, 2.45 Å). The kinase is depicted in yellow ribbons, and the hydrogen bonds are illustrated in blue dashed lines.

The co-crystal structure of ALK with compound **4-3** was consistent with the above expectations (Figure 8A).[148] A similar binding mode is observed in the co-crystal structure of **4-3** with TRKA (Figure 8B).[151] The compound is anchored to the hinge through three hydrogen bonds between the aminoindazole moiety and the backbone of residues Glu590 and Met592 (Glu1197 and Met1199 in ALK). The difluorobenzyl-indazole core creates favorable contacts with Ala542, Leu657 (Leu1256, and Val1130 in ALK), and the gatekeeper Phe589 (Leu1196 in ALK).[148] Moreover, the 3,5-difluorobenzyl moiety is involved in multiple interactions with the backbone carbonyls of Asp668 from the DFG motif (Asn1254 and Gly1269 in ALK). The central phenyl ring makes a hydrophobic contact with Leu516 (Leu1122 in ALK);

while the methylpiperazine is oriented towards the solvent front. In order to optimally fill the sugar pocket, the partially solvent-exposed tetrahydropyranyl moiety adopts a roughly orthogonal orientation with respect to the scaffold.[148]

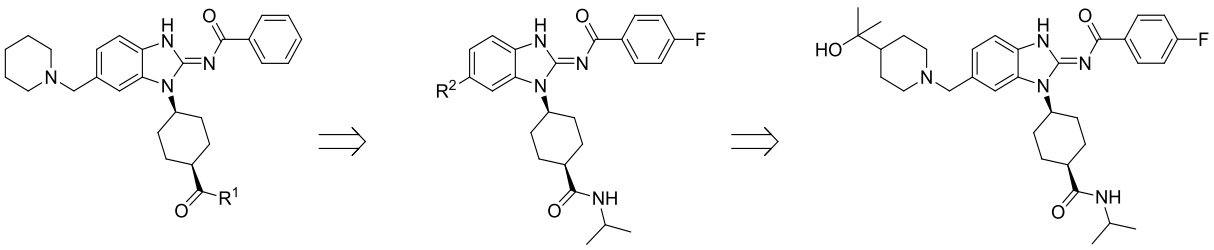

5: R^1=OMe;
5-1a: R^1=OEt;
5-1b: R^1=NHEt;
5-1c: R^1=N(Et)$_2$;
5-1d: R^1=NH$_2$;
5-1e: R^1=NH^{i}Pr;

5-2a, R^2=H;
5-2b, R^2=pyridin-2-yloxy;
5-2c, R^2=(4-(aminomethyl)piperidin-1-yl)methyl;
5-2d, R^2=(4-(carboxylic acid)piperidin-1-yl)methyl;

5-3 (Belizatinib, TSR-011)

Figure 9. Structural optimization from compound **5** to **5-3**.

Another drug discovery campaign centered on ALK serendipitously uncovered **5-3** (**Belizatinib**, **TSR-011**), a novel, potent TRK inhibitor (Figure 9).[152] Through HTS (high-throughput screening), Lewis *et al.* identified the ALK inhibitor **5** (ALK kinase IC_{50} = 0.003 μM, pALK cell IC_{50} = 0.054 μM; 64-fold, 103-fold, 15-fold selectivity over JAK2, SRC, and IGF1R, respectively),[152] which was co-crystalized with ALK (Figure 10A).[152] Through the benzoyl carbonyl oxygen and the benzimidazole NH, **5** was shown to bind to the hinge of ALK at Met1199 and the benzoyl ring was adjacent to the gatekeeper residue Leu1196. The *cis*-1,4 geometry of the cyclohexyl group pushes the methyl ester moiety into a hydrophobic pocket surrounded by Leu1256 and Gly1269. The piperidine moiety engages in Van der Waals interactions with two backbone carbonyls on the N-terminal lobe (Gly1121, Leu1122) in a shallow pocket on the surface of the protein at the entrance to the ATP binding pocket.[152]

To improve cell potency, selectivity, and metabolic stability, SAR optimization was completed. First, the methyl ester was replaced with different esters and amides (compounds **5-1a** to **5-1e**). The isopropyl amide compound **5-1e** displayed the best combination of activity and selectivity (ALK kinase IC_{50} = 0.002 μM, pALK cell IC_{50} = 0.054 μM; 813-fold, 429-fold, 36-fold selectivity over JAK2, SRC, and IGF1R, respectively).[152] To improve metabolic stability, a wide variety of modifications were investigated at the R^2 position. Figure 9 depicts some of these modifications, and the tertiary alcohol analogue **5-3** appeared optimal. Finally, different substitutions were introduced to the 4-fluoro phenyl ring; however, these derivatives either decreased selectivity or suffered from compromised cellular activity against

ALK.[152] When screening **5-3** against a kinase panel, **5-3** was found to have potent pan-TRK activity (IC_{50} for TRKA/B/C < 0.003 μM).[153] Currently, **5-3** is under a Phase 1/2 study in patients with advanced solid tumors and lymphomas. (NCT02048488).

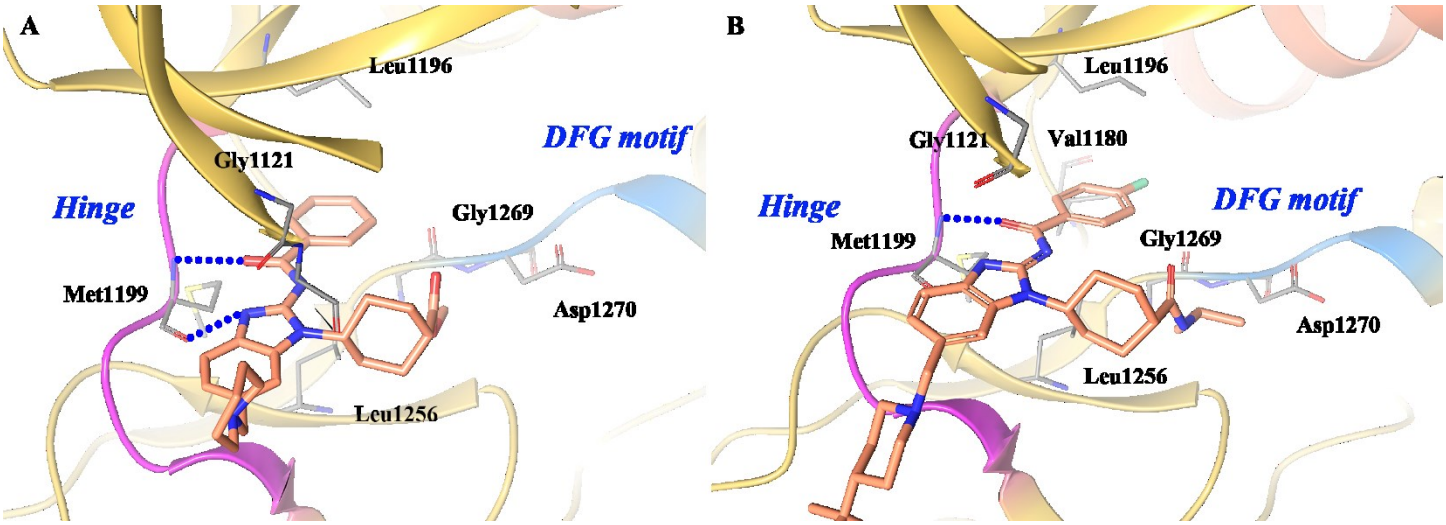

Figure 10. (A) Co-crystal structure of compound **5** in ALK (PDB ID: 4FOC, 1.7 Å); (B) Co-crystal structure of compound **5-3** in ALK (PDB ID: 4FOD, 2 Å). The kinase is depicted in yellow ribbons, and the hydrogen bonds are illustrated in blue dashed lines.

The co-crystal structure of **5-3** with ALK (Figure 10B) shows that **5-3** binds similar to **5** (Figure 10A).[152] Compound **5-3** pushes into the active site of the kinase in a pocket formed by Val1180 and Leu1256, and is in close proximity to the gatekeeper residue Leu1196. The iminobenzamide moiety adopts the exocyclic acylimine tautomer permitting key hydrogen bonding interactions with the hinge region residue Met1199. This tautomer is favored by extended π-delocalization into the pendant aryl ring, achieved by retaining a coplanar arrangement between benzamide and benzimidazole moieties.[152]

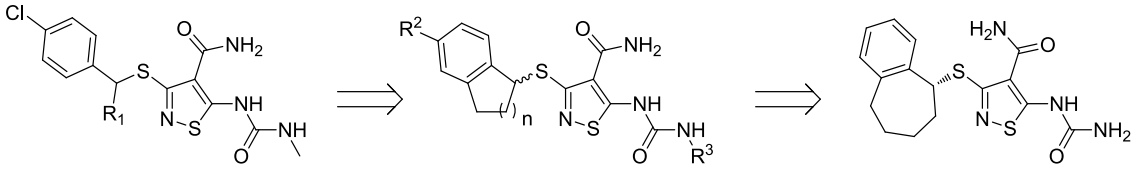

6: R^1=H;
6-1a: R^1=Me;
6-1b: R^1=(*R*)-Et;
6-1c: R^1=(*S*)-Et;
6-1d: R^1=^{n}Pr;
6-1e: R^1=Ph;

6-2a: R^2=Cl, R^3=H, n=1;
6-2b: R^2=Cl, R^3=Me, n=1;
6-2c: R^2=H, R^3=H, n=2;
6-2d: R^2=H, R^3=Me, n=2;
6-2e: R^2=H, R^3=H, n=3;
6-2f: (*S*) R^2=H, R^3=H, n=3

6-3 (Cpd5n)

Figure 11. Structural optimization from compound **6** to **6-3**.

Isothiazole derivatives have been identified as TRK inhibitors (Figure 11). From an HTS campaign directed at TRKA, Lippa *et al.* identified compound **6** (TRKA IC_{50}= 0.007 μM).[154] Initial SAR studies at R^1 determined that substitution at the benzylic α-position remarkably influenced TKRA activity and VEGFR2 selectivity. Small aliphatic chains were well tolerated (**6-1a**, **6-1b**, TRKA IC_{50}s were 0.003 μM and 0.004 μM, respectively), while larger substitutions significantly diminished activity (**6-1d**, **6-1e**, TRKA IC_{50}s were 0.035 μM and 2.6 μM, respectively).[154] The orientation of the R^1 substitution also played a key role: the (*R*)-ethyl enantiomer **6-1b** was >10-fold more active (TRKA IC_{50}, 0.004 μM *vs* 0.052 μM) and was >100-fold more selective (VEGFG2 selectivity, 1,300X *vs* 10X) than the (*S*)-enantiomer. SAR at R^2 and R^3 showed that substitution at these two positions are not necessary to maintain TRK activity (**6-2a to 6-2d**, TRKA IC_{50}s were 0.01 μM, 0.008 μM, 0.105 μM and 0.111 μM, respectively).[154] Further optimization identified that bicyclic moieties were important for TRK activity, especially the 7-membered ring system (compound **6-2e**, TRKA IC_{50}< 0.001 μM) and, consistent with previous data, the (*R*)-enantiomer was more active (**6-3** *vs* **6-2f**, TRKA IC_{50}s were <0.001 μM *vs* 0.091 μM,). Compound **6-3** (**Cpd5n**) had pico-molar kinase potency and single-digit nanomolar activity against TRK-driven cell growth.[154]

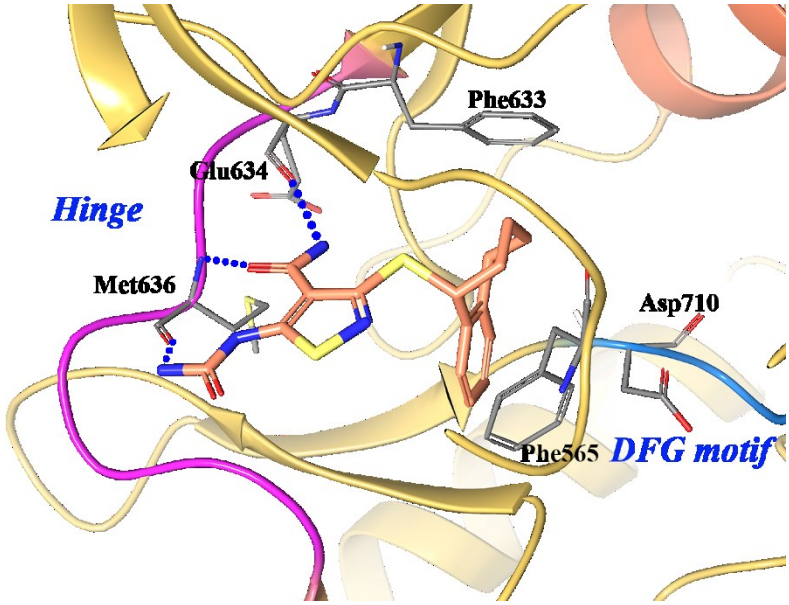

Figure 12. Co-crystal structure of compound **6-3** in TRKB (PDB ID: 4AT3, 1.77 Å). The kinase is depicted in yellow ribbons, and the hydrogen bonds are illustrated in blue dashed lines.

The co-crystal complex of **6-3** in TRKB was obtained and is shown in Figure 12.[73] The aliphatic portion of **6-3** is oriented towards the glycine-rich loop and exhibits clear, Type I binding.[73] The glycine-rich loop forms a cage around the inhibitor and engages in strong, hydrophobic interactions through Phe565. The urea and amide groups on the thiazole bind to the hinge of TRKB, forming three hydrogen bonds. The benzo-cycloheptene group is sandwiched between the gatekeeper Phe633 and glycine-rich loop Phe565 side chains, likely contributing to the stabilization of the TRKB DFG-in conformation.[73] This also explains the potency differences between the two enantiomers as the *S*-enantiomer could still bind the hinge but would clash with Phe565 due to difference in stereochemistry of the benzo-cycloheptene. The affinity of **6-3** for TRKB is also enhanced by several water-bridged hydrogen bonds between the inhibitor and the kinase.[73]

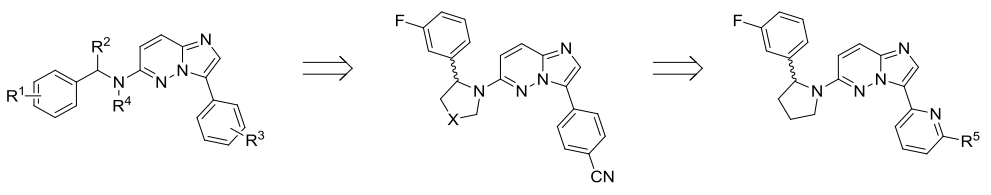

7: R^1=H, R^2=H, R^3=4-CN, R^4=H;
7-1a: R^1=H, R^2=H, R^3=3-CN, R^4=H;
7-1b: R^1=3-F, R^2=H, R^3=4-CN, R^4=H;
7-1c: R^1=3-F, R^2=H, R^3=N-methyltetrahydro-2H-pyran-4-carboxamide, R^4=H

7-2a: (racemic) X= CH_2CH_2;
7-2b: (racemic) X= OCH_2;
7-2c: (racemic) X= CH_2;
7-2d: (*S*) X= CH_2;
7-2e: (*R*) X= CH_2

7-3a: (racemic) R^5= H;

7-3b: (**GNF-8625**) (*R*) R^5=

Figure 13. Structural optimization from compound **7** to **7-3b**.

In another campaign to uncover novel TRK inhibitors, Choi *et al.* developed a series of substituted imidazopyridazine derivatives from compound **7** (TRKB IC_{50} = 0.083 μM) (Figure 13).[155] The crystal complex of **7** with TRKC (Figure 14A) shows that the ligand binds to the inactivated (DFG-out) form of the kinase and the imidazopyridazine warhead engages in a hydrogen bond at the hinge with Met620. The benzonitrile ring is wedged between Phe617 and Phe698, and the phenyl ring sits under the glycine-rich loop and faces the solvent front of the active site.[155]

Preliminary medicinal chemistry efforts focused SAR studies at R^1 to R^4, with the goal of identifying compounds with improved potency and pharmacokinetic properties suitable for in *vivo* profiling. Nitrile substitutions in the phenyl group (R^3) at the 3- or 4-position were equally tolerated (**7** *vs* **7-1a**, TRKA cell IC_{50}s = 0.85 μM and 0.74 μM). It was also observed that 3-substitution at the benzylamine phenyl ring (R^1) led to a 10-fold increase in potency (**7-1b**, TRKA cell IC_{50} = 0.076 μM).[155] Modifying the phenyl ring (R^3) with 3-F substitution at R^1 furnished many tolerated functional groups that could either increase solubility or further drive potency (i.e. compound **7-1c**, TRKA cell IC_{50} = 0.006 μM). Methylation of the benzylic amine (R^3) led to no significant change in potency indicating that the acidic proton on the benzylic amine does not hydrogen bond with TRK.[155] Cyclizing the benzyl amine moiety with the adjacent phenyl ring was performed to rigidify the structure and reduce conformational entropy. The fused, five-membered ring system was optimal for TRK inhibition and exhibited a preference for the *R*-enantiomer (**7-2a** to **7-2e**, TRKA cell IC_{50}s = 0.17 μM, 0.075 μM, 0.068 μM, 3.13 μM, and 0.021 μM, respectively). Derivatization at R^5 led to the discovery of the optimized compound **7-3b** (**GNF-8625**).[155] Compound **7-3b** demonstrated potent, antiproliferative activity against TRK transfected Ba/F3 and KM-12 cell lines (IC_{50} = 0.001 μM and 0.01 μM, respectively). In a KM-12-derived tumor xenograft, compound **7-3b** demonstrated antitumor efficacy in a dose dependent manner, inducing 20% tumor regression at a dose of 50 mg/kg BID.[155]

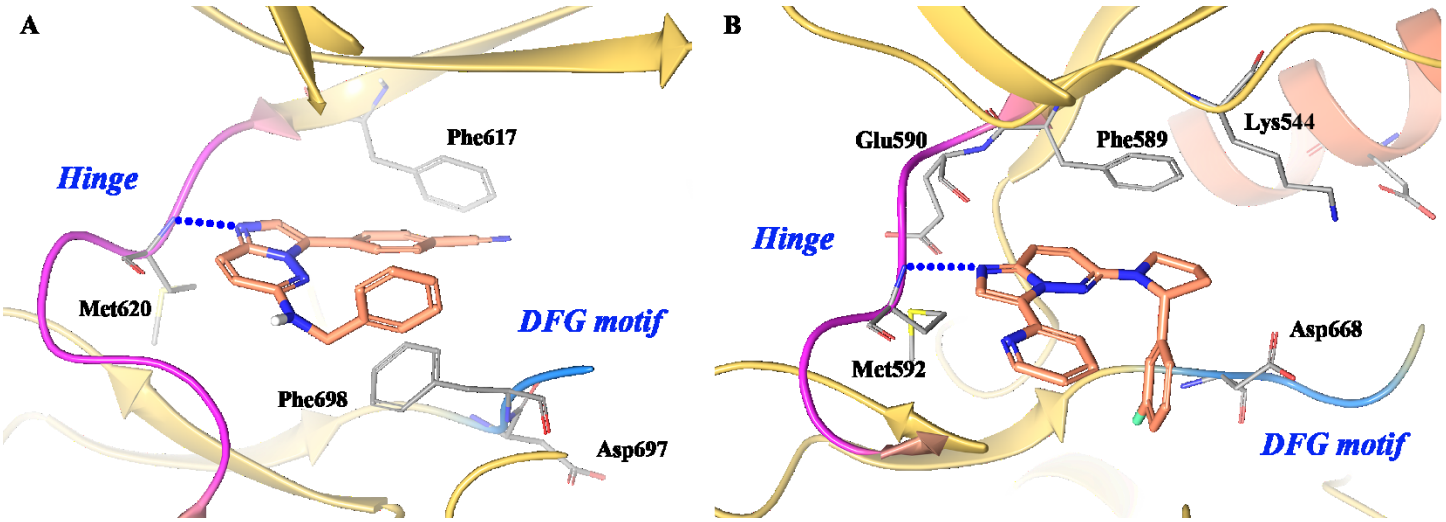

Figure 14. (A) Co-crystal structure of compound **7** in TRKC (PDB ID: 4YMJ, 2 Å); (B) Co-crystal structure of compound **7-3a** in TRKA (PDB ID: 4YNE, 2.02 Å). The kinase is depicted in yellow ribbons, and the hydrogen bonds are illustrated in blue dashed lines.

Imidazopyridazines are frequently incorporated into kinase inhibitors as they readily form a hydrogen bond at the hinge with the C-6 carbon oriented towards the solvent.[156] The warhead of **7-3a** is based on imidazopyridazine and was expected to bind TRKA akin to **7**. Surprisingly, the co-crystal structure of **7-3a** with TRKA revealed an unexpected 180° rotation of the imidazopyridazine core at the hinge (Figure 14B).[155] Only the (*R*)-enantiomer of **7-3a** is active because the 3-F-phenyl is optimally positioned downwards in the hydrophobic pocket. The moiety fills a pocket endogenously occupied by Phe669 and provides excellent shape complementary, likely contributing to increased affinity. Molecular modeling and crystallography studies indicated that two distinct binding modes exist (i.e. core flipping) with scaffold **7**.[155] Based on the different TRK co-crystal structures obtained with **7** and **7-3a**, it was concluded that the preferred binding mode depends on C-6 substitution. If the C-6 substitution is modified to (*R*)-phenylpyrrolidine, the "flipped" orientation is preferred as the pyrrolidine anchors the phenyl group in the hydrophobic pocket.[155] The phenomenon of 'core flipping' could be employed to generate compounds with activity in multiple kinase families. Based on the crystal structure, compound **7-3a** is a Type I kinase inhibitor.

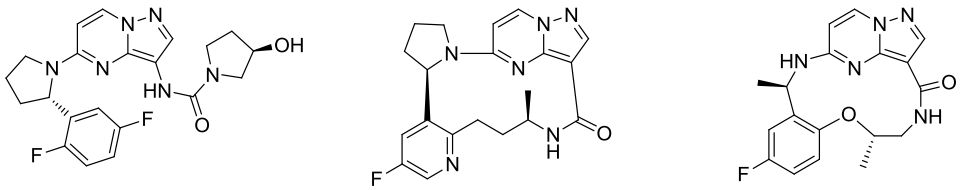

Figure 15. Chemical structures of compound **8**, and second generation TRK inhibitors **9** and **10**.

Compound **8** (**Larotrectinib**, **LOXO-101**) is another selective, pan-TRK inhibitor exhibiting low nanomolar cellular potency against the TRK family (IC_{50} ranging from 0.002 μM to 0.02 μM) with 100-fold selectivity over other kinases (Figure 15).[49, 157] The compound can induce cell-cycle arrest in the G1 phase and apoptosis in KM-12 cells.[49] Compound **8** is currently in a Phase 2, open-label study for patients with advanced solid tumors harboring a fusion of TRKA, TRKB, or TRKC (NCT02576431).[48] The medicinal chemistry effort leading to the discovery of this compound and its co-crystal complex with TRK have not been reported. However, because of the structure similarities between compounds **8** and **7-3b**, it can be inferred that **8** exhibits similar SAR properties to that of **7-3b**.

Second Generation Type I TRK Inhibitors

All first generation TRK inhibitors exhibit profound, upfront efficacy but eventually lose effectiveness due to the development of secondary mutations in the TRK kinase domain. After treatment with **8** or **4-3** mutations in the TRK kinase domain have been reported,[158] which renders further treatment ineffective.[47, 159] These mutations include $TRKA^{G595R}$ (and its paralogue $TRKC^{G623R}$) in the solvent front of the active site, $TRKA^{G667C}$ (and its paralogue $TRKC^{G696A}$) adjacent to the DFG motif, and $TRKA^{F589L}$ at the gatekeeper region.[47, 99, 159-161] $TRKA^{G595R}$ and $TRKA^{G667C}$ are analogous to ALK^{G1202R} and ALK^{G1269A}, respectively.[159] In TRKA, the native residues are important to accommodate **8** and **4-3**, while the mutations create steric clashes with the inhibitors. In addition, $TRKA^{G595R}$ increases ATP affinity to the kinase.[159] Structural modeling suggests that each mutation directly interferes with binding of **8**, **4-3**, and all other TRK tyrosine kinase inhibitors.[47, 160] Functional studies have subsequently confirmed that cancer cells harboring these mutations are cross-resistant to all TKIs with anti-TRK activity.[162-163]

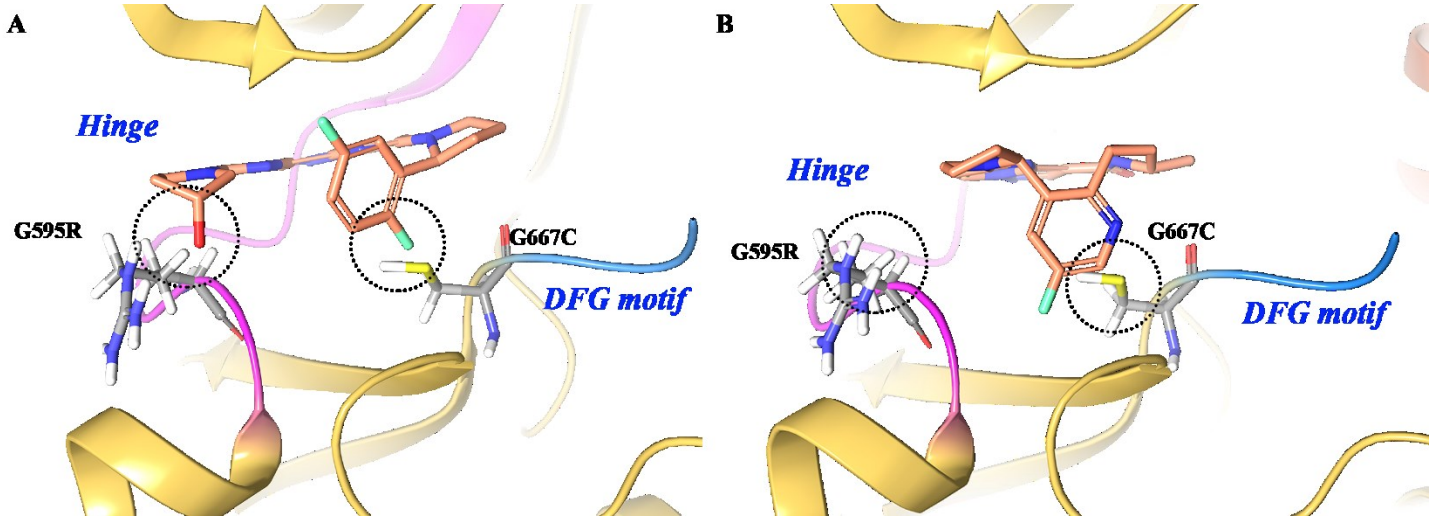

Figure 16. (A) Proposed binding and steric interactions of **8** with the TRKA double mutant G595R and G667C, (B) Proposed binding of **9** to the TRKA double mutant; steric interactions are not predicted between G595R and G667C. The kinase is depicted in yellow ribbons.[164]

To generate inhibitors that could overcome point mutations in TRK, compounds **9** (**LOXO-195**) and **24** (**TPX-0005**) were designed to limit the compound surface area in the active site. (Figure 16). Both compounds were designed as fused macrocycles to reduce unnecessary interactions at either end of the binding pocket. Modelling suggested that TRKA^{G595R} would introduce steric clashes between the arginine side chain and the hydroxypyrrolidine group of **8**, and TRKA^{G667C} would create steric clashes between the cysteine or alanine side chain and the difluorophenyl group of **8** (Figure E).[159] To determine the impact of TRK kinase mutations on inhibitor activity, **8** and **9** were tested against TRKA^{G595R}, TRKA^{G667C}, and TRKC^{G623R}. Compound **9** achieved low nanomolar inhibitory activity against all mutated kinase (IC_{50}s = 0.002 μM, 0.00098 μM, and 0.0023 μM); while compound **8** displayed significantly reduced inhibitory activity (IC_{50}s = 0.069 μM, 0.045 μM, and 0.048 μM).[159] An innovative first-in-human clinical trial has demonstrated efficacy of compound **9** in 2 patients who had developed acquired resistance to **8** mediated by secondary TRKA^{G595R} or TRKA^{G623R} mutations.[159] Compound **10**, an analogue to **9**, potently inhibited ROS1^{G2032R} (IC_{50} = 0.0084 μM), TRKA^{G595R} (IC_{50} = 0.0004 μM), TRKB^{G639R} (IC_{50} = 0.0019 μM) and TRKC^{G623R} (IC_{50} = 0.0004 μM).[165] **10** also exhibited activity in xenograft tumor models bearing WT and kinase domain mutations of ALK, ROS1 and TRKA.[165-166]

Other Type I TRK Inhibitors

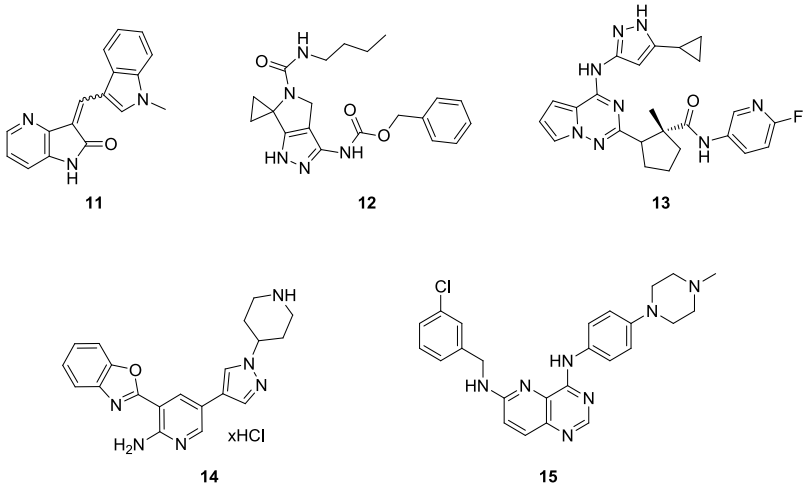

Figure 17. Chemical structures of other Type I TRK inhibitors

Several other TRK scaffolds have been reported that exhibit Type I characteristics and are summarized in the following section (Figure 17). Aza-oxindole and oxindoles were reported as potent TRK inhibitors by Wood *et* al.[167] The representative compound **11** exhibited pan-TRKA inhibitory activity (TRKA/B/C IC_{50}s = 0.030 μM, 0.007 μM, 0.005 μM, respectively) with selectivity in the greater kinome but also inhibited VEGFR2 (vascular endothelial growth factor receptor 2).[167-168] Compound **11** shares similarities in structure to other known VEGFR2 inhibitors, such as sunitinib, which likely accounts for its VEFGR2 profile.[167] Choe *et al.* reported a series of pyrrole[3,4-*c*]pyrazole TRKA inhibitors (Figure 17). The representative compound **12** inhibits TRKA with an IC_{50} of 0.019 μM. SAR studies indicated that the cyclopropyl and benzyl carbamate groups are essential for potency and removal of either resulted in a loss of activity.[169] Carboni *et al.* developed compound **13** as a dual IGF-1R/IR inhibitor (IC_{50} = 0.0018 μM and 0.0017 μM, respectively). Kinase profiling showed that compound **13** was active on several other kinases, including TRKA/B (IC_{50}s = 0.007 μM and 0.004 μM, respectively).[170] Cho *et al.* developed compound **14** as a c-MET inhibitor based on an aminopyridine core substituted with benzoxazole (IC_{50} = 0.08 μM).[171] Compound **14** was later identified to have activity against the mutant c-MET^{Y1230D} kinase (IC_{50} = 0.003 μM) and TRKA (IC_{50} = 0.039 μM).[172] Stachel *et al.* reported a series of pyrido[3,2-*d*]pyrimidine as TRKA inhibitors; the representative compound **15** had a TRKA IC_{50} of 0.011 μM and moderate cell activity (IC_{50}=1.688 μM).[173]

Radiolabeled Type I TRK Inhibitors

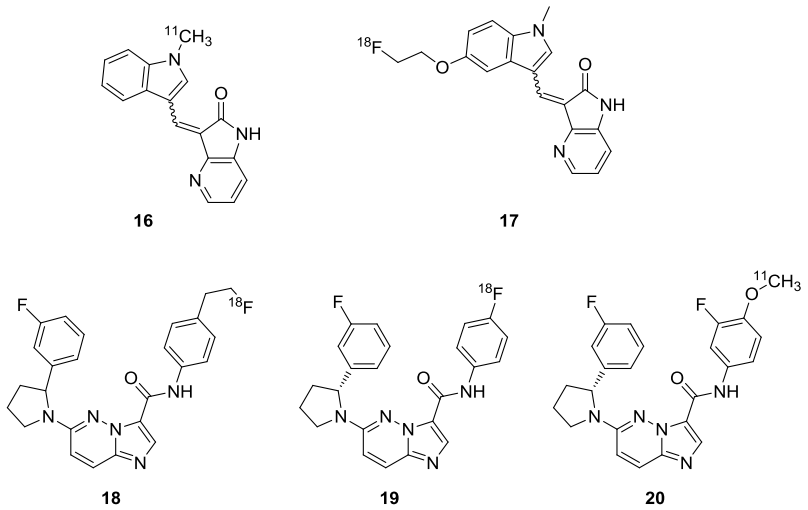

Figure 18. Chemical structures of representative radiolabeled Type I TRK Inhibitors.

Positron emission tomography (PET) is a non-invasive *in vivo* imaging technique that enables the visualization and quantification of the distribution of molecules labeled with positron-emitting isotopes. This method enables the evaluation of biochemical and physiological processes by monitoring the distribution and kinetics of a labeled molecule *in vivo*, and has found broad application in clinical practice (personalized treatments), research, and pharmaceutical development.[174-177]

Because of the clinical importance of TRK in cancer as well as the central nervous system, Bernard-Gauthier *et al* generated radiolabeled TRK ligands to assess and monitor TRKA/B/C levels in the brain. The TRK ligands were synthesized from known inhibitors using ^{11}C- or ^{18}F-labeled PET radiotracers suitable for *in vivo* imaging (compounds **16-20**) (Figure 18).[168, 178-182] These compounds demonstrated comparable activity and selectivity profiles to the unlabeled precursor.[180] Compound **16** displayed excellent TRK selectivity in a panel of brain and cancer relevant kinases and TRK-specific binding *in vitro* in rat brain and human neuroblastoma cryosections. The radio-compound also exhibited uniform regional brain distribution but was highly susceptible to CYP450 metabolism.[168] Nevertheless, TRK radio-compounds can prove instrumental in studying TRK biology, diagnosing TRK-positive disease, and determining drug disposition of TRK inhibitors in real time.[175, 177] It is worth noting that compound **19** was the first TRK radiotracer clinical lead involved in a non-human primate imaging study;[182] compound **20** was the first reported radiotracer used as an *in vivo* probe to explore endogenous kinase densities using PET neuroimaging in humans.[181]

Type II TRK Inhibitors

Type I TRK inhibitors are ATP competitive and typically possess pan-kinase activity. A method to increase kinase selectivity and potency is to generate inhibitors that bind in a Type II fashion.[183] Type II inhibitors are generally more active against tyrosine kinases, which can be exploited to increase selectivity and potency profiles.[184] TRK inhibitors that display Type II binding kinetics can be preferred depending on the biology being studied or the disease being treated. It is important to note that the most advanced TRK inhibitors in clinical trials are Type I (**8** and **4-3**). These inhibitors are being evaluated for anticancer properties and may have inhibition characteristics optimal for a tumor environment. In other therapeutic areas, such as the central nervous system (CNS) or pain management, TRK inhibitors with a Type II profile maybe preferred because, as a class, they are more selective than Type I inhibitors.[184] However, the typically larger molecular architecture of Type II compounds can cause less favorable drug-like properties, leading to development challenges. In the following section, the development of Type II TRK inhibitors is disclosed, and developmental efforts were primarily focused on optimizing for anticancer properties.

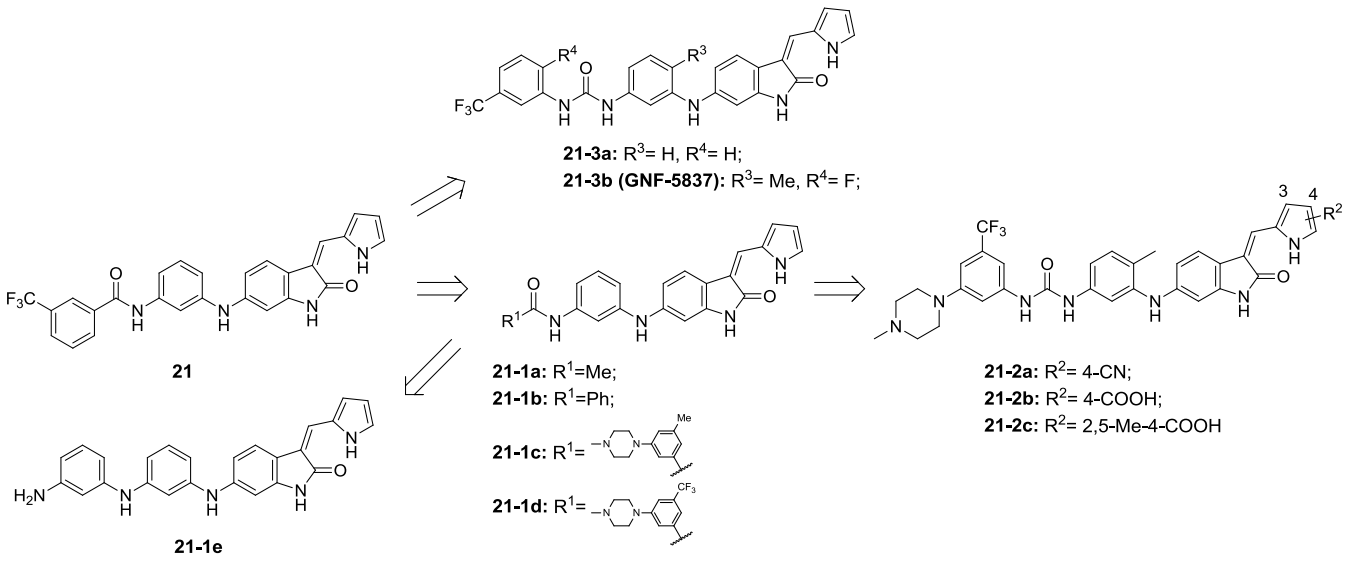

Figure 19. Structural optimization from compound **21** to **21-3b** (**GNF-5837**).

Albaugh *et al* identified Type II TRK inhibitors based on an oxindole-core (Figure 19).[185] Oxindole **21** inhibited Ba/F3-Tel-TRKA/B/C with IC_{50}s less than 0.06 μM. SAR studies at the R^1 position showed that the phenyl ring is critical for TRK specific inhibitory activity (**21-1a** *vs* **21-1b**, TRKA cell IC_{50}: 2.3 μM *vs* 0.91 μM).[185] To improve drug properties,

several basic groups were introduced at the terminal phenyl ring and were well tolerated and increased potency, but did not improve solubility. Substituting the aryl ring with 3-CF_3 at R^1 is crucial for TRK activity (**21-1c** and **21-1d,** TRKA cell IC_{50}: 0.39 μM and 0.013 μM 0.39 μM, respectively). Truncating the amide group to aniline resulted in a total loss of activity, indicating the amide is necessary for TRK activity (**21-1e**, TRKA cell IC_{50}> 10 μM).[185] Replacement of the pyrrole with other groups or methylation of the pyrrole nitrogen yielded significantly less potent compounds suggesting that the acidic proton on pyrrole is involved in a key hydrogen bond at the hinge region. Substitution on the pyrrole showed that carbolic acid at position 4 is preferred for potency and selectivity, with or without methyl substitution (**21-2a** to **21-2c,** TRKA cell IC_{50}: 0.014 μM, 0.01 μM, and 0.012 μM; selectivity: 43-fold, 150-fold and 108-fold, respectively).[185] Replacement of the amide with urea generated compounds with increased potency and selectivity over VEGFR2 (**21-3a**, TRKA cell IC_{50}= 0.004 μM, selectivity 130-fold).[185] Introduction of a methyl substitution at R^3 and a fluorine at R^4 generated compound **21-3b** (**GNF-5837**), which exhibits pan-TRK inhibition (TRKA/B/C IC_{50}s = 0.011μM, 0.009μM, 0.007 μM, respectively) and about 300-fold selectivity over VEGFR2 (IC_{50} = 3.0 μM). In BALB/c mice and Sprague–Dawley rats, compound **21-3b** demonstrated low drug clearance and moderate bioavailability. In mice bearing RIE xenografts expressing TRKA and NGF, compound **21-3b** (100 mg/kg/d P.O.) significantly inhibited tumor growth.[185]

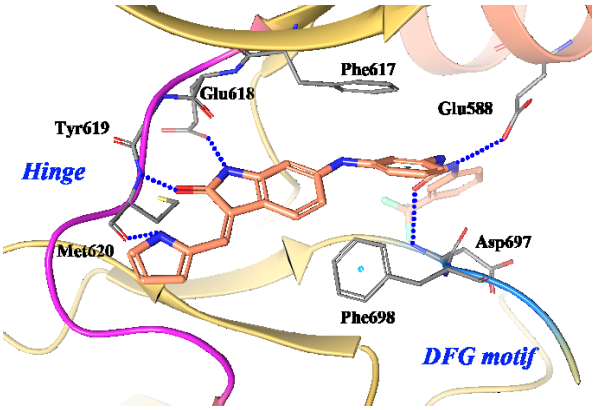

Figure 20. Co-crystal structure of compound **21-3a** in TRKC (PDB ID: 3V5Q, 2.2 Å). The kinase is depicted in yellow ribbons, and the hydrogen bonds are illustrated in blue dashed lines.

In the co-crystal structure of **21-3a** with TRKC (Figure 20), **21-3a** is found to bind to the kinase in a Type II manner.[185] The oxindole core and pyrrole nitrogen form key hydrogen bonds with hinge residues Glu618, Tyr619, and Met620. The urea functionality interacts with Glu588 from the α-C-helix and Asp697 from the DFG motif. In addition,

interactions occur at the phenyl bridge with Phe617 (gatekeeper) and a face to edge interaction with Phe698 from the DFG motif.[185]

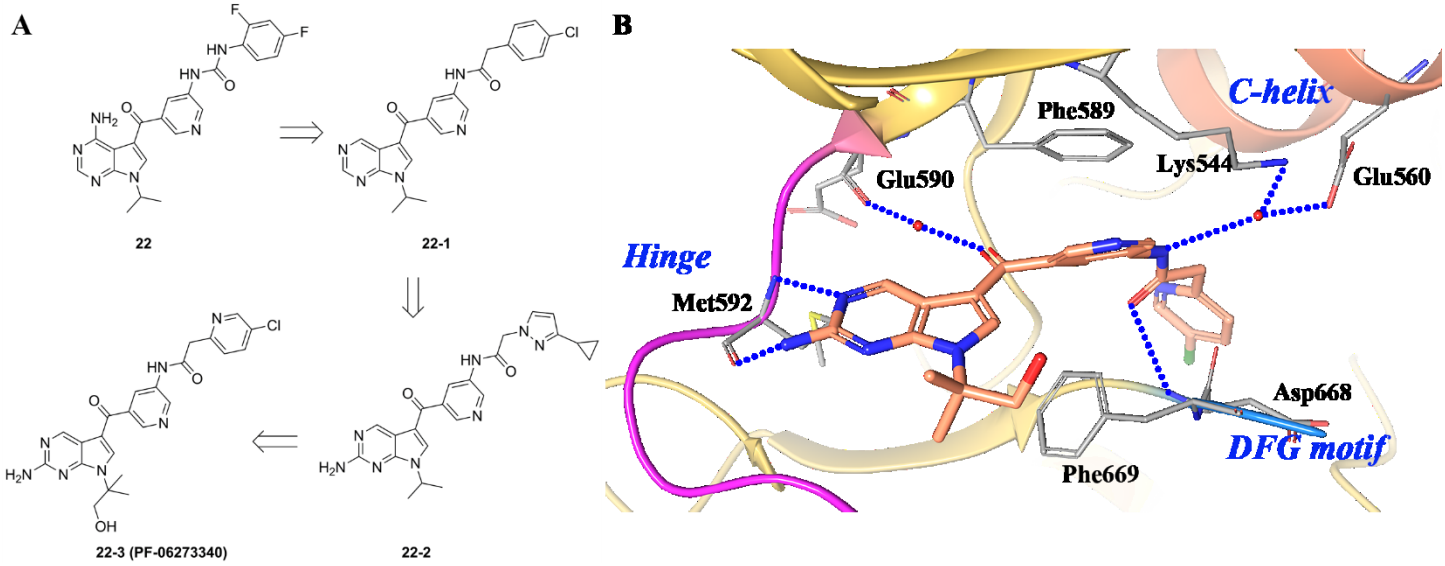

Figure 21. (A) Structural optimization from compound **22** to **22-3**; (B) Co-crystal structure of compound **22-3** with TRKA (PDB ID: 5JFX, 1.63 Å). The kinase is depicted in yellow ribbons, and the hydrogen bonds are illustrated in blue dashed lines.

Skerratt *et al.* reported a series of pyrrolopyrimidine derivatives as pan-TRK inhibitors (Figure 21A).[186] By employing a high-throughput TRKA/B cell screening assay, compound **22** was identified as a pan-TRK inhibitor (TRKA/B/C IC_{50}s = 0.002 μM, 0.005 μM, and 0.004 μM, respectively) with strong kinome selectivity but poor water solubility (< 0.3 μM).[186] To improve solubility, the urea group was replaced with an amide and the 4-NH_2 was removed to generate compound **22-1** (TRKA/B/C IC_{50}s = 0.012 μM, 0.004 μM, and 0.003 μM, respectively) with improved water solubility (~13.2 μM).[186] It was determined that the scaffold was likely metabolized by aldehyde oxidase and inhibited hERG (human Ether-à-go-go-Related Gene) potassium heart channels.[187-188] In order to reduce metabolic liabilities and off target toxicities, an amino group was added at the 2-position furnishing compound **22-2** (TRKA/B/C IC_{50}s = 0.008 μM, 0.005 μM, and 0.004 μM, respectively; solubility = 30 μM).[186] To further improve physical-chemical properties and aqueous solubility, a hydrophilic hydroxymethylene group was added to N-^{i}Pr motif and the terminal ring was replaced with pyridine to obtain compound **22-3** (**PF-06273340**). Compound **22-3** was a potent pan-TRK inhibitor (TRKA/B/C

IC_{50}s = 0.006 μM, 0.004 μM, and 0.003 μM, respectively; solubility= 131 μM) and exhibited selectivity over a large kinase panel.[186] Currently, Phase 1 clinical trials are ongoing to examine the activity of different doses of **22-3** on a panel of evoked pain tests in healthy male subjects (NCT02260947).

Figure 21B shows the co-crystal structure of **22-3** bound to TRKA and highlights key protein−ligand interactions.[186] Compound **22-3** binds to the DFG-out form of TRK, with the 2-aminopyrrolopyrimidine forming hydrogen bonds at the hinge and the ketone binding to Glu590 through a water contact.[186] Most kinase inhibitors engage in one or two interactions at the hinge, while **22-3** is found to engage in three. The central pyridine group of **22-3** engages in a double π-π stacking interaction with Phe589 (gatekeeper residue) and Phe669 (DFG motif). The carbonyl oxygen forms a hydrogen bond with the amide backbone of Asp668 (DFG motif) and the amide engages TRKA through a water contact between Lys544 and Glu560 from the c-Helix. The lipophilic back pocket accommodates the chloropyridine group.[186] Based on the binding characteristics of **22-3**, the inhibitor can be considered Type II.

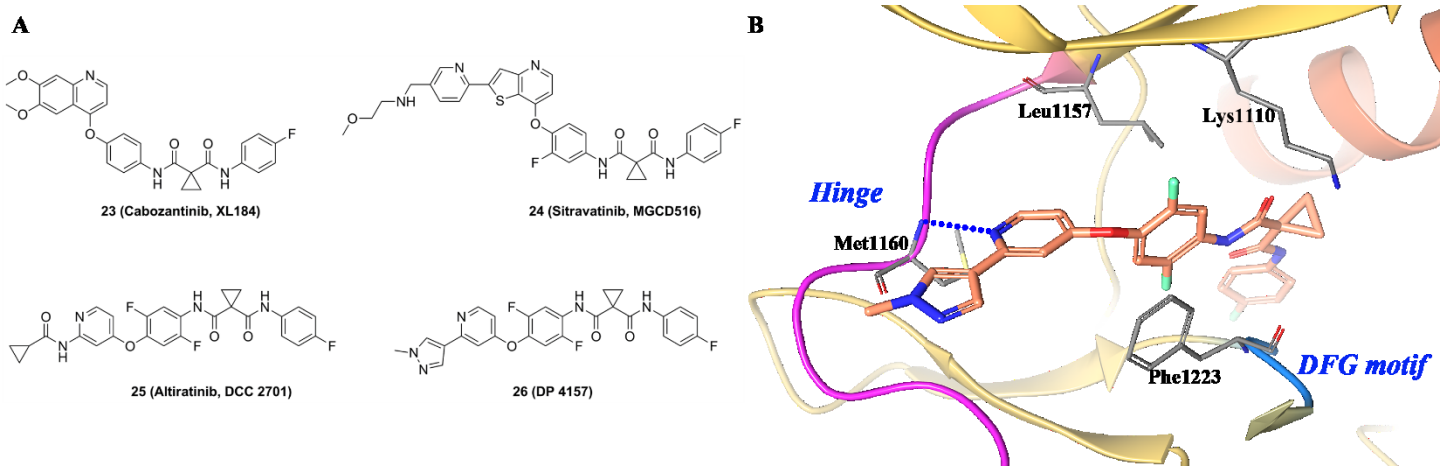

Figure 22. (A) Chemical structures of representative dicarboxamide TRKA inhibitors; (B) Co-crystal structure of compound **26** in c-MET (PDB ID: 5DG5, 2.6 Å). The kinase is depicted in yellow ribbons, and the hydrogen bonds are illustrated in blue dashed lines.

Compound **23** (**Cabozantinib**, **XL184**) is a multiple kinase inhibitor with activity against c-MET/VEGFR2 and was found to have a potent TRKB inhibitory activity (IC_{50} < 0.02 μM) (Figure 22A).[189] Compound **23** is currently under Phase 2 clinical trials in patients with RET fusion-gene non-small cell lung cancer and those with other activating genes,

such as ROS1, NTRK, MET or AXL (NCT01639508). Compound **24** (**Sitravatinib**, **MGCD516**) was developed by Patwardhan *et al.* as a potent multi-kinase inhibitor (Figure 22A) active against several kinases (IC_{50}s for AXL: 0.0015 μM, VEGFR2: 0.005 μM, FLT3: 0.008 μM, c-KIT: 0.006 μM, TRKA: 0.005 μM, and TRKB: 0.009 μM). Compound **24** blocked phosphorylation of several RTKs and induced potent anticancer effects *in vitro*; the compound was also active *in vivo* in MPNST (neurosarcoma) and LS141 (hybridoma) mouse xenograft models.[190] Compound **24** is currently under Phase 1 clinical development for patients with advanced solid tumor malignancies (NCT02219711). Compound **25** (**Altiratinib**, **DCC2701**) was reported by Smith *et al.* as a multi-targeted kinase inhibitor with preferential activity on MET, TIE-2, and VEGFR2 (IC_{50}s = 0.0027 μM, 0.008 μM, and 0.0092 μM, respectively) (Figure 22A). Subsequently, **25** was identified to exhibit activity as a pan-TRK inhibitor (TRKA/B/C IC_{50}s = 0.00085 μM, 0.0046 μM, and 0.0083 μM, respectively) and FLT3 inhibitor (IC_{50} 0.0093 μM).[191] In cell antiproliferative assays, compound **25** exhibited IC_{50}s of 0.00069 μM in K562 cells, 0.0012 μM in SK-N-SH cells, and 0.0014 μM in KM-12 cells. Compound **25** inhibited tumor growth in the MET-amplified MKN-45 xenograft model in a dose-dependent manner. Further, compound **25** can actively penetrate the blood-brain-barrier, indicating its potential for the treatment of brain cancers, brain metastases, and cancer pain. Compound **25** is currently under Phase 1 clinical development for patients with advanced solid tumors with NTRK or MET genomic alterations (NCT02228811).

Figure 22B illustrates the general Type II binding mode of the dicarboxamide kinase inhibitor class.[191] The pyridine of **26** (**DP4157**) binds to the hinge region and forms a hydrogen bond with Met1160. The central di-fluoro phenyl ring is in a hydrophobic pocket formed by Lys1110, Leu1157 and Phe1223, and engages in a π-π stacking interaction with Phe1223. The terminal para-fluoro phenyl ring binds in the allosteric pocket between the DFG motif and α-C-helix.[191]

Other Type II TRK Inhibitors

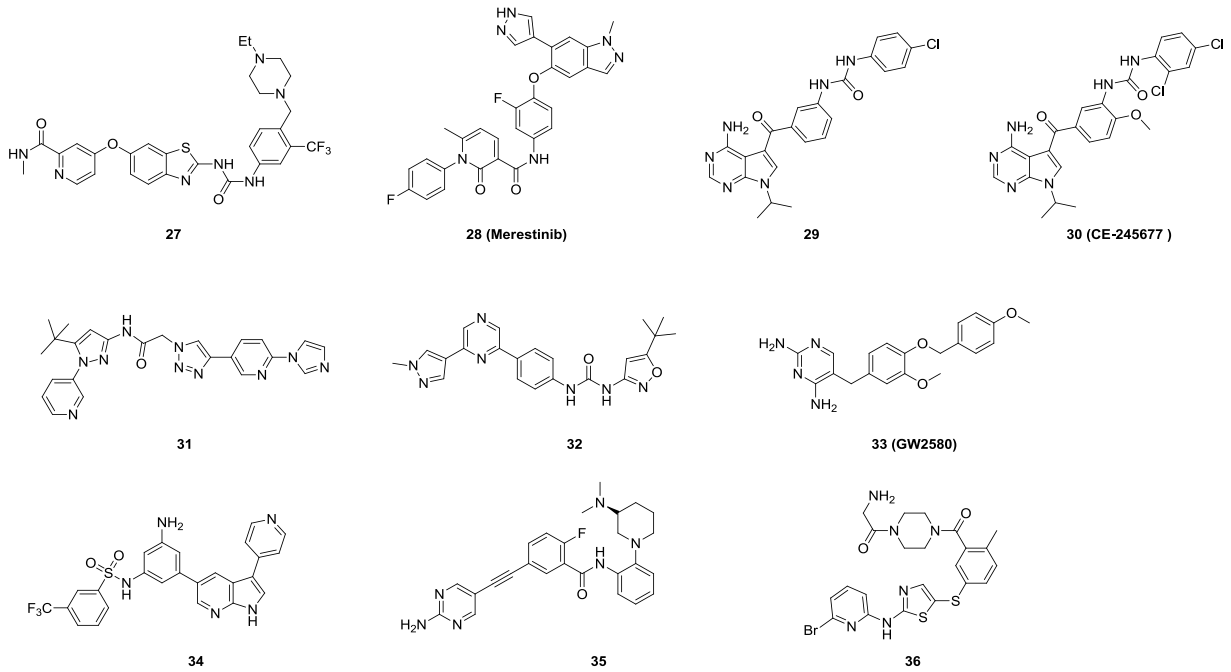

Figure 23. Chemical structures of other Type II TRK inhibitors

El-Damasy *et al.* reported benzothiazole derivative **27** as multi-targeted kinase inhibitors (Figure 23).[192] Compound **27** was active on several kinases with IC_{50} values below 0.1 μM (including VEGFR2, ABL, TRKA, TRKB, and TIE2 *et al.*). Specifically, the IC_{50}s for TRKA and TRKB were 0.0038 μM and 0.0044 μM, respectively. In antiproliferative studies, compound **27** was active against the KM-12 cell line with an IC_{50} of 0.019 μM. Arcari *et al.* reported a series of 4-aminopyrrolopyrimidine derivatives as TIE-2 inhibitors.[193] Compound **28** (Figure 23) was identified as a potent, pan kinase inhibitor with activity against c-MET (IC_{50} = 0.0047 μM) and RON (IC_{50} = 0.0012 μM) and exhibited anti-tumor activities in multiple mouse xenograft models.[157] Medicinal chemistry efforts led to the identification of compound **29** (Figure 23), which was found to be a TIE-2/TRKA dual inhibitor (IC_{50} for TIE-2 and TRKA were 0.0037 μM and 0.004 μM, respectively).[193] A close analogue of **29**, compound **30,** progressed to clinical trials, but the Phase I multiple dose trials were terminated due to the development of significant CNS adverse events, including cognitive deficits, personality changes, and sleep disturbances.[28, 186] Compound **31** (Figure 23) is another compound reported by Stachel *et al.*[173] with good TRK inhibitory activity (TRKA IC_{50} = 0.009 μM, cell IC_{50} = 0.007 μM). This compound was found to bind to the TRK kinase in the DFG-out conformation.[194] On compound **31**, the imidazole warhead binds to the hinge region, the central triazole ring forms an interaction with the gatekeeper residue, and the pyrazole occupies a

selectivity pocket normally occupied by Phe669. This inhibitor is very unique because of the innovative triazole linker and imidazole warhead. Frett *et al* described pyrazine-based derivatives as TRKA inhibitors (Figure 23).[195] Compound **32** had a TRKA IC_{50} of 0.005 μM (Figure 23), and modeling studies determined the compound binds in a typical Type II conformation. Compound **33** was initially reported by Conway *et al.* as a selective CSF-1R (colony stimulating factor 1 receptor) inhibitor (Figure 23), which completely inhibited CSF-1R *in vitro* at an IC_{50} of 0.06 μM but was inactive against 26 other kinases.[196] Later, the same authors found compound **33** also inhibited TRKA with an IC_{50} of 0.88 μM.[197].The radiolabeled analogue of **33** was reported by Bernard-Gauthier *et al*.[180] Bertrand *et al.* reported that compound **33** bound to TRKB in a DFG-out conformation.[73] Hong *et al.* reported a series of 3,5-disubstituted-7-azaindoles as TRK Inhibitors.[198] Further modification uncovered compound **34** (Figure 23), which is a pan-TRK inhibitor with selectivity over 30 kinases. The activity of compound **34** against TRK isoforms was equal (pan-TRK IC_{50} = ~0.001 μM), but was 100-fold more selective against other kinases. [198] Amino pyrimidine derivatives were developed as TIE-2 (tunica interna endothelial-2) inhibitors with compound **35** (Figure 23) exhibiting TIE-2 inhibition (IC_{50} = 0.005 μM) with almost equal TRKA inhibitory activity (IC_{50} = 0.008 μM).[199] Through screening of an in-house kinase library, Kim *et al.* found 2-amino-5-(thioaryl)thiazole to be a promising scaffold for TRK inhibition.[108] Further SAR investigation led to the identification of compound **36** (Figure 23) (TRKA IC_{50} = 0.0006 μM), which was selective over CDK, MET, and IGF-1R (IC_{50}s = 0.54 μM, >1 μM, and 0.43 μM, respectively).

Pseudo-Type II TRK Inhibitors

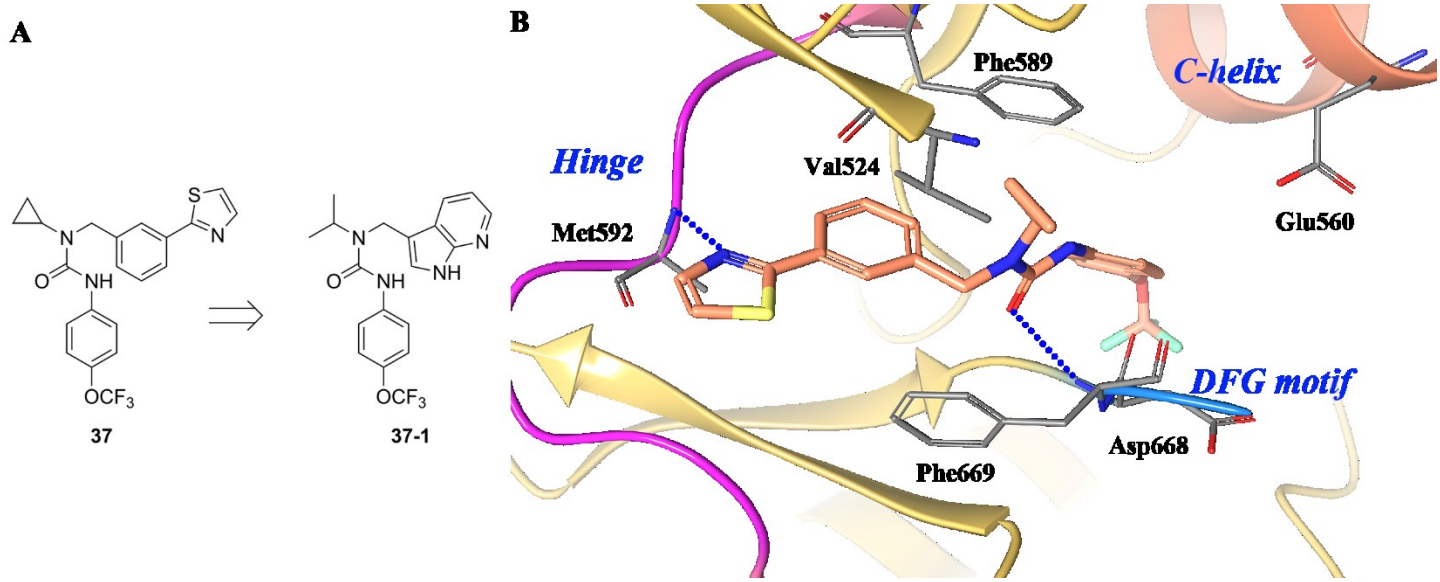

Figure 24. (A) Identification of compound **37-1**; (B) Co-crystal structure of compound **37** and its binding mode in TRKA (PDB ID: 4PMP, 1.8 Å). The kinase is depicted in yellow ribbons, and the hydrogen bonds are illustrated in blue dashed lines.

A quintessential property of Type II inhibitors is the formation of a strong hydrogen bond at the hinge region.[137] In certain inhibitors of TRK, however, the hydrogen bond at the hinge is abnormally weak with the majority of important interactions occurring in an adjacent allosteric pocket. This was first reported by Stachel *et al.* with the development of urea based compound **37** (Figure 24A) (TRKA kinase IC_{50} = 4.233 μM, cell IC_{50} = 0.549 μM).[173] Structure optimization resulted in the identification of compound **37-1** (TRKA kinase IC_{50} = 0.011 μM, cell IC_{50} = 0.003 μM). Figure 24B illustrates the binding mode of **37** with TRKA.[173] It is clear from this study that the compound bound to =TRKA in a DFG-out conformation, which is a typical feature for amide- and urea-linked Type II kinase inhibitors. However, **37** is structurally unlike any known Type II TRK inhibitor because of its low molecular weight and simple architecture.[173] At the ATP-binding site, the thiazole heterocycle forms a very weak hydrogen bond (3.45 Å) with the amide backbone of Met592. The benzylic ring is involved in hydrophobic interactions with the gatekeeper residue, Phe589. The para-trifluoromethoxyphenyl group occupies the hydrophobic pocket normally occupied by Phe669 in the DFG-in conformation. The amide carbonyl forms a hydrogen bond with Asp668 as is typical with most Type II kinase inhibitors.[137] A highly unique attribute to **37** is the cyclopropyl group, which occupies a hydrophobic cleft and is tucked

against Val524. This is an uncommon trait, as most kinase inhibitors are unsubstituted at this position and hydrogen bond to a glutamic acid on the α-C-helix.[173] One interpretation of the cyclopropyl SAR is that a critical hydrophobic mass is required to fill a small pocket near Val524 and Phe589. The placement of a hydrophobic group at this region is hypothesized to displace water, which would otherwise occupy the area.[173] These interactions suggest the compound exhibits binding properties more typical of a Type III inhibitor.

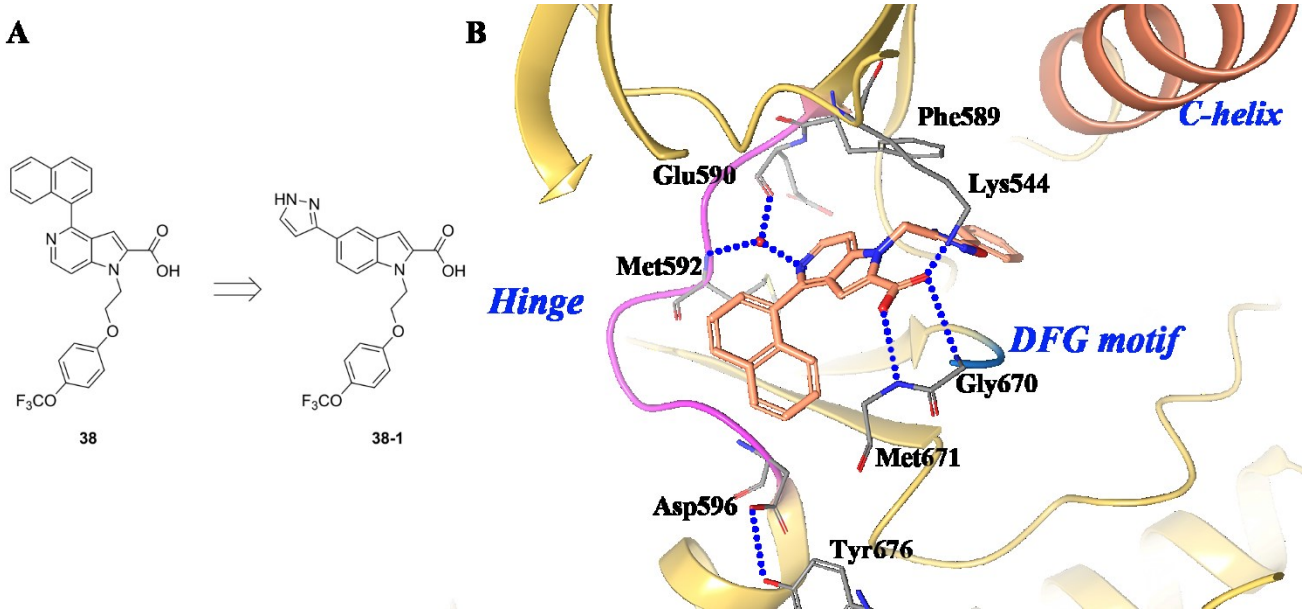

Figure 25. (A) Identification of compound **38-1**; (B) Co-crystal structure of compound **38** and its binding mode in TRKA (PDB ID: 4PMS, 2.8 Å). The kinase is depicted in yellow ribbons and the hydrogen bonds are illustrated in blue dashed lines.

In the same manuscript by Stachel *et al.*, the author discussed the development of compound **38** (TRKA kinase IC_{50} = 17.13 μM, cell IC_{50} = 1.162 μM) to compound **38-1** (TRKA kinase IC_{50} = 0.051 μM, cell IC_{50} = 0.029 μM) (Figure 25A).[173] Compound **38** was shown to bind to the DFG-out conformation of TRKA (Figure 25B).[173] The co-crystal structure revealed several unusual binding features. First, no direct interaction between the hinge backbone and the inhibitor was identified. Instead, the N5 nitrogen from the azaindole was shown to participate in a water-mediated hydrogen bond to the hinge region.[173] The naphthalene moiety was buried in the hydrophobic cleft at the front of the hinge

flanked by the activation loop residue Met671. One of the more unusual binding features is that the indole carboxylic acid interacts with two backbone amides in the activation loop. The unique interactions at the hinge and the activation loop regions anchor **38** to the ATP binding site. A third interaction was also evident between the carboxylic acid and Lys544 on the roof of the ATP binding pocket.[173] Compound **38** exhibited phosphorylation-dependent binding, which was due to the unusual conformation between the indole carboxylic acid and the activation loop. In the co-crystal structure, Tyr676 was involved in a hydrogen-bond interaction with Asp596. Since Tyr676 is a known phosphorylation site on TRKA, phospho-Tyr676 would disrupt this interaction with Asp596, forcing the activation loop away from the active site and stabilizing the active conformation. As such, the phosphorylated form of the enzyme is not able to bind compound **38**.[173] Because of the highly unique binding of **38** to TRKA, the compound exhibits a profile more typical of Type III.

Type III-JM TRK Inhibitors

TRKA activation triggers intracellular signaling cascades that increase the sensitivity of nociceptors, thus leading to chronic sensitization and pain.[200] However, TRKA/B/C share significant sequence homology at the kinase domain, which will make it extremely difficult to develop inhibitors selective for a single isoform. A method to circumvent selectivity issues is to develop allosteric inhibitors that do not bind to the highly conserved ATP active site. In an effort to identify TRKA specific inhibitors, Su *et al.* discovered compounds with novel scaffolds that bound to the juxtamembrane (JM) domain of TRKA.[138] The JM domain is located between the kinase domain and the transmembrane domain, and there is only 36% identity between TRKA and TRKB and 40% identity between TRKA and TRKC.[138] These findings provide the research community with a novel, exploitable region to generate TRK selective small molecule inhibitors.

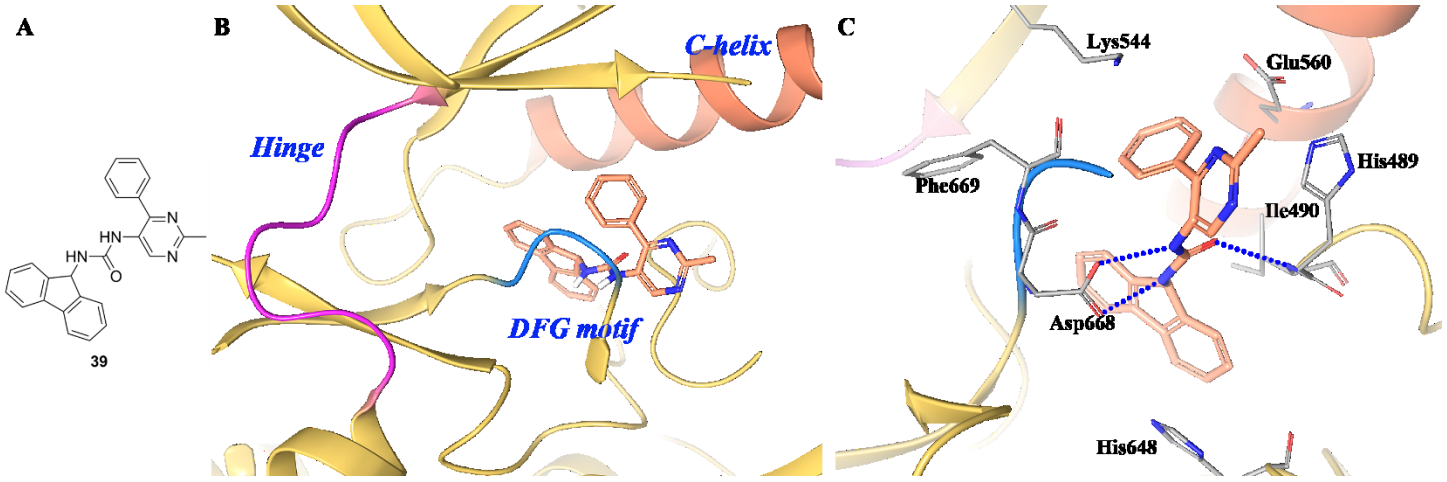

Figure 26. (A) Chemical structure of compound **39**; (B) Co-crystal structure of compound **39** in the allosteric pocket of TRKA (PDB ID: 5KMI, 1.87 Å); (C) Interactions of compound **39** with surrounding residues. The kinase is depicted in yellow ribbons and the hydrogen bonds are illustrated in blue dashed lines.

Compound **39** is a selective TRKA inhibitor (IC_{50}s for TRKA/B/C were 0.099 μM, > 81 μM and 25 μM, respectively) (Figure 26A).[138] In the co-crystal structure of **39** and TRKA (Figure 26B and Figure 26C), compound **36** bound behind the DFG motif opposite of the kinase active site.[138] The DFG motif was found in a DFG-out, inactive conformation, with Phe669 pointed toward the active site. Asp668, which coordinates to the phosphate groups on ATP, is away from the active site in the structure. The central urea of compound **39** makes two hydrogen bonds with Asp668. Asp668 is part of the DFG motif, and binding to compound **39** requires the DFG motif to be in the 'out' conformation.[138] The fluorine moiety of compound **39** occupies a relatively hydrophobic pocket formed primarily by aliphatic amino acids. The structure clearly reveals interactions at the JM region. Ile490, within the JM, sits on top of the fluorine moiety, aiding to the formation of the hydrophobic pocket [138] Similar to other TRKA co-crystal kinase structures, there is a shift in Phe646, which creates a pocket to accommodate the fluorine. The oxygen of the central urea in compound **39** forms a hydrogen bond with the amide nitrogen of Ile490. The phenyl moiety occupies a position between Lys544 of the β3 strand and Glu560 of the α-C-Helix.[138]

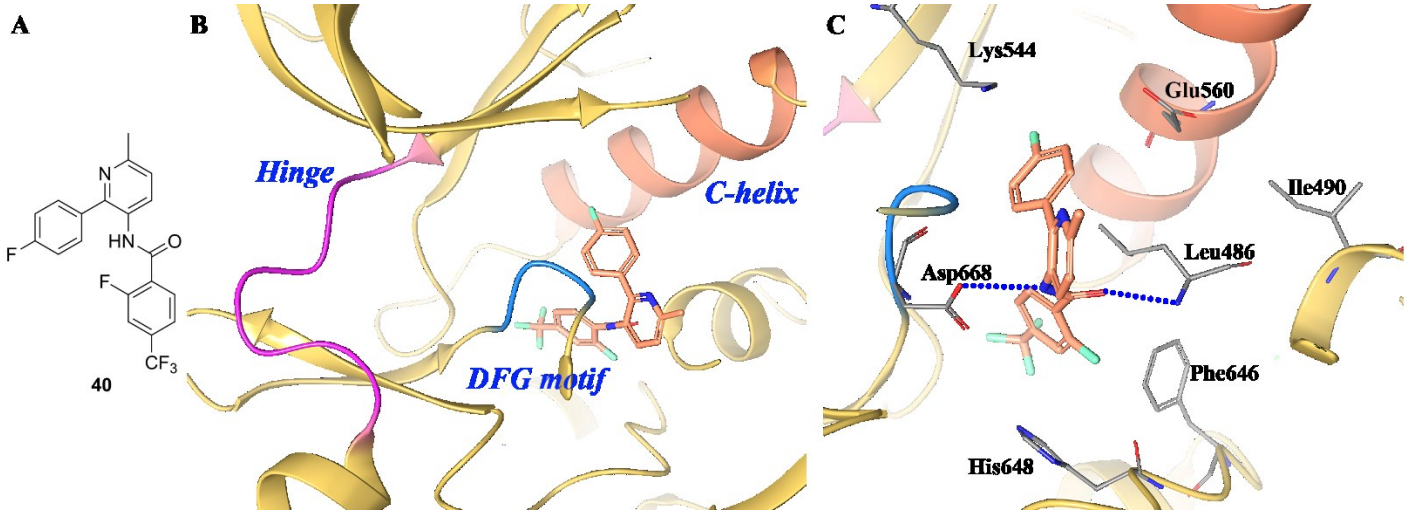

Figure 27. (A) Chemical structure of compound **40**; Co-crystal structure of compound **40** in the allosteric pocket of TRKA (PDB ID: 5KMK, 1.65 Å). (C) Interactions of compound **40** with surrounding residues. The kinase is depicted in yellow ribbons and the hydrogen bonds are illustrated in blue dashed lines.

Compound **40** is another selective TRKA inhibitor with interesting binding features (IC_{50}s for TRKA/B/C were 3.3 μM, >81.0 μM, and 27 μM, respectively) (Figure 27A).[138] The co-crystal structure of compound **40** revealed the compound bound to the same pocket as **39**, behind the DFG motif (Figure 27B and Figure 27C). The trifluorophenyl moiety of **40** sits in the pocket occupied by the fluorine of compound **39**. The central amide nitrogen is positioned close to the carboxylic acid of Asp668. The binding site is quite similar between the two structures except for the following differences: (1) for compound **39**, Ile490 packs above the phenyl ring, but Leu486 packs above the phenyl ring for **40**; (2) for **39**, Phe646 was displaced by the bulky moiety in the hydrophobic pocket, but for **40**, the smaller moiety accommodates Phe646 in a position closer to the active conformation.[138]

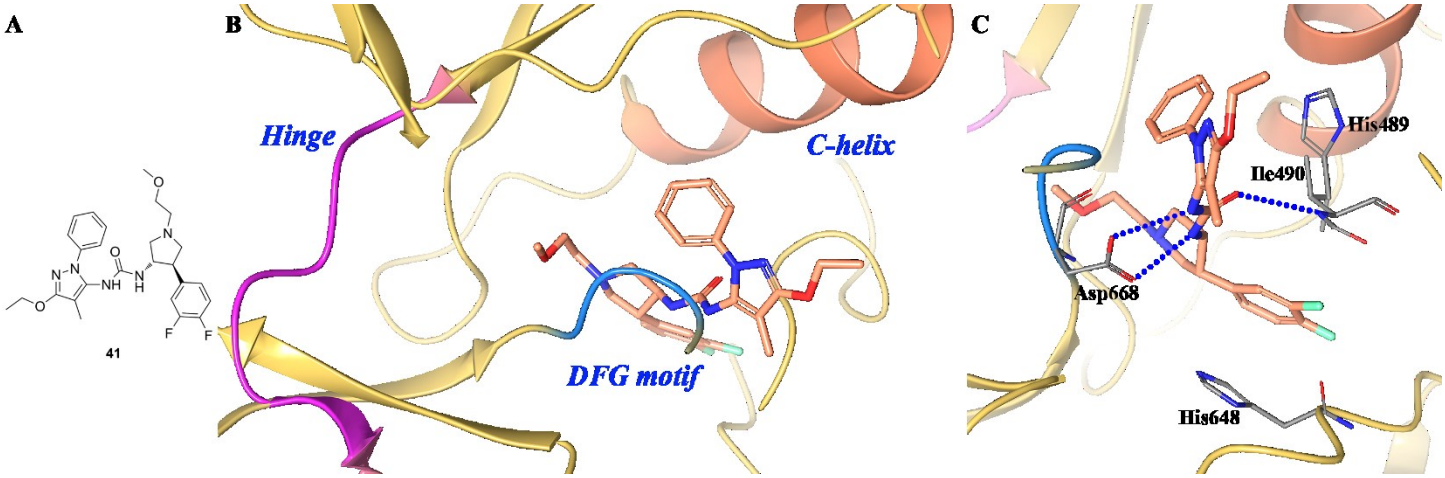

Figure 28. (A) Chemical structure of compound **41**; (B) Co-crystal structure of **41** bound in the allosteric pocket of TRKA (PDB ID: 5H3Q, 2.1 Å); (C) Interactions of compound **41** with surrounding residues. The kinase is depicted in yellow ribbons and the hydrogen bonds are illustrated in blue dashed lines.

A similar finding was also disclosed by Furuya *et al.*[200] Compound **41** (Figure 28A) showed potent inhibitory activity against TRKA (IC_{50} = 0.0027 μM) but was selective against TRKB and TRKC (IC_{50}s were 1.3 μM and 2.5 μM, respectively). Figure 28B and Figure 28C illustrate that compound **41** bound to the JM region of TRKA. The

configuration of the kinase domain and A loop is very similar to that observed for Apo TRKA.[200] **41** binds to the deep pocket formed by the DFG region of the A loop, glycine-rich loop (G loop), C-helix, and JM region. This pocket is completely separate from the ATP site. There are four key interactions that **41** creates at the binding region: (1) Asp668 of the DFG motif forms two hydrogen bonds with the urea moiety; (2) His489 interacts with the pyrazole ring via π-π interactions and with the ethoxy group via CH-π interactions; (3) Ile490 forms a hydrogen bond with the urea moiety and interacts with the difluorobenzene group of **41** via CH-π interactions; (4) His648 interacts with the difluorobenzene moiety through a π-π stacking interaction.[200] In addition to these, Leu486 is also involved in weak Van der Waals interactions with the methyl and ethoxyl groups of **41**. Interestingly, these amino acid residues are not conserved in TRKB nor TRKC but are integral for high binding affinity in TRKA.[200] Further exploitation of these TRKA specific amino acids could furnish numerous allosteric scaffolds with high TRKA selectivity.

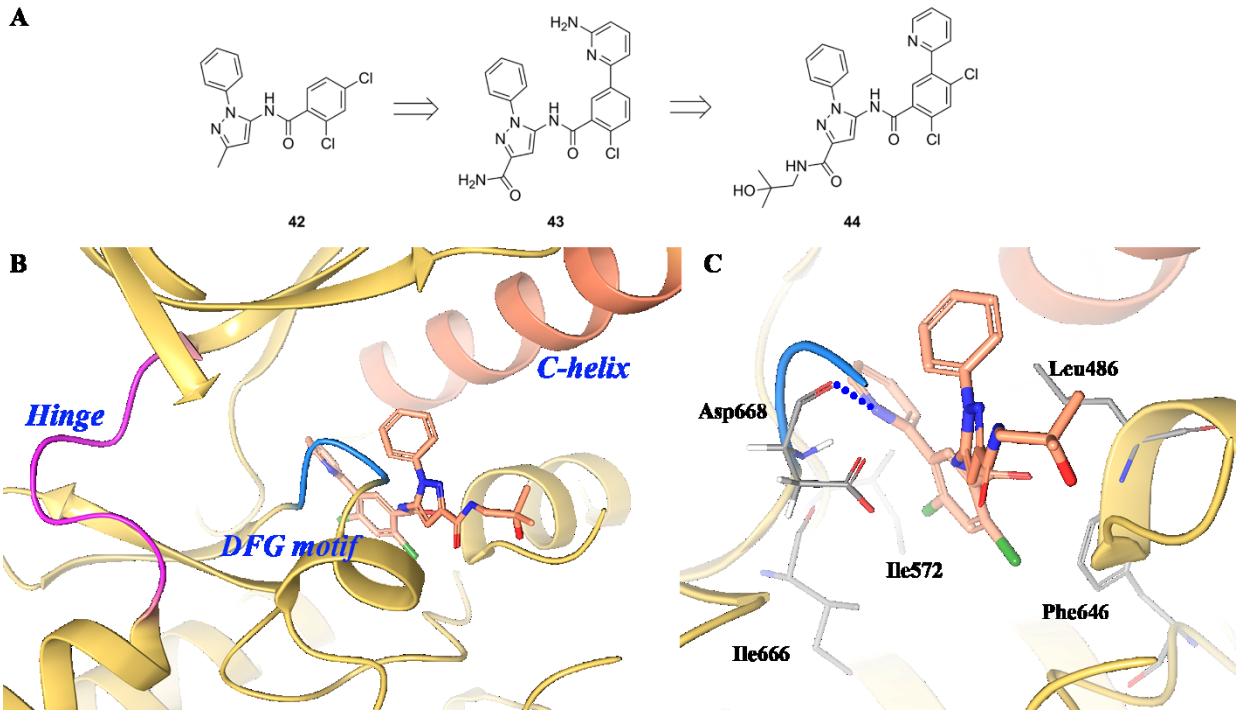

Figure 29. (A) Chemical structures of compounds **42**, **43**, and **44**; (B) Co-crystal structure of compound **44** bound to the allosteric pocket of TRKA (PDB ID: 6D20, 1.94 Å); (C) Interactions of compound **44** with surrounding residues. The kinase is depicted in yellow ribbons and the hydrogen bonds are illustrated in blue dashed lines.

Recently, Bagal *et al.* reported the discovery of a series of N-phenyl-pyrazole based compounds as selective TRKA inhibitors (Figure 29A).[201] The original hit **42** showed moderate TRKA inhibitory activity (TRKA cell IC_{50} = 3.3 μM) and >10-fold selective over TRKB/C (TRKB/C cell IC_{50}s > 50 μM). By introducing an amino-pyridine ring to the dichloro-phenyl ring and switching the methyl to an amide group, the resultant compound **43** demonstrated 66-fold improvement in TRKA potency (cell IC_{50} = 0.05 μM) and was >80-fold selective over TRKB/C (Cell IC_{50}s were 14 μM and 4.1 μM, respectively) with improved drug-like properties.[186] A variety of functional groups were evaluated on the pyridine and central phenyl ring, which led to the identification of **44** (TRKA/B/C IC_{50}s = 0.01 μM, 1.8 μM, and 0.7 μM, respectively) (Figure 29A). Compound **44** showed <15% inhibition against a panel of over 390 kinases at a concentration of 10 μM and was 72% orally bioavailable.[201] Figure 29B and Figure 29C illustrate the binding mode of **44** in the allosteric pocket of TRKA. The pyridyl nitrogen forms a hydrogen bond with the backbone of Asp668. The di-chloro central phenyl ring occupies the lipophilic pocket surrounded by Leu486, Ile572, Phe646 and Ile666. The terminal carbonyl group interacts with the side chain of Arg673 and the tertiary alcohol is exposed to the solvent front.[201]

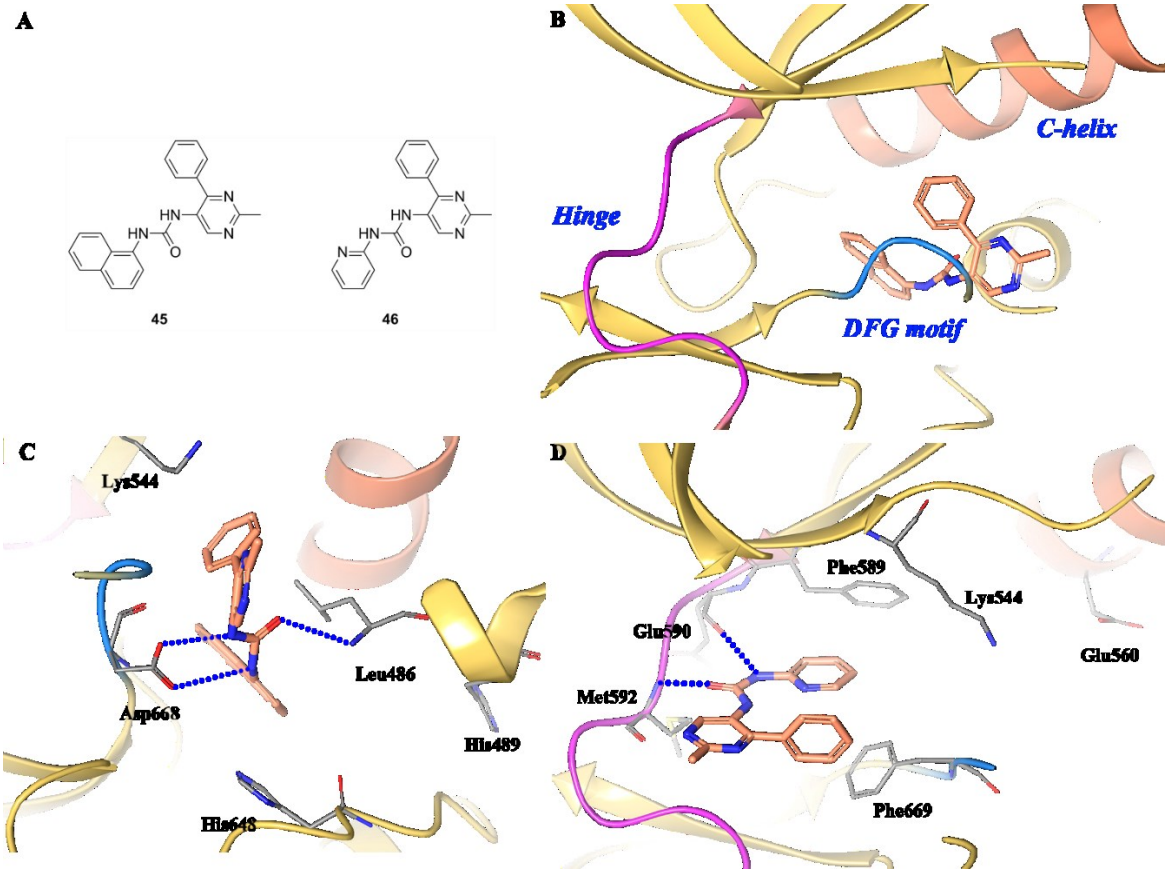

Figure 30. (A) Chemical structures of compounds **45** and **46**; (B) Co-crystal structure of compound **45** binding in the allosteric pocket of TRKA (PDB ID: 5KMM, 2.1 Å); (C) Interactions of compound **45** with surrounding residues; (D) Co-crystal structure of compound **46** in the active site of TRKA (PDB ID: 5KMO, 2.7 Å). The kinase is depicted in yellow ribbons and the hydrogen bonds are illustrated in blue dashed lines.

However, it is worth noting that two analogues of **39**, compounds **45** and **46** (by switching the fluorine moiety to naphthalene or pyridine), were also reported by Su *et al.* (Figure 30A).[138] These two compounds were active against TRKA and TRKC (**45**, TRKA/C IC_{50}s = 4.1 μM and 7.1 μM, respectively; **46**, TRKA/C IC_{50}s = 4.0 μM and 2.3 μM, respectively). Interactions of compound **45** with the kinase domain are similar to **39** but the JM interactions are altered as His489 is shifted away from to the compound (Figure 30B and Figure 30C). Instead of binding to the allosteric pocket, **46** binds to the active site in an atypical Type I conformation (Figure 30D). The urea carbonyl group forms a hydrogen bond with the hinge residue Met592, and the pyridine fragment has a weak π-π interaction with the DFG motif residue Phe669.[138] In this case, it is still uncertain whether compounds with such scaffolds will exhibit TRKA selectivity. It could be expected that only a subset of Type III inhibitors could be TRKA-selective because specific JM domain interactions are required for inhibition.[133]

Beyond compounds described above, there are three additional TRK inhibitors under clinical development with structures that have not been disclosed. These compounds include **PLX7486** (NCT01804530), **DS-6051B** (NCT02279433), and **F17752** (2013–003009–24).

Clinical Evaluation of TRK Inhibitors

Table 2. Reported drugs under clinical trials with known inhibitory activity of TRK kinases

NCT Identifier	Phase	Therapeutic Agent	Indication	Status	Patient Selection	Estimated Completion
NCT03213704	Phase II	Larotrectinib (**8**)	Pediatric Cancers	Recruiting	NTRK gene fusions	09/2024
NCT02637687	Phase II	Larotrectinib (**8**)	CNS Cancers	Recruiting	/	06/2019
NCT02576431	Phase II	Larotrectinib (**8**)	NTRK+ Solid Tumors	Recruiting	NTRK gene fusions	04/2018
NCT02122913	Phase I	Larotrectinib (**8**)	Solid Tumors	Recruiting	NTRK gene fusions	02/2017
NCT03215511	Phase I/II	LOXO-195 (**9**)	TRK Resistant Tumors	Recruiting	TRK-resistant lesions	08/2019
NCT02568267	Phase II	Entrectinib (**4-3**)	Solid Tumors	Recruiting	NTRK, ROS1, or ALK	10/2019

					gene rearrangements	
NCT02097810	Phase I	Entrectinib (**4-3**)	Advanced/Metastatic Cancer	Active	NTRK, ROS1, or ALK molecular alterations	06/2019
NCT02650401	Phase I	Entrectinib (**4-3**)	Pediatric and CNS Cancers	Recruiting	With or without NTRK, ROS1, or ALK gene fusions	08/2018
NCT01639508	Phase II	Cabozantinib (**23**)	Advanced NSCLC	Recruiting	RET, ROS1, or NTRK fusions or increased MET or AXL activity	07/2019
NCT02048488	Phase I/IIa	Belizatinib (**5-3**)	Solid Tumors and Lymphomas	Unknown	/	09/2016[+]
NCT02279433	Phase I	DS-6051b	Advanced Solid Tumors	Active	NTRK or ROS1 gene rearrangements	11/2019
NCT02675491	Phase I	DS-6051b	Advanced Solid Tumors	Active	NTRK or ROS1 gene rearrangements	09/2018
NCT02219711	Phase I	Sitravatinib (**24**)	Advanced Cancers	Recruiting	MET, NTRK, or DDR2 mutations, MET or KIT/PDGFRA/VEGFR2 gene amplification, MET, RET, AXL, NTRK1, or NTRK3 gene rearrangements, or CBL gene function mutations loss	12/2018
NCT01804530	Phase I	PLX7486	Advanced Solid Tumors	Terminated	NTRK point or fusion mutations	01/2018*
NCT02228811	Phase I	Altiratinib (**25**)	Advanced Solid Tumors	Terminated	NTRK or MET gene alterations	11/2017*

+ Study has passed its completion date and status has not been verified in more than two years

*Actual Primary Completion Date

All TRK-directed compounds under clinical investigation are pan-TRK inhibitors. This is likely due to the conservation of amino acids at the ATP binding domain of TRK isoforms. Pivotal TRK structural analysis completed by Bertrand, *et al.* only identified a two amino acid difference between the ATP binding site of TRKA and TRKB.[73] When analyzing TRKB and TRKC, all ATP binding site residues were identical.[73] Because all TRK inhibitors in clinical trials elicit activity by binding at the ATP binding site, they all possess pan-TRK activity. This activity profile is possibly beneficial because the inhibitors, in theory, can be utilized against a broad spectrum of tumors. However, this must be vetted cautiously, as dose-limiting toxicity can also increase based on inhibition profiles. An extensive, clinical overview for the development of TRK inhibitors has been reviewed by Lange, et al.[202]

Larotrectinib (**8**, LOXO-101) is under clinical investigation to treat melanoma, glioblastoma, NSCLC, pancreatic and ovarian cancers, and pediatric cancers. Following a single, oral dose, the unbound plasma concentration of

larotrectinib is sufficient to inhibit TRKA/B/C signaling without substantial inhibition of other kinases.[203] In a phase I study with larotrectinib, six patients with *NTRK* fusions with heavily pretreated advanced disease were enrolled (NCT02122913).[204] Of the six patients, three had partial responses within 3-4 months and one patient had a near-complete response after 8 months.[157] The drug was well tolerated, and the main side effects were fatigue, dizziness, and anemia. Larotrectinib was even well tolerated and efficacious in pediatric carcinomas harboring a TRK oncogene.[205-206] Due to the overall positive results of the phase I study, Bayer and Loxo Oncology initiated a multicenter phase II basket trial to evaluate larotrectinib in patients with an *NTRK* fusion oncogene (NCT02637687 and NCT02576431). The overall response rate to treatment was 75%, with 13% exhibiting a complete response.[99] At 1 year, 55% of the treated patients remained progression free. Based on the phase II results, larotrectinib has marked and durable antitumor efficacy in patients with *NTRK* fusions, regardless of age or tumor origin.[99, 207] Meeting future endpoints of clinical trials, such as median duration of response, progression-free survival, and overall survival, will further confirm the clinical utility of larotrectinib.

Entrectinib (**4-3**, RXDX-101) is a pan-kinase inhibitor under clinical development by Ignyta with activity against TRKA/B/C, ROS1, and ALK fusion oncogenes.[149] In a phase 1 clinical trial, 119 patients were treated with entrectinib split between two subgroups: ALKA-372-001, 54 patients, and STARTRK-1, 65 patients (NCT02097810).[208] Entrectinib was shown to be well tolerated and efficacious against *NTRK1/2/3* and *ALK* gene fusions, including patients with primary or secondary CNS disease.[208] The majority of treatment related toxicities were Grades 1-2 and reversible with cessation or modification of treatment.[208] In particular, responses were achieved regardless of histology, with responses observed in NSCLC, MASC, melanoma, glioneuronal tumor, colorectal cancer, and RCC.[208] Response rates were highest in *NTRK*-rearranged tumors, which provided first-time, clinical 'proof-of-concept' that *NTRK*-rearrangements are actionable drivers of tumor growth.[208] Because of the success of phase 1 studies, a global, multicenter phase II basket study (STARTRK-2) is currently recruiting patients with *NTRK*-, *ROS1*-, and *ALK*-rearranged tumors (NCT02568267).[209] These studies are being performed to confirm the results of the phase 1 study and to further establish the safety profile of entrectinib in a larger patient population. The clinical success of the phase 2 studies relies on the successful enrichment of patients with targetable gene fusions. Because of the rarity of *NTRK*-rearranged tumors and the success of the phase 1 trial, patients are being enrolled based on molecular, rather than histological, criteria.

Sitravatinib (**24**, MGCD516) is a multi-kinase inhibitor under clinical development by Mirati Therapeutics Inc. with activity against RTKs including MET, AXL, MER, and members of the VEGFR, PDGFR, DDR2, TRK and Eph families.[190] A phase 1/1b study is currently recruiting to evaluate dose and preliminary efficacy in patients harboring gene rearrangements involving *MET*, *RET*, *AXL*, or *NTRK1/2/3* (NCT02219711).[210] Based on pre-clinical data, sitravatinib is likely to be effective for metastatic, soft-tissue sarcomas. Similar to entrectinib, the clinical success of sitravatinib will rest on the ability to appropriately enrich patients for targetable, molecular lesions. Although blockade of multiple driver signaling pathways can be achieved with sitravatinib,[190] clinical investigation must identity a therapeutic window to safely target *NTRK* rearrangements without breaching dose-limiting toxicity on other kinase pathways.

DS-6051b is under clinical development by Daiichi Sankyo, Inc. for advanced solid tumors harboring *ROS1* or *NTRK1/2/3* rearrangements. A phase 1, two-part clinical trial is underway to determine dose-limiting toxicities and tumor response for up to two years (NCT02279433). Results from a phase 1 trial in Japanese subjects have already been published with dose-limiting toxicities experienced at the highest dose of 800 mg QD (NCT02675491).[211] Tolerability in American subjects was similar, with dose-limiting toxicities experienced at 800 and 1,200 mg QD.[212] Partial responses, based on tumor regression, were observed at or above the maximum tolerated dose warranting additional safety studies and better patient enrichment for a more durable, clinical response.

Cabozantinib (**23**, COMETRIQ®) is a pan-kinase inhibitor developed by Exelixis with FDA approval to treat metastatic medullary thyroid cancer (mMTC) and renal cell carcinoma (RCC). Cabozantinib was first approved to treat mMTC in 2012 and later, in 2016, it was approved for RCC. Because of its pan-kinase profile demonstrating activity against c-Met, RET, ROS1, ALK, VEGFR2, and TRK receptors, cabozantinib is under phase II clinical investigation for patients harboring *NTRK1* gene fusions in NSCLC (NCT01639508). In the same trial, the drug is being evaluated against patients with RET, ROS1, MET, and AXL oncogenes. Cabozantinib has been found to increase the risk of gastrointestinal perforations, fistulas, and hemorrhage and carries a black box warning for these side effects. In head-to-head studies, entrectinib exhibits stronger inhibition of *NTRK* fusion genes compared to cabozantinib, which suggests the clinical utility of entrectinib might be greater.[161] Further, cabozantinib inhibits VEGFR2 at an IC_{50} of 0.000035 μM[213] and other tyrosine kinases >0.001 μM, which positions cabozantinib as a highly potent, selective, and unique VEGFR2 inhibitor. The clinical utility of an inhibitor with strong VEGFR2 selectivity must be further evaluated for usefulness against TRK-

driven disease. Because of the pan-kinase profile of cabozantinib, clinical response against TRK cancers can be robust, but this also must be weighed against the high propensity for DLTs. Phase II clinical investigation will further evaluate the usefulness of cabozantinib in safely treating TRK-driven cancers.

A major clinical major consideration for TRK inhibitors is the propensity to select for drug resistant TRK mutations. For example, a metastatic colorectal cancer patient harboring a *NTRK1* gene fusion displayed a marked response to entrectinib.[160] However, after 4 months of treatment, entrectinib lost effectiveness in controlling tumor growth. By monitoring circulating tumor DNA (ctDNA), it was identified that the TRKA kinase domain underwent two different point mutations at G595R and G667C. These point mutations were also shown to limit the TRKA inhibitory activity of larotrectinib and belizatinib.[160] To overcome TRK resistant mutations, LOXO-195 (**9**) was developed, which is a constrained analogue of larotrectinib. Due to conformational limitations, steric interactions with TRKA G667C and TRKC G623R (homologous to TRKA G595R) are limited and kinase inhibitory activity is maintained. These results have been translated into clinical trials where patients have responded to LOXO-195 after failing treatment with larotrectinib.[159] Clinical trials for LOXO-195 are ongoing and are displaying the potential to extend durable remissions in patients with TRK-resistant lesions (NCT03215511).

Conclusion and Future Perspective for TRK Inhibitors

The use of kinase-directed precision medicine has been heavily pursued since the discovery and development of imatinib.[42] Kinases have since emerged as one of the most intensely pursued drug targets in oncology research due to highly druggable active sites and their critical roles in cellular signaling. However, there has yet to be a clinically approved inhibitor for the TRK-receptor tyrosine kinase despite its intimate involvement in tumor pathology and disease. The vast majority of kinase inhibitors developed for TRK exhibit limited selectivity against any of the three isoforms (TRKA/B/C) and are active in the greater kinome. These types of inhibitors will have limited utility as tools to further study TRK biology but have exhibited excellent therapeutic potential in clinical trials, especially when patients treated with TRK inhibitors are selected based on their molecular pathology. To further study TRK biology, it will be beneficial to utilize highly selective inhibitors with activity specific for a single, TRK isoform, such as **41** for TRKA. This will permit the inhibition of a single enzyme in the TRK family, which can help identify isoform importance and interplay in a variety of preclinical TRK-models. It is important to note that TRK singling, specifically via their corresponding growth

factors,[214] has been implicated in mediating and modulating the pain response. As such beyond cancer, TRK inhibitors are being evaluated in clinical trials as agents to reduce neuropathic pain (NCT03346330).

The most clinically advanced TRK inhibitors include entrectinib, a pan-TRK, ALK and ROS inhibitor, and larotrectinib, a specific, pan-TRK inhibitor. Both larotrectinib and entrectinib have achieved orphan designation from regulatory authorities.[48] A recent report of the clinical activity of entrectinib in 55 TRK mutant patients displayed an 80% overall response rate with long-lasting responses in 71% of patients (> 12-months).[100] An aspect that needs to be considered in the development of TRK inhibitors is, given their role in the nervous system, the possibility of adverse neuropsychiatric effects. One parameter that may influence this property is activity in the greater kinome and, another, the ability to cross the blood-brain barrier. Noteworthy, the most advanced TRK inhibitors under clinical development, such as larotrectinib and entrectinib, exhibited neurotoxicity. This is likely due to target specificity, although they are able to penetrate the blood-brain barrier and exert therapeutic effects against brain metastases.[48] The identification of the clinical candidate PF-06273340 (**22-3**) provides a strategy to deliver peripherally restricted and orally bioavailable compounds, which was to design compounds in physicochemical space appropriate for absorption across the gastrointestinal epithelium while, simultaneously, engineering the compounds as substrates for blood–brain barrier efflux transporters.[186, 201]

As observed with all kinase inhibitors, TRK resistance to precision medicine is a major therapeutic limitation for durable efficacy. To overcome resistance, LOXO-195 was developed and is exhibiting effectiveness to induce remissions in patients that have failed larotrectinib treatment. The exact duration of remission is being investigated in clinical trials, and the development of LOXO-195 is a hopeful addition for treating TRK-driven disease. Clinical studies have confirmed the importance of selecting patients based on molecular criteria, and this enrichment will become even more important when transitioning from 1st to 2nd generation TRK inhibitors. Although all evaluation of TRK precision medicine is in the early stages of clinical development, significant breakthroughs have been uncovered for the treatment and management of TRK-driven tumors. With the completion of clinical studies incorporating larger patient populations it is expected that TRK precision medicine will continue to exhibit efficacy. Larger clinical studies will also illuminate if selective (larotrectinib) or pan-kinase inhibitors (entrectinib) are more appropriate for treating TRK malignancies. With the advent of routine molecular profiling of tumors, patients will be treated with TRK precision medicine to induce a

tailored response. This will translate to customized treatment profiles that will better target the unique pathology of a patient's tumor.

Author Information

Corresponding Authors

*B. F.; e-mail, BAFrett@uams.edu

*H. L.: e-mail, HLi2@uams.edu

Notes

The authors declare no competing financial interest.

Biographies

Wei Yan received his Ph.D. from East China University of Science and Technology, Shanghai, China, and worked jointly at Shanghai Institute of Materia Medica, Chinese Academy of Sciences. Following, he worked at WuXi AppTec as a process chemistry scientist. He is currently a postdoctoral researcher at the University of Arkansas for Medical Sciences. His expertise is in medicinal chemistry and process chemistry for pilot plant manufacture of APIs.

Naga Rajiv Lakkaniga is currently a Ph.D candidate in the Department of Pharmaceutical Sciences, University of Arkansas for Medical Sciences. He received a Bachelors in Pharmacy and Master of Pharmacy in Pharmaceutical Chemistry from Birla Institute of Technology and Science- Pilani, India. His current research is focused on discovering novel small molecule kinase inhibitors for anti-cancer therapy using synthetic medicinal chemistry, and employing computational methods for lead optimization and conformational study of protein kinases.

Gunaganti Naresh received his Ph.D. in Organic and Medicinal Chemistry from CSIR-Central Drug Research Institute-Jawaharlal Nehru University, New Delhi, India. Later, he joined the University of Arizona as a postdoctoral research associate under Dr. Hong-yu Li. He is currently working as a postdoctoral research associate at University of Arkansas for Medical Sciences in the area of kinase drug discovery. He is interested in developing irreversible inhibitors for various kinases using synthetic and medicinal chemistry tools.

Fengping Lv received his Ph. D. in Organic Chemistry from East China Normal University under the supervision of Professor Wenhao Hu. He completed his postdoctoral trainings at University of Arkansas for Medical Sciences in the field of drug discovery research of kinase inhibitors for cancer. He is currently a faulty member of Shaoxing University Yuanpei College, and focused on translational targeted cancer drug development.

Francesca Carlomagno is Professor of General Pathology at the University of Naples Federico II, Dept. Molecular Medicine and Medical Biotechnology. She is also associated to the Institute of Experimental Endocrinology and Oncology of the National Research Council (IEOS, CNR). She received her MD degree and PhD from the University of Naples Federico II. She was a visiting fellow at NCI, NIH and completed her postdoctoral trainings at Cambridge University and Federico II University. Her research is on the molecular biology of cancer with a specific interest in antineoplastic, targeted therapy using small molecule kinase inhibitors. More recently in her lab new projects related to alteration of DNA replication and iron metabolism are being conducted with the aim to identify new pathways relevant for cancer.

Massimo Santoro is Professor of General Pathology at the University of Naples Federico II, Dept. of Molecular Medicine and Medical Biotechnology. He graduated in Medicine and Surgery at the University of Naples Federico II and then pursued a PhD degree in Molecular Pathology. He has been a fellow at NCI, NIH. His main interest has been molecular genetics of thyroid cancer. He participated to the identification of RET gene fusions in papillary thyroid cancer and activating point mutations in medullary thyroid cancer.

Neil McDonald is currently a Senior Group Leader at the Francis Crick Institute. He is also Professor in Structural Biology at Birkbeck College, London. He received his Ph.D. degree from the University of London, and did his postdoctoral training at Columbia University, NY. He previously worked at Cancer Research UK Labs in London where he focused on the structural biology of oncology targets. His current research interests are neurotrophic factor receptors and their downstream signaling pathways, in particular Rho-GTPase activated protein kinases.

Brendan Frett is an Assistant Professor of Pharmaceutical Sciences in the College of Pharmacy at the University of Arkansas for Medical Sciences. He received his Ph.D. degree from the University of Arizona, where he co-discovered a clinical candidate in IND studies. He has successfully transferred academic-based discoveries to pharmaceutical

companies for clinical development. He is interested in pursuing translational research projects, where research completed in his laboratory can directly help patients.

Hong-yu Li is a Professor of Medicinal Chemistry at the University of Arkansas for Medical Sciences (UAMS). He is also an Arkansas Research Alliance (ARA) Scholar, the Helen Adams & ARA endowed chair in drug discovery, and co-director for the Therapeutics Science Program, Winthrop P Rockefeller Cancer Institute. He received his Ph.D. degree from the University of Tokyo and did postdoctoral trainings at Columbia University and Harvard University. He previously worked at Eli Lilly and the University of Arizona where he focused on oncology drug discovery. His current research interests are in chemical biology and drug discovery, especially for oncology related targets and phenotypes. In his lab at UAMS, a robust oncology pipeline is under development exploiting single agent polypharmacology and synergistic medicinal chemistry approaches.

Abbreviations used

AKT, v-akt murine thymoma viral oncogene homologue; ALIS, automated ligand identification system; ALK, anaplastic lymphoma kinase; AML, acute myeloid leukemia; ATP, adenosine triphosphate; BDNF, brain-derived neurotrophic factor; CDK, cyclin-dependent kinase; CML, chronic myelogenous leukemia; DAG, diacyl-glycerol; DDR2, Discoidin domain-containing receptor 2; ERK, extracellular signal-regulated kinase; FDA, food and drug administration; FLT3, fms-like tyrosine kinase 3; Glio, glioblastoma; GRB2, growth factor receptor-bound protein 2; hERG, human ether-a-go-go-related gene; IC, intrahepatic cholangiocarcinoma; IGF1R, insulin-like growth factor 1; IP3, inositol trisphosphate; MASC, mammary analogue secretory carcinomas; MEK, mitogen-activated protein kinase; NGF, nerve growth factor; NT3, neurotrophin-3; PH, pleckstrin homology; PI3K, phosphatidylinositol-4,5-bisphosphate 3-kinase; PLCγ, phospholipase C-γ; PKC, protein kinase C; PTC, papillary thyroid cancer; PDGFR, Platelet-derived growth factor receptor; P-gp, P-glycoprotein; QSAR, quantitative structure–activity relationship; RAF, rapidly accelerated fibrosarcoma oncogene; RAS, rat sarcoma oncogene; RET rearranged during transfection; Ron, recepteur d'origine nantais;; RTK, receptor tyrosine kinases; SHC, Src homology 2 domain containing; TIE-2 ,tunica interna endothelial-2; TRK, tropomyosin receptor kinase; VEGFR2, vascular endothelial growth factor receptor 2;

References

1. Carter, A. R.; Chen, C.; Schwartz, P. M.; Segal, R. A. Brain-derived neurotrophic factor modulates cerebellar plasticity and synaptic ultrastructure. *J Neurosci* **2002**, *22* (4), 1316-1327.
2. Lai, K. O.; Wong, A. S.; Cheung, M. C.; Xu, P.; Liang, Z.; Lok, K. C.; Xie, H.; Palko, M. E.; Yung, W. H.; Tessarollo, L.; Cheung, Z. H.; Ip, N. Y. TrkB phosphorylation by Cdk5 is required for activity-dependent structural plasticity and spatial memory. *Nat Neurosci* **2012**, *15* (11), 1506-1515.
3. Ren, K.; Dubner, R. Pain facilitation and activity-dependent plasticity in pain modulatory circuitry: role of BDNF-TrkB signaling and NMDA receptors. *Mol Neurobiol* **2007**, *35* (3), 224-235.
4. Schuman, E. M. Neurotrophin regulation of synaptic transmission. *Curr Opin Neurobiol* **1999**, *9* (1), 105-109.
5. Kang, H.; Jia, L. Z.; Suh, K. Y.; Tang, L.; Schuman, E. M. Determinants of BDNF-induced hippocampal synaptic plasticity: role of the Trk B receptor and the kinetics of neurotrophin delivery. *Learn Mem* **1996**, *3* (2-3), 188-196.
6. McAllister, A. K.; Katz, L. C.; Lo, D. C. Neurotrophins and synaptic plasticity. *Annu Rev Neurosci* **1999**, *22*, 295-318.
7. Schinder, A. F.; Poo, M. The neurotrophin hypothesis for synaptic plasticity. *Trends Neurosci* **2000**, *23* (12), 639-645.
8. Huang, E. J.; Reichardt, L. F. Trk receptors: roles in neuronal signal transduction. *Annu Rev Biochem* **2003**, *72*, 609-642.
9. Bartkowska, K.; Paquin, A.; Gauthier, A. S.; Kaplan, D. R.; Miller, F. D. Trk signaling regulates neural precursor cell proliferation and differentiation during cortical development. *Development* **2007**, *134* (24), 4369-4380.
10. Islam, O.; Loo, T. X.; Heese, K. Brain-derived neurotrophic factor (BDNF) has proliferative effects on neural stem cells through the truncated TRK-B receptor, MAP kinase, AKT, and STAT-3 signaling pathways. *Curr Neurovasc Res* **2009**, *6* (1), 42-53.
11. Meakin, S. O.; MacDonald, J. I.; Gryz, E. A.; Kubu, C. J.; Verdi, J. M. The signaling adapter FRS-2 competes with Shc for binding to the nerve growth factor receptor TrkA. A model for discriminating proliferation and differentiation. *J Biol Chem* **1999**, *274* (14), 9861-9870.
12. Kumar, S.; Kahn, M. A.; Dinh, L.; de Vellis, J. NT-3-mediated TrkC receptor activation promotes proliferation and cell survival of rodent progenitor oligodendrocyte cells in vitro and in vivo. *J Neurosci Res* **1998**, *54* (6), 754-765.
13. Matsumoto, K.; Wada, R. K.; Yamashiro, J. M.; Kaplan, D. R.; Thiele, C. J. Expression of brain-derived neurotrophic factor and p145TrkB affects survival, differentiation, and invasiveness of human neuroblastoma cells. *Cancer Res* **1995**, *55* (8), 1798-1806.
14. Zhang, Y. Z.; Moheban, D. B.; Conway, B. R.; Bhattacharyya, A.; Segal, R. A. Cell surface Trk receptors mediate NGF-induced survival while internalized receptors regulate NGF-induced differentiation. *J Neurosci* **2000**, *20* (15), 5671-5678.
15. Barnabe-Heider, F.; Miller, F. D. Endogenously produced neurotrophins regulate survival and differentiation of cortical progenitors via distinct signaling pathways. *J Neurosci* **2003**, *23* (12), 5149-5160.
16. Eggert, A.; Ikegaki, N.; Liu, X.; Chou, T. T.; Lee, V. M.; Trojanowski, J. Q.; Brodeur, G. M. Molecular dissection of TrkA signal transduction pathways mediating differentiation in human neuroblastoma cells. *Oncogene* **2000**, *19* (16), 2043-2051.
17. DiCicco-Bloom, E.; Friedman, W. J.; Black, I. B. NT-3 stimulates sympathetic neuroblast proliferation by promoting precursor survival. *Neuron* **1993**, *11* (6), 1101-1011.
18. Glass, D. J.; Nye, S. H.; Hantzopoulos, P.; Macchi, M. J.; Squinto, S. P.; Goldfarb, M.; Yancopoulos, G. D. Trkl3 mediates BDNF/NT-3-dependent survival and proliferation in fibroblasts lacking the low affinity NGF receptor. *Cell* **1991**, *66* (2), 405-413.
19. Cohen, R. I.; Marmur, R.; Norton, W. T.; Mehler, M. F.; Kessler, J. A. Nerve growth factor and neurotrophin-3 differentially regulate the proliferation and survival of developing rat brain oligodendrocytes. *J Neurosci* **1996**, *16* (20), 6433-6442.
20. Ibanez, C. F.; Ebendal, T.; Barbany, G.; Murray-Rust, J.; Blundell, T. L.; Persson, H. Disruption of the low affinity receptor-binding site in NGF allows neuronal survival and differentiation by binding to the trk gene product. *Cell* **1992**, *69* (2), 329-341.

21. Lavenius, E.; Gestblom, C.; Johansson, I.; Nanberg, E.; Pahlman, S. Transfection of Trk-a into human neuroblastoma-cells restores their ability to differentiate in response to nerve growth-factor. *Cell Growth Differ* **1995**, *6* (6), 727-736.
22. Chao, M. V. Neurotrophins and their receptors: a convergence point for many signalling pathways. *Nat Rev Neurosci* **2003**, *4* (4), 299-309.
23. Bapat, A. A.; Hostetter, G.; Von Hoff, D. D.; Han, H. Perineural invasion and associated pain in pancreatic cancer. *Nat Rev Cancer* **2011**, *11* (10), 695-707.
24. Miknyoczki, S. J.; Wan, W.; Chang, H.; Dobrzanski, P.; Ruggeri, B. A.; Dionne, C. A.; Buchkovich, K. The neurotrophin-trk receptor axes are critical for the growth and progression of human prostatic carcinoma and pancreatic ductal adenocarcinoma xenografts in nude mice. *Clin Cancer Res* **2002**, *8* (6), 1924-1931.
25. Desmet, C. J.; Peeper, D. S. The neurotrophic receptor TrkB: a drug target in anti-cancer therapy? *Cell Mol Life Sci* **2006**, *63* (7-8), 755-759.
26. Rubin, J. B.; Segal, R. A. Growth, survival and migration: the Trk to cancer. *Cancer Treat Res* **2003**, *115*, 1-18.
27. Brodeur, G. M.; Minturn, J. E.; Ho, R.; Simpson, A. M.; Iyer, R.; Varela, C. R.; Light, J. E.; Kolla, V.; Evans, A. E. Trk receptor expression and inhibition in neuroblastomas. *Clin Cancer Res* **2009**, *15* (10), 3244-3250.
28. Wang, T.; Yu, D.; Lamb, M. L. Trk kinase inhibitors as new treatments for cancer and pain. *Expert Opin Ther Pat* **2009**, *19* (3), 305-319.
29. Weeraratna, A. T.; Dalrymple, S. L.; Lamb, J. C.; Denmeade, S. R.; Miknyoczki, S.; Dionne, C. A.; Isaacs, J. T. Pan-trk inhibition decreases metastasis and enhances host survival in experimental models as a result of its selective induction of apoptosis of prostate cancer cells. *Clin Cancer Res* **2001**, *7* (8), 2237-2245.
30. Weeraratna, A. T.; Arnold, J. T.; George, D. J.; DeMarzo, A.; Isaacs, J. T. Rational basis for Trk inhibition therapy for prostate cancer. *Prostate* **2000**, *45* (2), 140-148.
31. Thiele, C. J.; Li, Z.; McKee, A. E. On Trk--the TrkB signal transduction pathway is an increasingly important target in cancer biology. *Clin Cancer Res* **2009**, *15* (19), 5962-5967.
32. Melck, D.; De Petrocellis, L.; Orlando, P.; Bisogno, T.; Laezza, C.; Bifulco, M.; Di Marzo, V. Suppression of nerve growth factor Trk receptors and prolactin receptors by endocannabinoids leads to inhibition of human breast and prostate cancer cell proliferation. *Endocrinology* **2000**, *141* (1), 118-126.
33. Nakagawara, A. Trk receptor tyrosine kinases: A bridge between cancer and neural development. *Cancer Lett* **2001**, *169* (2), 107-114.
34. Sakamoto, Y.; Kitajima, Y.; Edakuni, G.; Sasatomi, E.; Mori, M.; Kitahara, K.; Miyazaki, K. Expression of Trk tyrosine kinase receptor is a biologic marker for cell proliferation and perineural invasion of human pancreatic ductal adenocarcinoma. *Oncol Rep* **2001**, *8* (3), 477-484.
35. Schneider, M. B.; Standop, J.; Ulrich, A.; Wittel, U.; Friess, H.; Andren-Sandberg, A.; Pour, P. M. Expression of nerve growth factors in pancreatic neural tissue and pancreatic cancer. *J Histochem Cytochem* **2001**, *49* (10), 1205-1210.
36. McGregor, L. M.; McCune, B. K.; Graff, J. R.; McDowell, P. R.; Romans, K. E.; Yancopoulos, G. D.; Ball, D. W.; Baylin, S. B.; Nelkin, B. D. Roles of trk family neurotrophin receptors in medullary thyroid carcinoma development and progression. *Proc Natl Acad Sci U S A* **1999**, *96* (8), 4540-4545.
37. Sclabas, G. M.; Fujioka, S.; Schmidt, C.; Li, Z.; Frederick, W. A.; Yang, W.; Yokoi, K.; Evans, D. B.; Abbruzzese, J. L.; Hess, K. R.; Zhang, W.; Fidler, I. J.; Chiao, P. J. Overexpression of tropomysin-related kinase B in metastatic human pancreatic cancer cells. *Clin Cancer Res* **2005**, *11* (2 Pt 1), 440-449.
38. Sugimoto, T.; Kuroda, H.; Horii, Y.; Moritake, H.; Tanaka, T.; Hattori, S. Signal transduction pathways through TRK-A and TRK-B receptors in human neuroblastoma cells. *Jpn J Cancer Res* **2001**, *92* (2), 152-160.
39. Borrello, M. G.; Bongarzone, I.; Plerotti, M. A.; Luksch, R.; Gasparini, M.; Collini, P.; Pllotti, S.; Rlzzetti, M. G.; Mondellini, P.; De Bernardi, B.; Di Martino, D.; Garaventa, A.; Brisigotti, M.; Tonini, G. P. trk andret proto-oncogene expression in human neuroblastoma specimens: High frequency of trk expression in non-advanced stages. *Int J Cancer* **1993**, *54* (4), 540-545.
40. Okada, Y.; Eibl, G.; Guha, S.; Duffy, J. P.; Reber, H. A.; Hines, O. J. Nerve growth factor stimulates MMP-2 expression and activity and increases invasion by human pancreatic cancer cells. *Clin Exp Metastasis* **2004**, *21* (4), 285-292.

41. Sapio, M. R.; Posca, D.; Raggioli, A.; Guerra, A.; Marotta, V.; Deandrea, M.; Motta, M.; Limone, P. P.; Troncone, G.; Caleo, A.; Rossi, G.; Fenzi, G.; Vitale, M. Detection of RET/PTC, TRK and BRAF mutations in preoperative diagnosis of thyroid nodules with indeterminate cytological findings. *Clin Endocrinol (Oxf)* **2007**, *66* (5), 678-683.
42. Druker, B. J.; Tamura, S.; Buchdunger, E.; Ohno, S.; Segal, G. M.; Fanning, S.; Zimmermann, J.; Lydon, N. B. Effects of a selective inhibitor of the Abl tyrosine kinase on the growth of Bcr-Abl positive cells. *Nat Med* **1996**, *2* (5), 561-566.
43. Vaishnavi, A.; Le, A. T.; Doebele, R. C. TRKing down an old oncogene in a new era of targeted therapy. *Cancer Discov* **2015**, *5* (1), 25-34.
44. Amatu, A.; Sartore-Bianchi, A.; Siena, S. NTRK gene fusions as novel targets of cancer therapy across multiple tumour types. *ESMO Open* **2016**, *1* (2), e000023.
45. Stransky, N.; Cerami, E.; Schalm, S.; Kim, J. L.; Lengauer, C. The landscape of kinase fusions in cancer. *Nat Commun* **2014**, *5*, 4846.
46. Dela Cruz, C. S.; Tanoue, L. T.; Matthay, R. A. Lung cancer: epidemiology, etiology, and prevention. *Clin Chest Med* **2011**, *32* (4), 605-644.
47. Drilon, A.; Li, G.; Dogan, S.; Gounder, M.; Shen, R.; Arcila, M.; Wang, L.; Hyman, D. M.; Hechtman, J.; Wei, G.; Cam, N. R.; Christiansen, J.; Luo, D.; Maneval, E. C.; Bauer, T.; Patel, M.; Liu, S. V.; Ou, S. H.; Farago, A.; Shaw, A.; Shoemaker, R. F.; Lim, J.; Hornby, Z.; Multani, P.; Ladanyi, M.; Berger, M.; Katabi, N.; Ghossein, R.; Ho, A. L. What hides behind the MASC: clinical response and acquired resistance to entrectinib after ETV6-NTRK3 identification in a mammary analogue secretory carcinoma (MASC). *Ann Oncol* **2016**, *27* (5), 920-926.
48. Khotskaya, Y. B.; Holla, V. R.; Farago, A. F.; Shaw, K. R. M.; Meric-Bernstam, F.; Hong, D. S. Targeting TRK family proteins in cancer. *Pharmacol Ther* **2017**, *173*, 58-66.
49. Vaishnavi, A.; Capelletti, M.; Le, A. T.; Kako, S.; Butaney, M.; Ercan, D.; Mahale, S.; Davies, K. D.; Aisner, D. L.; Pilling, A. B.; Berge, E. M.; Kim, J.; Sasaki, H.; Park, S.; Kryukov, G.; Garraway, L. A.; Hammerman, P. S.; Haas, J.; Andrews, S. W.; Lipson, D.; Stephens, P. J.; Miller, V. A.; Varella-Garcia, M.; Janne, P. A.; Doebele, R. C. Oncogenic and drug-sensitive NTRK1 rearrangements in lung cancer. *Nat Med* **2013**, *19* (11), 1469-1472.
50. Martin-Zanca, D.; Hughes, S. H.; Barbacid, M. A human oncogene formed by the fusion of truncated tropomyosin and protein tyrosine kinase sequences. *Nature* **1986**, *319* (6056), 743-748.
51. Ardini, E.; Bosotti, R.; Borgia, A. L.; De Ponti, C.; Somaschini, A.; Cammarota, R.; Amboldi, N.; Raddrizzani, L.; Milani, A.; Magnaghi, P.; Ballinari, D.; Casero, D.; Gasparri, F.; Banfi, P.; Avanzi, N.; Saccardo, M. B.; Alzani, R.; Bandiera, T.; Felder, E.; Donati, D.; Pesenti, E.; Sartore-Bianchi, A.; Gambacorta, M.; Pierotti, M. A.; Siena, S.; Veronese, S.; Galvani, A.; Isacchi, A. The TPM3-NTRK1 rearrangement is a recurring event in colorectal carcinoma and is associated with tumor sensitivity to TRKA kinase inhibition. *Mol Oncol* **2014**, *8* (8), 1495-1507.
52. Tacconelli, A.; Farina, A. R.; Cappabianca, L.; Gulino, A.; Mackay, A. R. Alternative TrkAIII splicing: a potential regulated tumor-promoting switch and therapeutic target in neuroblastoma. *Future Oncol* **2005**, *1* (5), 689-698.
53. Greco, A.; Miranda, C.; Pierotti, M. A. Rearrangements of NTRK1 gene in papillary thyroid carcinoma. *Mol Cell Endocrinol* **2010**, *321* (1), 44-49.
54. Kralik, J. M.; Kranewitter, W.; Boesmueller, H.; Marschon, R.; Tschurtschenthaler, G.; Rumpold, H.; Wiesinger, K.; Erdel, M.; Petzer, A. L.; Webersinke, G. Characterization of a newly identified ETV6-NTRK3 fusion transcript in acute myeloid leukemia. *Diagn Pathol* **2011**, *6*, 19.
55. Frattini, V.; Trifonov, V.; Chan, J. M.; Castano, A.; Lia, M.; Abate, F.; Keir, S. T.; Ji, A. X.; Zoppoli, P.; Niola, F.; Danussi, C.; Dolgalev, I.; Porrati, P.; Pellegatta, S.; Heguy, A.; Gupta, G.; Pisapia, D. J.; Canoll, P.; Bruce, J. N.; McLendon, R. E.; Yan, H.; Aldape, K.; Finocchiaro, G.; Mikkelsen, T.; Prive, G. G.; Bigner, D. D.; Lasorella, A.; Rabadan, R.; Iavarone, A. The integrated landscape of driver genomic alterations in glioblastoma. *Nat Genet* **2013**, *45* (10), 1141-1149.
56. Ricarte-Filho, J. C.; Li, S.; Garcia-Rendueles, M. E.; Montero-Conde, C.; Voza, F.; Knauf, J. A.; Heguy, A.; Viale, A.; Bogdanova, T.; Thomas, G. A.; Mason, C. E.; Fagin, J. A. Identification of kinase fusion oncogenes in post-Chernobyl radiation-induced thyroid cancers. *J Clin Invest* **2013**, *123* (11), 4935-4944.
57. Leeman-Neill, R. J.; Kelly, L. M.; Liu, P.; Brenner, A. V.; Little, M. P.; Bogdanova, T. I.; Evdokimova, V. N.; Hatch, M.; Zurnadzy, L. Y.; Nikiforova, M. N.; Yue, N. J.; Zhang, M.; Mabuchi, K.; Tronko, M. D.; Nikiforov, Y. E. ETV6-NTRK3 is a common chromosomal rearrangement in radiation-associated thyroid cancer. *Cancer* **2014**, *120* (6), 799-807.
58. Segal, R. A. Selectivity in neurotrophin signaling: theme and variations. *Annu Rev Neurosci* **2003**, *26*, 299-330.

59. Greco, A.; Mariani, C.; Miranda, C.; Lupas, A.; Pagliardini, S.; Pomati, M.; Pierotti, M. A. The DNA rearrangement that generates the Trk-T3 oncogene involves a nnovel gene on chromosome-3 whose product has a potential coiled-coil domain. *Mol Cell Biol* **1995**, *15* (11), 6118-6127.
60. Mitra, G.; Martin-Zanca, D.; Barbacid, M. Identification and biochemical characterization of p70TRK, product of the human TRK oncogene. *Proc Natl Acad Sci U S A* **1987**, *84* (19), 6707-6711.
61. Greco, A.; Fusetti, L.; Miranda, C.; Villa, R.; Zanotti, S.; Pagliardini, S.; Pierotti, M. A. Role of the TFG N-terminus and coiled-coil domain in the transforming activity of the thyroid TRK-T3 oncogene. *Oncogene* **1998**, *16* (6), 809-816.
62. Gysin, S.; Salt, M.; Young, A.; McCormick, F. Therapeutic strategies for targeting ras proteins. *Genes Cancer* **2011**, *2* (3), 359-372.
63. Martin-Zanca, D.; Oskam, R.; Mitra, G.; Copeland, T.; Barbacid, M. Molecular and biochemical characterization of the human trk proto-oncogene. *Mol Cell Biol* **1989**, *9* (1), 24-33.
64. Ultsch, M. H.; Wiesmann, C.; Simmons, L. C.; Henrich, J.; Yang, M.; Reilly, D.; Bass, S. H.; de Vos, A. M. Crystal structures of the neurotrophin-binding domain of TrkA, TrkB and TrkC. *J Mol Biol* **1999**, *290* (1), 149-159.
65. Wiesmann, C.; Ultsch, M. H.; Bass, S. H.; de Vos, A. M. Crystal structure of nerve growth factor in complex with the ligand-binding domain of the TrkA receptor. *Nature* **1999**, *401* (6749), 184-188.
66. Schneider, R.; Schweiger, M. A novel modular mosaic of cell adhesion motifs in the extracellular domains of the neurogenic trk and trkB tyrosine kinase receptors. *Oncogene* **1991**, *6* (10), 1807-1811.
67. Geetha, T.; Rege, S. D.; Mathews, S. E.; Meakin, S. O.; White, M. F.; Babu, J. R. Nerve growth factor receptor TrkA, a new receptor in insulin signaling pathway in PC12 cells. *J Biol Chem* **2013**, *288* (33), 23807-23813.
68. Kaplan, D. R.; Hempstead, B. L.; Martin-Zanca, D.; Chao, M. V.; Parada, L. F. The trk proto-oncogene product: a signal transducing receptor for nerve growth factor. *Science* **1991**, *252* (5005), 554-558.
69. Squinto, S. P.; Stitt, T. N.; Aldrich, T. H.; Davis, S.; Blanco, S. M.; RadzieJewski, C.; Glass, D. J.; Masiakowski, P.; Furth, M. E.; Valenzuela, D. M.; Distefano, P. S.; Yancopoulos, G. D. TrkB encodes a functional receptor for brain-derived neurotrophic factor and neurotrophin-3 but not nerve growth factor. *Cell* **1991**, *65* (5), 885-893.
70. Klein, R.; Jing, S. Q.; Nanduri, V.; O'Rourke, E.; Barbacid, M. The trk proto-oncogene encodes a receptor for nerve growth factor. *Cell* **1991**, *65* (1), 189-197.
71. Lamballe, F.; Klein, R.; Barbacid, M. TrkC, a new member of the trk family of tyrosine protein kinases, is a receptor for neurotrophin-3. *Cell* **1991**, *66* (5), 967-979.
72. Yuen, E. C.; Mobley, W. C. Early BDNF, NT-3, and NT-4 signaling events. *Exp Neurol* **1999**, *159* (1), 297-308.
73. Bertrand, T.; Kothe, M.; Liu, J.; Dupuy, A.; Rak, A.; Berne, P. F.; Davis, S.; Gladysheva, T.; Valtre, C.; Crenne, J. Y.; Mathieu, M. The crystal structures of trkA and trkB suggest key regions for achieving selective inhibition. *J Mol Biol* **2012**, *423* (3), 439-453.
74. Cherry, M.; Williams, D. H. Recent kinase and kinase inhibitor X-ray structures: mechanisms of inhibition and selectivity insights. *Curr Med Chem* **2004**, *11* (6), 663-673.
75. Jing, S. Q.; Tapley, P.; Barbacid, M. Nerve growth-factor mediates signal transduction through Trk homodimer receptors. *Neuron* **1992**, *9* (6), 1067-1079.
76. Cunningham, M. E.; Stephens, R. M.; Kaplan, D. R.; Greene, L. A. Autophosphorylation of activation loop tyrosines regulates signaling by the TRK nerve growth factor receptor. *J Biol Chem* **1997**, *272* (16), 10957-10967.
77. Cunningham, M. E.; Greene, L. A. A function-structure model for NGF-activated TRK. *EMBO J* **1998**, *17* (24), 7282-7293.
78. Middlemas, D. S.; Meisenhelder, J.; Hunter, T. Identification of Trkb autophosphorylation sites and evidence that phospholipase C-gamma-1 is a substrate of the Trkb receptor. *J Biol Chem* **1994**, *269* (7), 5458-5466.
79. Loeb, D. M. S., R. M.; Copeland, T.; Kaplan, D. R.; Greene, L. A. A Trk nerve growth factor (NGF) receptor point mutation affecting interaction with phospholipase C-gamma 1 abolishes NGF-promoted peripherin induction but not neurite outgrowth. *J Biol Chem* **1994**, *269* (12), 8901-8910.
80. Obermeier, A.; Lammers, R.; Wiesmuller, K. H.; Jung, G.; Schlessinger, J.; Ullrich, A. Identification of Trk binding sites for SHC and phosphatidylinositol 3'-kinase and formation of a multimeric signaling complex. *J Biol Chem* **1993**, *268* (31), 22963-22966.

81. Obermeier, A.; Bradshaw, R. A.; Seedorf, K.; Choidas, A.; Schlessinger, J.; Ullrich, A. Neuronal differentiation signals are controlled by nerve growth factor receptor/Trk binding sites for SHC and PLC gamma. *EMBO J* **1994**, *13* (7), 1585-1590.
82. Stephens, R. M.; Loeb, D. M.; Copeland, T. D.; Pawson, T.; Greene, L. A.; Kaplan, D. R. Trk receptors use redundant signal transduction pathways involving SHC and PLC-γ1 to mediate NGF responses. *Neuron* **1994**, *12* (3), 691-705.
83. Patapoutian, A.; Reichardt, L. F. Trk receptors: mediators of neurotrophin action. *Curr Opin Neurobiol* **2001**, *11* (3), 272-280.
84. Songyang, Z.; Margolis, B.; Chaudhuri, M.; Shoelson, S. E.; Cantley, L. C. The phosphotyrosine interaction domain of SHC recognizes tyrosine-phosphorylated NPXY motif. *J Biol Chem* **1995**, *270* (25), 14863-14866.
85. Lowenstein, E. J.; Daly, R. J.; Batzer, A. G.; Li, W.; Margolis, B.; Lammers, R.; Ullrich, A.; Skolnik, E. Y.; Bar-Sagi, D.; Schlessinger, J. The SH2 and SH3 domain-containing protein GRB2 links receptor tyrosine kinases to ras signaling. *Cell* **1992**, *70* (3), 431-442.
86. Bonfini, L.; Karlovich, C. A.; Dasgupta, C.; Banerjee, U. The Son of sevenless gene product: a putative activator of Ras. *Science* **1992**, *255* (5044), 603-606.
87. Nishida, E.; Gotoh, Y. The map kinase sascade is essential for diverse signal transduction pathways. *Trends Biochem Sci* **1993**, *18* (4), 128-131.
88. Atwal, J. K.; Massie, B.; Miller, F. D.; Kaplan, D. R. The TrkB-Shc site signals neuronal survival and local axon growth via MEK and PI3-kinase. *Neuron* **2000**, *27* (2), 265-277.
89. Fishell, G.; Blazeski, R.; Godement, P.; Rivas, R.; Wang, L. C.; Mason, C. A. Optical microscopy. 3. Tracking fluorescently labeled neurons in developing brain. *FASEB J* **1995**, *9* (5), 324-334.
90. Datta, K.; Bellacosa, A.; Chan, T. O.; Tsichlis, P. N. Akt is a direct target of the phosphatidylinositol 3-kinase - Activation by growth factors, v-src and v-Ha-ras, in Sf9 and mammalian cells. *J Biol Chem* **1996**, *271* (48), 30835-30839.
91. Hemmings, B. A. Update: Signal transduction - PH domains - A universal membrane adapter. *Science* **1997**, *275* (5308), 1899-1899.
92. Alessi, D. R.; James, S. R.; Downes, C. P.; Holmes, A. B.; Gaffney, P. R. J.; Reese, C. B.; Cohen, P. Characterization of a 3-phosphoinositide-dependent protein kinase which phosphorylates and activates protein kinase Bα. *Current Biology* **1997**, *7* (4), 261-269.
93. Andjelkovic, M.; Alessi, D. R.; Meier, R.; Fernandez, A.; Lamb, N. J.; Frech, M.; Cron, P.; Cohen, P.; Lucocq, J. M.; Hemmings, B. A. Role of translocation in the activation and function of protein kinase B. *J Biol Chem* **1997**, *272* (50), 31515-31524.
94. Burgering, B. M.; Coffer, P. J. Protein kinase B (c-Akt) in phosphatidylinositol-3-OH kinase signal transduction. *Nature* **1995**, *376* (6541), 599-602.
95. Dudek, H.; Datta, S. R.; Franke, T. F.; Birnbaum, M. J.; Yao, R.; Cooper, G. M.; Segal, R. A.; Kaplan, D. R.; Greenberg, M. E. Regulation of neuronal survival by the serine-threonine protein kinase Akt. *Science* **1997**, *275* (5300), 661-665.
96. Crowder, R. J.; Freeman, R. S. Phosphatidylinositol 3-kinase and Akt protein kinase are necessary and sufficient for the survival of nerve growth factor-dependent sympathetic neurons. *J Neurosci* **1998**, *18* (8), 2933-2943.
97. Yao, R.; Cooper, G. M. Requirement for phosphatidylinositol-3 kinase in the prevention of apoptosis by nerve growth factor. *Science* **1995**, *267* (5206), 2003-2006.
98. Zirrgiebel, U.; Ohga, Y.; Carter, B.; Berninger, B.; Inagaki, N.; Thoenen, H.; Lindholm, D. Characterization of TrkB receptor-mediated signaling pathways in rat cerebellar granule neurons: involvement of protein kinase C in neuronal survival. *J Neurochem* **2002**, *65* (5), 2241-2250.
99. Drilon, A.; Laetsch, T. W.; Kummar, S.; DuBois, S. G.; Lassen, U. N.; Demetri, G. D.; Nathenson, M.; Doebele, R. C.; Farago, A. F.; Pappo, A. S.; Turpin, B.; Dowlati, A.; Brose, M. S.; Mascarenhas, L.; Federman, N.; Berlin, J.; El-Deiry, W. S.; Baik, C.; Deeken, J.; Boni, V.; Nagasubramanian, R.; Taylor, M.; Rudzinski, E. R.; Meric-Bernstam, F.; Sohal, D. P. S.; Ma, P. C.; Raez, L. E.; Hechtman, J. F.; Benayed, R.; Ladanyi, M.; Tuch, B. B.; Ebata, K.; Cruickshank, S.; Ku, N. C.; Cox, M. C.; Hawkins, D. S.; Hong, D. S.; Hyman, D. M. Efficacy of larotrectinib in TRK fusion-positive cancers in adults and children. *N Engl J Med* **2018**, *378* (8), 731-739.

100. Andre, F. Developing anticancer drugs in orphan molecular entities - a paradigm under construction. *N Engl J Med* **2018**, *378* (8), 763-765.
101. Harada, T.; Yatabe, Y.; Takeshita, M.; Koga, T.; Yano, T.; Wang, Y.; Giaccone, G. Role and relevance of TrkB mutations and expression in non-small cell lung cancer. *Clin Cancer Res* **2011**, *17* (9), 2638-2645.
102. Farago, A. F.; Le, L. P.; Zheng, Z.; Muzikansky, A.; Drilon, A.; Patel, M.; Bauer, T. M.; Liu, S. V.; Ou, S. H.; Jackman, D.; Costa, D. B.; Multani, P. S.; Li, G. G.; Hornby, Z.; Chow-Maneval, E.; Luo, D.; Lim, J. E.; Iafrate, A. J.; Shaw, A. T. Durable clinical response to entrectinib in NTRK1-rearranged non-small cell lung cancer. *J Thorac Oncol* **2015**, *10* (12), 1670-1674.
103. Coulier, F.; Kumar, R.; Ernst, M.; Klein, R.; Martin-Zanca, D.; Barbacid, M. Human trk oncogenes activated by point mutation, in-frame deletion, and duplication of the tyrosine kinase domain. *Mol Cell Biol* **1990**, *10* (8), 4202-4210.
104. Arevalo, J. C.; Conde, B.; Hempstead, B. I.; Chao, M. V.; Martin-Zanca, D.; Perez, P. A novel mutation within the extracellular domain of TrkA causes constitutive receptor activation. *Oncogene* **2001**, *20* (10), 1229-1234.
105. Tomasson, M. H.; Xiang, Z.; Walgren, R.; Zhao, Y.; Kasai, Y.; Miner, T.; Ries, R. E.; Lubman, O.; Fremont, D. H.; McLellan, M. D.; Payton, J. E.; Westervelt, P.; DiPersio, J. F.; Link, D. C.; Walter, M. J.; Graubert, T. A.; Watson, M.; Baty, J.; Heath, S.; Shannon, W. D.; Nagarajan, R.; Bloomfield, C. D.; Mardis, E. R.; Wilson, R. K.; Ley, T. J. Somatic mutations and germline sequence variants in the expressed tyrosine kinase genes of patients with de novo acute myeloid leukemia. *Blood* **2008**, *111* (9), 4797-4808.
106. Tacconelli, A.; Farina, A. R.; Cappabianca, L.; Desantis, G.; Tessitore, A.; Vetuschi, A.; Sferra, R.; Rucci, N.; Argenti, B.; Screpanti, I.; Gulino, A.; Mackay, A. R. TrkA alternative splicing: a regulated tumor-promoting switch in human neuroblastoma. *Cancer Cell* **2004**, *6* (4), 347-360.
107. Reuther, G. W.; Lambert, Q. T.; Caligiuri, M. A.; Der, C. J. Identification and characterization of an activating TrkA deletion mutation in acute myeloid leukemia. *Mol Cell Biol* **2000**, *20* (23), 8655-8666.
108. Kim, S. H.; Tokarski, J. S.; Leavitt, K. J.; Fink, B. E.; Salvati, M. E.; Moquin, R.; Obermeier, M. T.; Trainor, G. L.; Vite, G. G.; Stadnick, L. K.; Lippy, J. S.; You, D.; Lorenzi, M. V.; Chen, P. Identification of 2-amino-5-(thioaryl)thiazoles as inhibitors of nerve growth factor receptor TrkA. *Bioorg Med Chem Lett* **2008**, *18* (2), 634-639.
109. Gupta, A.; Dixon, E. Epidemiology and risk factors: intrahepatic cholangiocarcinoma. *Hepatobiliary Surg Nutr* **2017**, *6* (2), 101-104.
110. Selikoff, I. J. Epidemiology of gastrointestinal cancer. *Environ Health Perspect* **1974**, *9*, 299-305.
111. Kim, J.; Lee, Y.; Cho, H. J.; Lee, Y. E.; An, J.; Cho, G. H.; Ko, Y. H.; Joo, K. M.; Nam, D. H. NTRK1 fusion in glioblastoma multiforme. *PLoS One* **2014**, *9* (3), e91940.
112. Sharma, C. An analysis of trends of incidence and cytohistological correlation of papillary carcinoma of the thyroid gland with evaluation of discordant cases. *J Cytol* **2016**, *33* (4), 192-198.
113. Rubin, B. P.; Chen, C.-J.; Morgan, T. W.; Xiao, S.; Grier, H. E.; Kozakewich, H. P.; Perez-Atayde, A. R.; Fletcher, J. A. Congenital mesoblastic nephroma t(12;15) is associated with ETV6-NTRK3 gene fusion. *Am J Pathol* **1998**, *153* (5), 1451-1458.
114. Chien, L. N.; Gittleman, H.; Ostrom, Q. T.; Hung, K. S.; Sloan, A. E.; Hsieh, Y. C.; Kruchko, C.; Rogers, L. R.; Wang, Y. F.; Chiou, H. Y.; Barnholtz-Sloan, J. S. Comparative brain and central nervous system tumor incidence and survival between the United States and Taiwan based on population-based registry. *Front Public Health* **2016**, *4*, 151.
115. Wu, G.; Diaz, A. K.; Paugh, B. S.; Rankin, S. L.; Ju, B.; Li, Y.; Zhu, X.; Qu, C.; Chen, X.; Zhang, J.; Easton, J.; Edmonson, M.; Ma, X.; Lu, C.; Nagahawatte, P.; Hedlund, E.; Rusch, M.; Pounds, S.; Lin, T.; Onar-Thomas, A.; Huether, R.; Kriwacki, R.; Parker, M.; Gupta, P.; Becksfort, J.; Wei, L.; Mulder, H. L.; Boggs, K.; Vadodaria, B.; Yergeau, D.; Russell, J. C.; Ochoa, K.; Fulton, R. S.; Fulton, L. L.; Jones, C.; Boop, F. A.; Broniscer, A.; Wetmore, C.; Gajjar, A.; Ding, L.; Mardis, E. R.; Wilson, R. K.; Taylor, M. R.; Downing, J. R.; Ellison, D. W.; Zhang, J.; Baker, S. J. The genomic landscape of diffuse intrinsic pontine glioma and pediatric non-brainstem high-grade glioma. *Nat Genet* **2014**, *46* (5), 444-450.
116. Mourad, M.; Jetmore, T.; Jategaonkar, A. A.; Moubayed, S.; Moshier, E.; Urken, M. L. Epidemiological trends of head and neck cancer in the United States: a SEER population study. *J Oral Maxillofac Surg* **2017**, *75* (12), 2562-2572.
117. Pao, W.; Girard, N. New driver mutations in non-small-cell lung cancer. *Lancet Oncol.* **2011**, *12* (2), 175-180.
118. Damjanov, I.; Skenderi, F.; Vranic, S. Mammary analogue secretory carcinoma (MASC) of the salivary gland: a new tumor entity. *Bosn J Basic Med Sci* **2016**, *16* (3), 237-238.

119. Eguchi M; M, E.-I. Absence of t(12;15) associated ETV6-NTRK3 fusion transcripts in pediatric acute leukemias. *Med Pediatr Oncol.* **2001**, *37* (4), 417.
120. Roberts, K. G.; Gu, Z.; Payne-Turner, D.; McCastlain, K.; Harvey, R. C.; Chen, I. M.; Pei, D.; Iacobucci, I.; Valentine, M.; Pounds, S. B.; Shi, L.; Li, Y.; Zhang, J.; Cheng, C.; Rambaldi, A.; Tosi, M.; Spinelli, O.; Radich, J. P.; Minden, M. D.; Rowe, J. M.; Luger, S.; Litzow, M. R.; Tallman, M. S.; Wiernik, P. H.; Bhatia, R.; Aldoss, I.; Kohlschmidt, J.; Mrozek, K.; Marcucci, G.; Bloomfield, C. D.; Stock, W.; Kornblau, S.; Kantarjian, H. M.; Konopleva, M.; Paietta, E.; Willman, C. L.; Mullighan, C. G. High frequency and poor outcome of philadelphia chromosome-like acute lymphoblastic leukemia in adults. *J Clin Oncol* **2017**, *35* (4), 394-401.
121. Fancelli, D.; Moll, J.; Varasi, M.; Bravo, R.; Artico, R.; Berta, D.; Bindi, S.; Cameron, A.; Candiani, I.; Cappella, P.; Carpinelli, P.; Croci, W.; Forte, B.; Giorgini, M. L.; Klapwijk, J.; Marsiglio, A.; Pesenti, E.; Rocchetti, M.; Roletto, F.; Severino, D.; Soncini, C.; Storici, P.; Tonani, R.; Zugnoni, P.; Vianello, P. 1,4,5,6-tetrahydropyrrolo[3,4-c]pyrazoles: identification of a potent Aurora kinase inhibitor with a favorable antitumor kinase inhibition profile. *J Med Chem* **2006**, *49* (24), 7247-7251.
122. Wiesner, T.; He, J.; Yelensky, R.; Esteve-Puig, R.; Botton, T.; Yeh, I.; Lipson, D.; Otto, G.; Brennan, K.; Murali, R.; Garrido, M.; Miller, V. A.; Ross, J. S.; Berger, M. F.; Sparatta, A.; Palmedo, G.; Cerroni, L.; Busam, K. J.; Kutzner, H.; Cronin, M. T.; Stephens, P. J.; Bastian, B. C. Kinase fusions are frequent in Spitz tumours and spitzoid melanomas. *Nat Commun* **2014**, *5*, 3116.
123. Turbeville, S.; Francis, K. M.; Behm, I.; Chiu, G. R.; Sanchez, H.; Morrison, B.; Rowe, J. M. Prevalence and incidence of acute myeloid leukemia may be higher than currently accepted estimates among the $\geqslant$65 year-old population in the United States. *Blood* **2014**, *124*.
124. Knezevich, S.; McFadden, D.; Tao, W.; Lim, J.; Sorensen, P. A novel ETV6-NTRK3 gene fusion in congenital fibrosarcoma. *Nat Genet.* **1998**, *18* (2), 184-187.
125. Lee, S. G.; Jung, S. P.; Lee, H. Y.; Kim, S.; Kim, H. Y.; Kim, I.; Bae, J. W. Secretory breast carcinoma: A report of three cases and a review of the literature. *Oncol Lett* **2014**, *8* (2), 683-686.
126. Russell, J. P.; Powell, D. J.; Cunnane, M.; Greco, A.; Portella, G.; Santoro, M.; Fusco, A.; Rothstein, J. L. The TRK-T1 fusion protein induces neoplastic transformation of thyroid epithelium. *Oncogene* **2000**, *19* (50), 5729-5735.
127. Ranzi, V.; Meakin, S. O.; Miranda, C.; Mondellini, P.; Pierotti, M. A.; Greco, A. The signaling adapters fibroblast growth factor receptor substrate 2 and 3 are activated by the thyroid TRK oncoproteins. *Endocrinology* **2003**, *144* (3), 922-928.
128. Miranda, C.; Greco, A.; Miele, C.; Pierotti, M. A.; Van Obberghen, E. IRS-1 and IRS-2 are recruited by TrkA receptor and oncogenic TRK-T1. *J Cell Physiol* **2001**, *186* (1), 35-46.
129. Roccato, E.; Miranda, C.; Ranzi, V.; Gishizki, M.; Pierotti, M. A.; Greco, A. Biological activity of the thyroid TRK-T3 oncogene requires signalling through Shc. *Br J Cancer* **2002**, *87* (6), 645-653.
130. Morrison, K. B.; Tognon, C. E.; Garnett, M. J.; Deal, C.; Sorensen, P. H. ETV6-NTRK3 transformation requires insulin-like growth factor 1 receptor signaling and is associated with constitutive IRS-1 tyrosine phosphorylation. *Oncogene* **2002**, *21* (37), 5684-5695.
131. Tognon, C.; Garnett, M.; Kenward, E.; Kay, R.; Morrison, K.; Sorensen, P. H. B. The chimeric protein tyrosine kinase ETV6-NTRK3 requires both Ras-Erk1/2 and PI3-kinase-Akt signaling for fibroblast transformation. *Cancer Res* **2001**, *61* (24), 8909-8916.
132. Edel, M. J.; Shvarts, A.; Medema, J. P.; Bernards, R. An in vivo functional genetic screen reveals a role for the TRK-T3 oncogene in tumor progression. *Oncogene* **2004**, *23* (29), 4959-4965.
133. Bailey, J. J.; Schirrmacher, R.; Farrell, K.; Bernard-Gauthier, V. Tropomyosin receptor kinase inhibitors: an updated patent review for 2010-2016-Part I. *Expert Opin Ther Pat* **2017**, *27* (6), 733-751.
134. Bailey, J. J.; Schirrmacher, R.; Farrell, K.; Bernard-Gauthier, V. Tropomyosin receptor kinase inhibitors: an updated patent review for 2010-2016-Part II. *Expert Opin Ther Pat* **2017**, *27* (7), 831-849.
135. McCarthy, C.; Walker, E. Tropomyosin receptor kinase inhibitors: a patent update 2009-2013. *Expert Opin Ther Pat* **2014**, *24* (7), 731-744.
136. Cowan-Jacob, S. W.; Jahnke, W.; Knapp, S. Novel approaches for targeting kinases: allosteric inhibition, allosteric activation and pseudokinases. *Future Med Chem* **2014**, *6* (5), 541-561.

137. Wu, P.; Nielsen, T. E.; Clausen, M. H. FDA-approved small-molecule kinase inhibitors. *Trends Pharmacol Sci* **2015**, *36* (7), 422-439.
138. Su, H. P.; Rickert, K.; Burlein, C.; Narayan, K.; Bukhtiyarova, M.; Hurzy, D. M.; Stump, C. A.; Zhang, X.; Reid, J.; Krasowska-Zoladek, A.; Tummala, S.; Shipman, J. M.; Kornienko, M.; Lemaire, P. A.; Krosky, D.; Heller, A.; Achab, A.; Chamberlin, C.; Saradjian, P.; Sauvagnat, B.; Yang, X.; Ziebell, M. R.; Nickbarg, E.; Sanders, J. M.; Bilodeau, M. T.; Carroll, S. S.; Lumb, K. J.; Soisson, S. M.; Henze, D. A.; Cooke, A. J. Structural characterization of nonactive site, TrkA-selective kinase inhibitors. *Proc Natl Acad Sci U S A* **2017**, *114* (3), E297-E306.
139. Wang, T.; Lamb, M. L.; Scott, D. A.; Wang, H.; Block, M. H.; Lyne, P. D.; Lee, J. W.; Davies, A. M.; Zhang, H. J.; Zhu, Y.; Gu, F.; Han, Y.; Wang, B.; Mohr, P. J.; Kaus, R. J.; Josey, J. A.; Hoffmann, E.; Thress, K.; Macintyre, T.; Wang, H.; Omer, C. A.; Yu, D. Identification of 4-aminopyrazolylpyrimidines as potent inhibitors of Trk kinases. *J Med Chem* **2008**, *51* (15), 4672-4684.
140. Thress, K.; Macintyre, T.; Wang, H.; Whitston, D.; Liu, Z. Y.; Hoffmann, E.; Wang, T.; Brown, J. L.; Webster, K.; Omer, C.; Zage, P. E.; Zeng, L.; Zweidler-McKay, P. A. Identification and predinical characterization of AZ-23, a novel, selective, and orally bioavailable inhibitor of the Trk kinase pathway. *Mol Cancer Ther* **2009**, *8* (7), 1818-1827.
141. Wang, T.; Lamb, M. L.; Block, M. H.; Davies, A. M.; Han, Y. X.; Hoffmann, E.; Ioannidis, S.; Josey, J. A.; Liu, Z. Y.; Lyne, P. D.; MacIntyre, T.; Mohr, P. J.; Omer, C. A.; Sjogren, T.; Thress, K.; Wang, B.; Wang, H. Y.; Yu, D. W.; Zhangt, H. J. Discovery of disubstituted imidazo 4,5-b pyridines and purines as potent TrkA inhibitors. *ACS Med Chem Lett* **2012**, *3* (9), 705-709.
142. Carrera, A. C.; Alexandrov, K.; Roberts, T. M. The conserved lysine of the catalytic domain of protein kinases is actively involved in the phosphotransfer reaction and not required for anchoring ATP. *Proc Natl Acad Sci U S A* **1993**, *90* (2), 442-446.
143. Brasca, M. G.; Amboldi, N.; Ballinari, D.; Cameron, A.; Casale, E.; Cervi, G.; Colombo, M.; Colotta, F.; Croci, V.; D'Alessio, R.; Fiorentini, F.; Isacchi, A.; Mercurio, C.; Moretti, W.; Panzeri, A.; Pastori, W.; Pevarello, P.; Quartieri, F.; Roletto, F.; Traquandi, G.; Vianello, P.; Vulpetti, A.; Ciomei, M. Identification of N,1,4,4-tetramethyl-8-{[4-(4-methylpiperazin-1-yl)phenyl]amino}-4,5-dihydro-1H-py razolo[4,3-h]quinazoline-3-carboxamide (PHA-848125), a potent, orally available cyclin dependent kinase inhibitor. *J Med Chem* **2009**, *52* (16), 5152-5163.
144. Albanese, C.; Alzani, R.; Amboldi, N.; Degrassi, A.; Festuccia, C.; Fiorentini, F.; Gravina, G.; Mercurio, C.; Pastori, W.; Brasca, M.; Pesenti, E.; Galvani, A.; Ciomei, M. Anti-tumour efficacy on glioma models of PHA-848125, a multi-kinase inhibitor able to cross the blood-brain barrier. *Br J Pharmacol* **2013**, *169* (1), 156-166.
145. Albanese, C.; Alzani, R.; Amboldi, N.; Avanzi, N.; Ballinari, D.; Brasca, M. G.; Festuccia, C.; Fiorentini, F.; Locatelli, G.; Pastori, W.; Patton, V.; Roletto, F.; Colotta, F.; Galvani, A.; Isacchi, A.; Moll, J.; Pesenti, E.; Mercurio, C.; Ciomei, M. Dual targeting of CDK and tropomyosin receptor kinase families by the oral inhibitor PHA-848125, an agent with broad-spectrum antitumor efficacy. *Mol Cancer Ther* **2010**, *9* (8), 2243-2254.
146. Gillies, R. J.; Verduzco, D.; Gatenby, R. A. Evolutionary dynamics of carcinogenesis and why targeted therapy does not work. *Nat Rev Cancer* **2012**, *12* (7), 487-493.
147. Bossi, R. T.; Saccardo, M. B.; Ardini, E.; Menichincheri, M.; Rusconi, L.; Magnaghi, P.; Orsini, P.; Avanzi, N.; Borgia, A. L.; Nesi, M.; Bandiera, T.; Fogliatto, G.; Bertrand, J. A. Crystal structures of anaplastic lymphoma kinase in complex with ATP competitive inhibitors. *Biochemistry (Mosc)* **2010**, *49* (32), 6813-6825.
148. Menichincheri, M.; Ardini, E.; Magnaghi, P.; Avanzi, N.; Banfi, P.; Bossi, R.; Buffa, L.; Canevari, G.; Ceriani, L.; Colombo, M.; Corti, L.; Donati, D.; Fasolini, M.; Felder, E.; Fiorelli, C.; Fiorentini, F.; Galvani, A.; Isacchi, A.; Borgia, A. L.; Marchionni, C.; Nesi, M.; Orrenius, C.; Panzeri, A.; Pesenti, E.; Rusconi, L.; Saccardo, M. B.; Vanotti, E.; Perrone, E.; Orsini, P. Discovery of entrectinib: A new 3-aminoindazole as a potent anaplastic lymphoma kinase (ALK), c-ros oncogene 1 kinase (ROS1), and pan-tropomyosine receptor kinases (Pan-TRKs) inhibitor. *J Med Chem* **2016**, *59* (7), 3392-3408.
149. Ardini, E.; Menichincheri, M.; Banfi, P.; Bosotti, R.; De Ponti, C.; Pulci, R.; Ballinari, D.; Ciomei, M.; Texido, G.; Degrassi, A.; Avanzi, N.; Amboldi, N.; Saccardo, M. B.; Casero, D.; Orsini, P.; Bandiera, T.; Mologni, L.; Anderson, D.; Wei, G.; Harris, J.; Vernier, J. M.; Li, G.; Felder, E.; Donati, D.; Isacchi, A.; Pesenti, E.; Magnaghi, P.; Galvani, A. Entrectinib, a pan-TRK, ROS1, and ALK inhibitor with activity in multiple molecularly defined cancer indications. *Mol Cancer Ther* **2016**, *15* (4), 628-639.

150. Ardini, E.; Borgia, A. L.; De Ponti, C.; Amboldi, N.; Ballinari, D.; Saccardo, M. B.; Magnaghi, P.; Pesenti, E.; Isacchi, A.; Galvani, A. Identification and preclinical characterization of NMS-P626, a potent, selective and orally bioavailable TrkA inhibitor with anti-tumor activity in a TrkA-dependent colorectal cancer. *Ejc Supplements* **2010**, *8* (7), 39-40.
151. Jin, L.; Yan, S.; Wei, G.; Li, G.; Harris, J.; Vernier, J.-M. The structure of TRKA kinase domain bound to the inhibitor Entrectinib., DOI: 10.2210/pdb5KVT/pdb.
152. Lewis, R. T.; Bode, C. M.; Choquette, D. M.; Potashman, M.; Romero, K.; Stellwagen, J. C.; Teffera, Y.; Moore, E.; Whittington, D. A.; Chen, H.; Epstein, L. F.; Emkey, R.; Andrews, P. S.; Yu, V. L.; Saffran, D. C.; Xu, M.; Drew, A.; Merkel, P.; Szilvassy, S.; Brake, R. L. The discovery and optimization of a novel class of potent, selective, and orally bioavailable anaplastic lymphoma kinase (ALK) inhibitors with potential utility for the treatment of cancer. *J Med Chem* **2012**, *55* (14), 6523-6540.
153. Sachdev, J.; Arkenau, H. T.; Infante, J. R.; Mita, M. M.; Anthony, S. P.; Natale, R. B.; Ejadi, S.; Wilcoxen, K.; Kansra, V.; Laken, H.; Hughes, L.; Martell, R.; Weiss, G. J. 506 Phase (Ph) 1/2a study of TSR-011, a potent inhibitor of ALK and TRK, in advanced solid tumors including crizotinib-resistant ALK positive non-small cell lung cancer. *Eur J Cancer* **2014**, *50*, 165.
154. Lippa, B.; Morris, J.; Corbett, M.; Kwan, T. A.; Noe, M. C.; Snow, S. L.; Gant, T. G.; Mangiaracina, M.; Coffey, H. A.; Foster, B.; Knauth, E. A.; Wessel, M. D. Discovery of novel isothiazole inhibitors of the TrkA kinase: Structure-activity relationship, computer modeling, optimization, and identification of highly potent antagonists. *Bioorg Med Chem Lett* **2006**, *16* (13), 3444-3448.
155. Choi, H. S.; Rucker, P. V.; Wang, Z.; Fan, Y.; Albaugh, P.; Chopiuk, G.; Gessier, F.; Sun, F.; Adrian, F.; Liu, G.; Hood, T.; Li, N.; Jia, Y.; Che, J.; McCormack, S.; Li, A.; Li, J.; Steffy, A.; Culazzo, A.; Tompkins, C.; Phung, V.; Kreusch, A.; Lu, M.; Hu, B.; Chaudhary, A.; Prashad, M.; Tuntland, T.; Liu, B.; Harris, J.; Seidel, H. M.; Loren, J.; Molteni, V. (R)-2-Phenylpyrrolidine substituted imidazopyridazines: a new class of potent and selective pan-TRK inhibitors. *ACS Med Chem Lett* **2015**, *6* (5), 562-567.
156. Sato, Y.; Onozaki, Y.; Sugimoto, T.; Kurihara, H.; Kamijo, K.; Kadowaki, C.; Tsujino, T.; Watanabe, A.; Otsuki, S.; Mitsuya, M.; Iida, M.; Haze, K.; Machida, T.; Nakatsuru, Y.; Komatani, H.; Kotani, H.; Iwasawa, Y. Imidazopyridine derivatives as potent and selective polo-like kinase (PLK) inhibitors. *Bioorg Med Chem Lett* **2009**, *19* (16), 4673-4678.
157. Doebele, R. C.; Davis, L. E.; Vaishnavi, A.; Le, A. T.; Estrada-Bernal, A.; Keysar, S.; Jimeno, A.; Varella-Garcia, M.; Aisner, D. L.; Li, Y.; Stephens, P. J.; Morosini, D.; Tuch, B. B.; Fernandes, M.; Nanda, N.; Low, J. A. An oncogenic NTRK fusion in a patient with soft-tissue sarcoma with response to the tropomyosin-related kinase inhibitor LOXO-101. *Cancer Discov* **2015**, *5* (10), 1049-1057.
158. Parikh, A. R.; Corcoran, R. B. Fast-TRKing drug development for rare molecular targets. *Cancer Discov* **2017**, *7* (9), 934-936.
159. Drilon, A.; Nagasubramanian, R.; Blake, J. F.; Ku, N.; Tuch, B. B.; Ebata, K.; Smith, S.; Lauriault, V.; Kolakowski, G. R.; Brandhuber, B. J.; Larsen, P. D.; Bouhana, K. S.; Winski, S. L.; Hamor, R.; Wu, W. I.; Parker, A.; Morales, T. H.; Sullivan, F. X.; DeWolf, W. E.; Wollenberg, L. A.; Gordon, P. R.; Douglas-Lindsay, D. N.; Scaltriti, M.; Benayed, R.; Raj, S.; Hanusch, B.; Schram, A. M.; Jonsson, P.; Berger, M. F.; Hechtman, J. F.; Taylor, B. S.; Andrews, S.; Rothenberg, S. M.; Hyman, D. M. A next-generation TRK kinase inhibitor overcomes acquired resistance to prior TRK kinase inhibition in patients with TRK fusion-positive solid tumors. *Cancer Discov* **2017**, *7* (9), 963-972.
160. Russo, M.; Misale, S.; Wei, G.; Siravegna, G.; Crisafulli, G.; Lazzari, L.; Corti, G.; Rospo, G.; Novara, L.; Mussolin, B.; Bartolini, A.; Cam, N.; Patel, R.; Yan, S. Q.; Shoemaker, R.; Wild, R.; Di Nicolantonio, F.; Sartore-Bianchi, A.; Li, G.; Siena, S.; Bardelli, A. Acquired resistance to the TRK inhibitor entrectinib in colorectal cancer. *Cancer Discov* **2016**, *6* (1), 36-44.
161. Fuse, M. J.; Okada, K.; Oh-Hara, T.; Ogura, H.; Fujita, N.; Katayama, R. Mechanisms of resistance to NTRK inhibitors and therapeutic strategies in NTRK1-rearranged cancers. *Mol Cancer Ther* **2017**, *16* (10), 2130-2143.
162. Drilon, A.; De Braud, F. G.; Siena, S.; Ou, S.-H. I.; Patel, M.; Ahn, M.-J.; Lee, J.; Bauer, T. M.; Farago, A. F.; Liu, S. V.; Reddinger, N.; Patel, R.; Luo, D.; Maneval, E. C.; Multani, P. S.; Doebele, R. C.; Shaw, A. T. Abstract CT007: Entrectinib, an oral pan-Trk, ROS1, and ALK inhibitor in TKI-naïve patients with advanced solid tumors harboring gene rearrangements: Updated phase I results. *Cancer Res* **2016**, *76* (14 Supplement), CT007.
163. Estrada-Bernal, A.; Le, A. T.; Tuch, B.; Kutateladze, T.; Doebele, R. C. Abstract C65: TRK kinase domain mutations that induce resistance to a pan-TRK inhibitor. *Mol Cancer Ther* **2016**, *14* (12 Supplement 2), C65.

164. The molecular docking was carried out using AutoDock4. The TRKA protein crystal structure was downloaded from the protein data bank (PDB ID: 4AOJ). Amino acid mutations were carried out using Maestro 2018-2, and the figures were generated by Maestro 2018-2.
165. Cui, J. J.; Zhai, D.; Deng, W.; Rogers, E.; Huang, Z.; Whitten, J.; Li, Y. TPX-0005, a novel ALK/ROS1/TRK inhibitor, effectively inhibited a broad spectrum of mutations including solvent front ALK G1202R, ROS1 G2032R and TRKA G595R mutants. *Eur J Cancer* **2016**, *69*, S32-S32.
166. Cui, J. J.; Rogers, E.; Zhai, D. Y.; Deng, W.; Huang, Z. D.; Whitten, J.; Li, Y. S. Ending the endless acquired tyrosine kinase resistance mutations - Design of TPX-0005, a multi-target ALK/ROS1/TRK inhibitor with broad spectrum activity against wild-type and mutants including ALK G1202R, ROS1 G2032R and TRKA G595R. *Cancer Res* **2016**, *76*.
167. Wood, E. R.; Kuyper, L.; Petrov, K. G.; Hunter, R. N.; Harris, P. A.; Lackey, K. Discovery and in vitro evaluation of potent TrkA kinase inhibitors: oxindole and aza-oxindoles. *Bioorg Med Chem Lett* **2004**, *14* (4), 953-957.
168. Bernard-Gauthier, V.; Aliaga, A.; Aliaga, A.; Boudjemeline, M.; Hopewell, R.; Kostikov, A.; Rosa-Neto, P.; Thiel, A.; Schirrmacher, R. Syntheses and evaluation of carbon-11-and fluorine-18-radiolabeled pan-tropomyosin receptor kinase (Trk) inhibitors: Exploration of the 4-aza-2-oxindole scaffold as Trk PET imaging agents. *ACS Chem Neurosci* **2015**, *6* (2), 260-276.
169. Choe, H.; Son, Y. H.; Byun, B. J.; Choi, S. U.; Lee, K. Identification of pyrrole[3,4-c]pyrazoles as potent tropomyosin receptor kinase A (TrkA) inhibitors. *B Korean Chem Soc* **2016**, *37* (8), 1378-1380.
170. Carboni, J. M.; Wittman, M.; Yang, Z.; Lee, F.; Greer, A.; Hurlburt, W.; Hillerman, S.; Cao, C.; Cantor, G. H.; Dell-John, J.; Chen, C.; Discenza, L.; Menard, K.; Li, A.; Trainor, G.; Vyas, D.; Kramer, R.; Attar, R. M.; Gottardis, M. M. BMS-754807, a small molecule inhibitor of insulin-like growth factor-1R/IR. *Mol Cancer Ther* **2009**, *8* (12), 3341-3349.
171. Cho, S. Y.; Han, S. Y.; Ha, J. D.; Ryu, J. W.; Lee, C. O.; Jung, H.; Kang, N. S.; Kim, H. R.; Koh, J. S.; Lee, J. Discovery of aminopyridines substituted with benzoxazole as orally active c-Met kinase inhibitors. *Bioorg Med Chem Lett* **2010**, *20* (14), 4223-4227.
172. Han, S. Y.; Lee, C. O.; Ahn, S. H.; Lee, M. O.; Kang, S. Y.; Cha, H. J.; Cho, S. Y.; Ha, J. D.; Ryu, J. W.; Jung, H.; Kim, H. R.; Koh, J. S.; Lee, J. Evaluation of a multi-kinase inhibitor KRC-108 as an anti-tumor agent in vitro and in vivo. *Invest New Drugs* **2012**, *30* (2), 518-523.
173. Stachel, S. J.; Sanders, J. M.; Henze, D. A.; Rudd, M. T.; Su, H. P.; Li, Y.; Nanda, K. K.; Egbertson, M. S.; Manley, P. J.; Jones, K. L.; Brnardic, E. J.; Green, A.; Grobler, J. A.; Hanney, B.; Leitl, M.; Lai, M. T.; Munshi, V.; Murphy, D.; Rickert, K.; Riley, D.; Krasowska-Zoladek, A.; Daley, C.; Zuck, P.; Kane, S. A.; Bilodeau, M. T. Maximizing diversity from a kinase screen: identification of novel and selective pan-Trk inhibitors for chronic pain. *J Med Chem* **2014**, *57* (13), 5800-5816.
174. Rohren, E. M.; Turkington, T. G.; Coleman, R. E. Clinical applications of PET in oncology. *Radiology* **2004**, *231* (2), 305-332.
175. Rudin, M.; Weissleder, R. Molecular imaging in drug discovery and development. *Nat Rev Drug Discov* **2003**, *2* (2), 123-131.
176. Slobbe, P.; Poot, A. J.; Windhorst, A. D.; van Dongen, G. A. PET imaging with small-molecule tyrosine kinase inhibitors: TKI-PET. *Drug Discov Today* **2012**, *17* (21-22), 1175-1187.
177. Bernard-Gauthier, V.; Bailey, J. J.; Berke, S.; Schirrmacher, R. Recent advances in the development and application of radiolabeled kinase inhibitors for PET imaging. *Molecules* **2015**, *20* (12), 22000-22027.
178. Bernard-Gauthier, V.; Bailey, J. J.; Aliaga, A.; Kostikov, A.; Rosa-Neto, P.; Wuest, M.; Brodeur, G. M.; Bedell, B. J.; Wuest, F.; Schirrmacher, R. Development of subnanomolar radiofluorinated (2-pyrrolidin-1-yl)imidazo 1,2-b pyridazine pan-Trk inhibitors as candidate PET imaging probes. *Medchemcomm* **2015**, *6* (12), 2184-2193.
179. Bernard-Gauthier, V.; Mahringer, A.; Vesnaver, M.; Fricker, G.; Schirrmacher, R. Design and synthesis of a fluorinated quinazoline-based type-II Trk inhibitor as a scaffold for PET radiotracer development. *Bioorg Med Chem Lett* **2017**, *27* (12), 2771-2775.
180. Bernard-Gauthier, V.; Schirrmacher, R. 5-(4-((4-[(18)F]Fluorobenzyl)oxy)-3-methoxybenzyl)pyrimidine-2,4-diamine: a selective dual inhibitor for potential PET imaging of Trk/CSF-1R. *Bioorg Med Chem Lett* **2014**, *24* (20), 4784-4790.
181. Bernard-Gauthier, V.; Bailey, J. J.; Mossine, A. V.; Lindner, S.; Vomacka, L.; Aliaga, A.; Shao, X.; Quesada, C. A.; Sherman, P.; Mahringer, A.; Kostikov, A.; Grand'Maison, M.; Rosa-Neto, P.; Soucy, J. P.; Thiel, A.; Kaplan, D. R.; Fricker,

G.; Wangler, B.; Bartenstein, P.; Schirrmacher, R.; Scott, P. J. H. A kinome-wide selective radiolabeled TrkB/C inhibitor for in vitro and in vivo neuroimaging: synthesis, preclinical evaluation, and first-in-human. *J Med Chem* **2017**, *60* (16), 6897-6910.
182. Bernard-Gauthier, V.; Mossine, A. V.; Mahringer, A.; Aliaga, A.; Bailey, J. J.; Shao, X.; Stauff, J.; Arteaga, J.; Sherman, P.; Grand'Maison, M.; Rochon, P. L.; Wangler, B.; Wangler, C.; Bartenstein, P.; Kostikov, A.; Kaplan, D. R.; Fricker, G.; Rosa-Neto, P.; Scott, P. J. H.; Schirrmacher, R. Identification of [(18)F]TRACK, a fluorine-18-labeled tropomyosin receptor kinase (Trk) inhibitor for PET imaging. *J Med Chem* **2018**, *61* (4), 1737-1743.
183. Pargellis, C.; Tong, L.; Churchill, L.; Cirillo, P. F.; Gilmore, T.; Graham, A. G.; Grob, P. M.; Hickey, E. R.; Moss, N.; Pav, S.; Regan, J. Inhibition of p38 MAP kinase by utilizing a novel allosteric binding site. *Nat Struct Biol* **2002**, *9* (4), 268-272.
184. Davis, M. I.; Hunt, J. P.; Herrgard, S.; Ciceri, P.; Wodicka, L. M.; Pallares, G.; Hocker, M.; Treiber, D. K.; Zarrinkar, P. P. Comprehensive analysis of kinase inhibitor selectivity. *Nat Biotechnol* **2011**, *29* (11), 1046-1051.
185. Albaugh, P.; Fan, Y.; Mi, Y.; Sun, F. X.; Adrian, F.; Li, N. X.; Jia, Y.; Sarkisova, Y.; Kreusch, A.; Hood, T.; Lu, M.; Liu, G. X.; Huang, S. L.; Liu, Z. S.; Loren, J.; Tuntland, T.; Karanewsky, D. S.; Seidel, H. M.; Molteni, V. Discovery of GNF-5837, a selective TRK inhibitor with efficacy in rodent cancer tumor models. *ACS Med Chem Lett* **2012**, *3* (2), 140-145.
186. Skerratt, S. E.; Andrews, M.; Bagal, S. K.; Bilsland, J.; Brown, D.; Bungay, P. J.; Cole, S.; Gibson, K. R.; Jones, R.; Morao, I.; Nedderman, A.; Omoto, K.; Robinson, C.; Ryckmans, T.; Skinner, K.; Stupple, P.; Waldron, G. The discovery of a potent, selective, and peripherally restricted pan-Trk inhibitor (PF-06273340) for the treatment of pain. *J Med Chem* **2016**, *59* (22), 10084-10099.
187. Pryde, D. C.; Dalvie, D.; Hu, Q.; Jones, P.; Obach, R. S.; Tran, T. D. Aldehyde oxidase: an enzyme of emerging importance in drug discovery. *J Med Chem* **2010**, *53* (24), 8441-8460.
188. Pryde, D. C.; Tran, T. D.; Jones, P.; Duckworth, J.; Howard, M.; Gardner, I.; Hyland, R.; Webster, R.; Wenham, T.; Bagal, S.; Omoto, K.; Schneider, R. P.; Lin, J. Medicinal chemistry approaches to avoid aldehyde oxidase metabolism. *Bioorg Med Chem Lett* **2012**, *22* (8), 2856-2860.
189. Yakes, F. M.; Chen, J.; Tan, J.; Yamaguchi, K.; Shi, Y.; Yu, P.; Qian, F.; Chu, F.; Bentzien, F.; Cancilla, B.; Orf, J.; You, A.; Laird, A. D.; Engst, S.; Lee, L.; Lesch, J.; Chou, Y. C.; Joly, A. H. Cabozantinib (XL184), a novel MET and VEGFR2 inhibitor, simultaneously suppresses metastasis, angiogenesis, and tumor growth. *Mol Cancer Ther* **2011**, *10* (12), 2298-2308.
190. Patwardhan, P. P.; Ivy, K. S.; Musi, E.; de Stanchina, E.; Schwartz, G. K. Significant blockade of multiple receptor tyrosine kinases by MGCD516 (Sitravatinib), a novel small molecule inhibitor, shows potent anti-tumor activity in preclinical models of sarcoma. *Oncotarget* **2016**, *7* (4), 4093-4109.
191. Smith, B. D.; Kaufman, M. D.; Leary, C. B.; Turner, B. A.; Wise, S. C.; Ahn, Y. M.; Booth, R. J.; Caldwell, T. M.; Ensinger, C. L.; Hood, M. M.; Lu, W. P.; Patt, T. W.; Patt, W. C.; Rutkoski, T. J.; Samarakoon, T.; Telikepalli, H.; Vogeti, L.; Vogeti, S.; Yates, K. M.; Chun, L.; Stewart, L. J.; Clare, M.; Flynn, D. L. Altiratinib inhibits tumor growth, invasion, angiogenesis, and microenvironment-mediated drug resistance via balanced inhibition of MET, TIE2, and VEGFR2. *Mol Cancer Ther* **2015**, *14* (9), 2023-2034.
192. El Zein, N.; D'Hondt, S.; Sariban, E. Crosstalks between the receptors tyrosine kinase EGFR and TrkA and the GPCR, FPR, in human monocytes are essential for receptors-mediated cell activation. *Cell Signal* **2010**, *22* (10), 1437-1447.
193. Arcari, J. T.; Beebe, J. S.; Berliner, M. A.; Bernardo, V.; Boehm, M.; Borzillo, G. V.; Clark, T.; Cohen, B. D.; Connell, R. D.; Frost, H. N.; Gordon, D. A.; Hungerford, W. M.; Kakar, S. M.; Kanter, A.; Keene, N. F.; Knauth, E. A.; Lagreca, S. D.; Lu, Y.; Martinez-Alsina, L.; Marx, M. A.; Morris, J.; Patel, N. C.; Savage, D.; Soderstrom, C. I.; Thompson, C.; Tkalcevic, G.; Tom, N. J.; Vajdos, F. F.; Valentine, J. J.; Vincent, P. W.; Wessel, M. D.; Chen, J. M. Discovery and synthesis of novel 4-aminopyrrolopyrimidine Tie-2 kinase inhibitors for the treatment of solid tumors. *Bioorg Med Chem Lett* **2013**, *23* (10), 3059-3063.
194. Kufareva, I.; Abagyan, R. Type-II kinase inhibitor docking, screening, and profiling using modified structures of active kinase states. *J Med Chem* **2008**, *51* (24), 7921-7932.
195. Frett, B.; McConnell, N.; Wang, Y.; Xu, Z.; Ambrose, A.; Li, H. Y. Identification of pyrazine-based TrkA inhibitors: design, synthesis, evaluation, and computational modeling studies. *Medchemcomm* **2014**, *5* (10), 1507-1514.

196. Conway, J. G.; McDonald, B.; Parham, J.; Keith, B.; Rusnak, D. W.; Shaw, E.; Jansen, M.; Lin, P.; Payne, A.; Crosby, R. M.; Johnson, J. H.; Frick, L.; Lin, M. H.; Depee, S.; Tadepalli, S.; Votta, B.; James, I.; Fuller, K.; Chambers, T. J.; Kull, F. C.; Chamberlain, S. D.; Hutchins, J. T. Inhibition of colony-stimulating-factor-1 signaling in vivo with the orally bioavailable cFMS kinase inhibitor GW2580. *Proc Natl Acad Sci U S A* **2005**, *102* (44), 16078-16083.
197. Conway, J. G.; Pink, H.; Bergquist, M. L.; Han, B.; Depee, S.; Tadepalli, S.; Lin, P.; Crumrine, R. C.; Binz, J.; Clark, R. L.; Selph, J. L.; Stimpson, S. A.; Hutchins, J. T.; Chamberlain, S. D.; Brodie, T. A. Effects of the cFMS kinase inhibitor 5-(3-methoxy-4-((4-methoxybenzyl)oxy)benzyl)pyrimidine-2,4-diamine (GW2580) in normal and arthritic rats. *J Pharmacol Exp Ther* **2008**, *326* (1), 41-50.
198. Hong, S.; Kim, J.; Seo, J. H.; Jung, K. H.; Hong, S. S.; Hong, S. Design, synthesis, and evaluation of 3,5-disubstituted 7-azaindoles as Trk inhibitors with anticancer and antiangiogenic activities. *J Med Chem* **2012**, *55* (11), 5337-5349.
199. Cee, V. J.; Albrecht, B. K.; Geuns-Meyer, S.; Hughes, P.; Bellon, S.; Bready, J.; Caenepeel, S.; Chaffee, S. C.; Coxon, A.; Emery, M.; Fretland, J.; Gallant, P.; Gu, Y.; Hodous, B. L.; Hoffman, D.; Johnson, R. E.; Kendall, R.; Kim, J. L.; Long, A. M.; McGowan, D.; Morrison, M.; Olivieri, P. R.; Patel, V. F.; Polverino, A.; Powers, D.; Rose, P.; Wang, L.; Zhao, H. Alkynylpyrimidine amide derivatives as potent, selective, and orally active inhibitors of Tie-2 kinase. *J Med Chem* **2007**, *50* (4), 627-640.
200. Furuya, N.; Momose, T.; Katsuno, K.; Fushimi, N.; Muranaka, H.; Handa, C.; Ozawa, T.; Kinoshita, T. The juxtamembrane region of TrkA kinase is critical for inhibitor selectivity. *Bioorg Med Chem Lett* **2017**, *27* (5), 1233-1236.
201. Bagal, S. K.; Omoto, K.; Blakemore, D. C.; Bungay, P. J.; Bilsland, J. G.; Clarke, P. J.; Corbett, M. S.; Cronin, C. N.; Cui, J. J.; Dias, R.; Flanagan, N. J.; Greasley, S. E.; Grimley, R.; Johnson, E.; Fengas, D.; Kitching, L.; Kraus, M. L.; McAlpine, I.; Nagata, A.; Waldron, G. J.; Warmus, J. S. Discovery of allosteric, potent, subtype selective, and peripherally restricted TrkA kinase inhibitors. *J Med Chem* **2018**, DOI: 10.1021/acs.jmedchem.8b00280.
202. Lange, A. M.; Lo, H. W. Inhibiting TRK proteins in clinical cancer therapy. *Cancers (Basel)* **2018**, *10* (4), 105.
203. Burris, H. A.; Shaw, A. T.; Bauer, T. M.; Farago, A. F.; Doebele, R. C.; Smith, S.; Nanda, N.; Cruickshank, S.; Low, J. A.; Brose, M. S. Abstract 4529: Pharmacokinetics (PK) of LOXO-101 during the first-in-human Phase I study in patients with advanced solid tumors: Interim update. *Cancer Res* **2015**, *75* (15 Supplement), 4529.
204. Hyman, D. M.; Laetsch, T. W.; Kummar, S.; DuBois, S. G.; Farago, A. F.; Pappo, A. S.; Demetri, G. D.; El-Deiry, W. S.; Lassen, U. N.; Dowlati, A.; Brose, M. S.; Boni, V.; Turpin, B.; Nagasubramanian, R.; Cruickshank, S.; Cox, M. C.; Ku, N. C.; Hawkins, D. S.; Hong, D. S.; Drilon, A. E. The efficacy of larotrectinib (LOXO-101), a selective tropomyosin receptor kinase (TRK) inhibitor, in adult and pediatric TRK fusion cancers. *J Clin Oncol* **2017**, *35* (18_suppl), LBA2501.
205. Laetsch, T. W.; DuBois, S. G.; Nagasubramanian, R.; Turpin, B.; Mascarenhas, L.; Federman, N.; Reynolds, M.; Smith, S.; Cruickshank, S.; Cox, M. C.; Pappo, A. S.; Hawkins, D. S. A pediatric phase I study of larotrectinib, a highly selective inhibitor of the tropomyosin receptor kinase (TRK) family. *J Clin Oncol* **2017**, *35* (15_suppl), 10510.
206. Laetsch, T. W.; DuBois, S. G.; Mascarenhas, L.; Turpin, B.; Federman, N.; Albert, C. M.; Nagasubramanian, R.; Davis, J. L.; Rudzinski, E.; Feraco, A. M.; Tuch, B. B.; Ebata, K. T.; Reynolds, M.; Smith, S.; Cruickshank, S.; Cox, M. C.; Pappo, A. S.; Hawkins, D. S. Larotrectinib for paediatric solid tumours harbouring NTRK gene fusions: phase 1 results from a multicentre, open-label, phase 1/2 study. *Lancet Oncol.* **2018**, *19* (5), 705-714.
207. Sidaway, P. Targeted therapy: Larotrectinib effective against TRK-fusion-positive cancers. *Nat Rev Clin Oncol* **2018**, *15* (5), 264.
208. Drilon, A.; Siena, S.; Ou, S. I.; Patel, M.; Ahn, M. J.; Lee, J.; Bauer, T. M.; Farago, A. F.; Wheler, J. J.; Liu, S. V.; Doebele, R.; Giannetta, L.; Cerea, G.; Marrapese, G.; Schirru, M.; Amatu, A.; Bencardino, K.; Palmeri, L.; Sartore-Bianchi, A.; Vanzulli, A.; Cresta, S.; Damian, S.; Duca, M.; Ardini, E.; Li, G.; Christiansen, J.; Kowalski, K.; Johnson, A. D.; Patel, R.; Luo, D.; Chow-Maneval, E.; Hornby, Z.; Multani, P. S.; Shaw, A. T.; De Braud, F. G. Safety and antitumor activity of the multitargeted pan-TRK, ROS1, and ALK inhibitor entrectinib: combined results from two phase I trials (ALKA-372-001 and STARTRK-1). *Cancer Discov* **2017**, *7* (4), 400-409.
209. Pishvaian, M. J.; Rolfo, C. D.; Liu, S. V.; Multani, P. S.; Maneval, E. C.; Garrido-Laguna, I. Clinical benefit of entrectinib for patients with metastatic pancreatic cancer who harbor NTRK and ROS1 fusions. *J Clin Oncol* **2018**, *36* (4_suppl), 521
210. Werner, T.; Heist, R.; Carvajal, R.; Adkins, D.; Alva, A.; Goel, S.; Hong, D.; Bazhenova, L.; Saleh, M.; Siegel, R.; Kyriakopoulos, C.; Blakely, C.; Eaton, K.; Lauer, R.; Wang, D.; Schwartz, G.; Neuteboom, S.; Potvin, D.; Faltaos, D.; Chen, I.;

Christensen, J.; Levisetti, M.; Chao, R.; Bauer, T. P2.06-001 A study of MGCD516, a receptor tyrosine kinase (RTK) inhibitor, in molecularly selected patients with NSCLC or other advanced solid tumors. *J Thorac Oncol* **2017**, *12* (1), S1068-S1069.

211. Takeda, M.; Seto, T.; Fujiwara, Y.; Yamamoto, N.; Nosaki, K.; Toyozawa, R.; Abe, C.; Shiga, R.; Nakamaru, K.; Nakagawa, K. 1362PSafety and clinical activity of DS-6051b, a ROS1/NTRK inhibitor, in Japanese patients with NSCLC harboring ROS1 fusion gene. *Annals of Oncology* **2017**, *28* (suppl_5).

212. Papadopoulos, K. P.; Borazanci, E.; Von Hoff, D.; Gandhi, L.; Patnaik, A.; Tachibana, M.; Zahir, H.; Gajee, R.; Goldberg, T.; Senaldi, G.; Ou, S.-H. Abstract CT024: First-in-human phase 1 dose-escalation study of DS-6051b, an oral ROS1 and NTRK inhibitor, in subjects with advanced solid tumors. *Cancer Res* **2016**, *76* (14 Supplement), CT024.

213. You, W. K.; Sennino, B.; Williamson, C. W.; Falcon, B.; Hashizume, H.; Yao, L. C.; Aftab, D. T.; McDonald, D. M. VEGF and c-Met blockade amplify angiogenesis inhibition in pancreatic islet cancer. *Cancer Res* **2011**, *71* (14), 4758-4768.

214. Pezet, S.; McMahon, S. B. Neurotrophins: mediators and modulators of pain. *Annu Rev Neurosci* **2006**, *29*, 507-538.

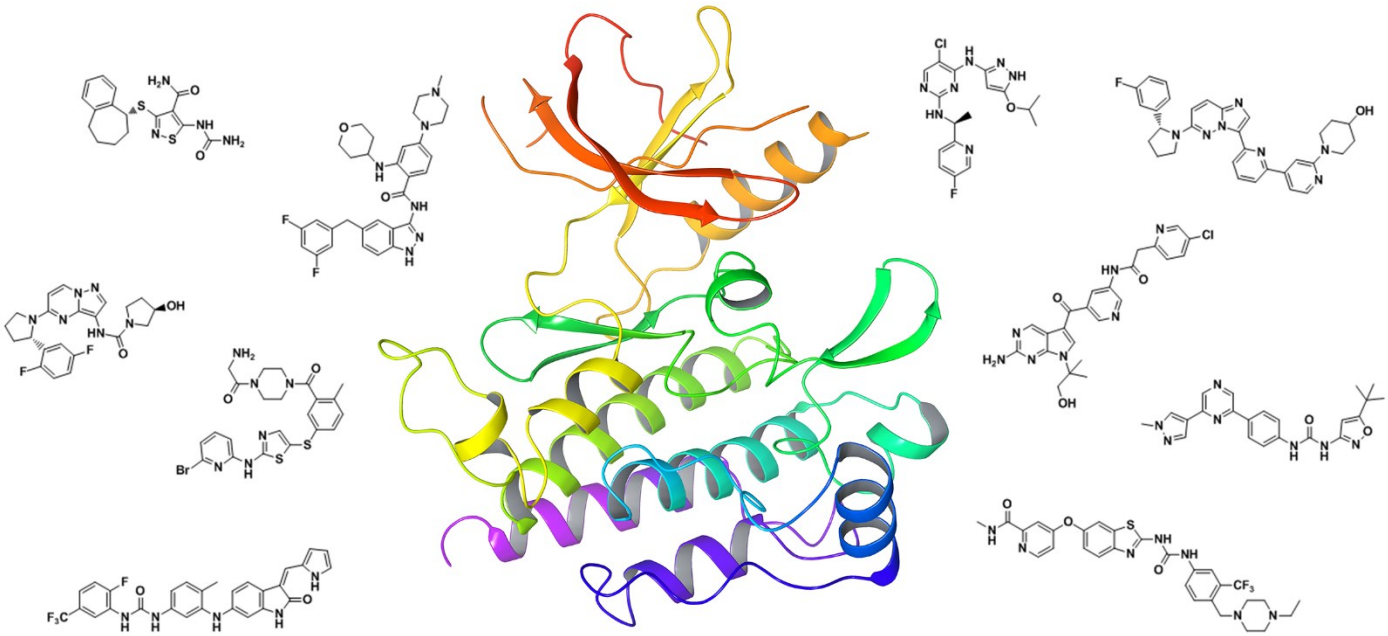

TRK Kinase

Table of Contents graphic